Title
Study of the bio-tribo-mechanical characteristics of orthopedic-grade polymers

Author
Roy, Anurag

Publication Date
2024

Study of the Bio-Tribo-Mechanical Characteristics of Orthopedic-Grade Polymers

By

Anurag Roy

A dissertation submitted in partial satisfaction of the

requirements for the degree of

Doctor of Philosophy

in

Engineering - Mechanical Engineering

in the

Graduate Division

of the

University of California, Berkeley

Committee in charge:

Professor Lisa A. Pruitt, Chair
Professor Grace Gu
Professor Andrew Minor

Spring 2024

Abstract

Study of the Bio-Tribo-Mechanical Characteristics of Orthopedic-Grade Polymers

by

Anurag Roy

Doctor of Philosophy in Engineering – Mechanical Engineering

University of California, Berkeley

Professor Lisa A. Pruitt, Chair

Osteoarthritis is an affliction whereby the articular cartilage present in the joint space starts to progressively degrade, causing mild to excruciating pain (depending on the stage of osteoarthritic joints) and severely affecting mobility and the quality of life of patients. Advanced stage osteoarthritic joints need a surgical intervention in the form of total joint replacement (TJR) as a 'cure'. TJRs encompass total knee replacements, total hip replacements, total shoulder replacements, and more. Ultra-high molecular weight polyethylene (UHMWPE) has been used as a bearing material in TJRs for over six decades owing to a slew of attributes it exhibits including but not limited to exceptional energetic toughness, mechanical integrity, and biocompatibility. However, given the hostile environment that the orthopedic grade polymers experience in-vivo, there are reports of TJR failure induced through wear (caused by the constant articulation of the mechanical components in TJRs), fatigue (owing to the cyclic nature of biomechanical stresses), and corrosion (given the saline ambience inside the body). Consequently, new polymer bearing materials like Polyether ether ketone (PEEK) and PEEK composites are increasingly being explored in the orthopedics community to overcome the aforementioned challenges. Alongside, there is a push towards improving the surface attributes of the TJR components given that wear, fatigue-induced wear, and corrosion are primarily surface and sub-surface phenomenon, and researchers in this field are looking into varied surface modification techniques from plasma surface treatment to coatings to post-processing and compositional changes through alloying to address persistent problems with TJRs.

This thesis delves into the bio-tribo-mechanical characteristics of both of these orthopedic-grade polymers, namely, UHMWPE and PEEK. First, an overview of the fatigue of polymers with special focus on UHMWPE is provided to lay the groundwork. Next, a deep dive into the tribological, mechanical, and biocompatibility aspects of PEEK and its composites is undertaken and their suitability for use in TJRs as a potential substitute for UHMWPE is thoroughly understood. Thereafter, some initial findings concerning the fatigue crack initiation phenomenon in UHMWPE from clinically relevant stress concentrations in TJR components like notches are duly reported. Finally, a perspective on bringing about a fundamental shift in the orthopedics realm by employing surface modification techniques such as Diamond-like Carbon (DLC) overcoats on TJR components to mitigate problems such as wear, corrosion, and metal-ion release plaguing modern-day TJR systems is discussed for future researchers interested in this field.

ACKNOWLEDGEMENTS

I want to thank my PhD advisor Prof. Lisa A. Pruitt, my MS advisor Prof. K. Komvopoulos, my letter writers Prof. Z. Al Balushi and Prof. H. Weller, fellowship and funding agencies, faculty who instructed classes I took, professors with whom I taught courses, my quals and thesis committee members, labmates, collaborators, departmental staff, campus colleagues, mentors, peer-support group, Toastmasters on Campus group, grad community, friends, and family for their invaluable support. Gratitude is such a beautiful thing that if you know, you know. It is heartfelt in a way that science can't measure and there are countless people who helped in my doctoral quest, such that I might go out of pages before that endless list might even be close to finishing. A quote from my favorite movie 'Silver Linings Playbook' is pertinent here- "The world will break your heart ten ways to Sunday, that's guaranteed, and I can't begin to explain that…… but guess what? Sunday is my favorite day again….. I think of everything everyone did for me and I feel like a very lucky guy…." Very succinctly summarizes how I feel about the Berkeley chapter!

Table of Contents

List of Figures

List of Tables

Chapter 1 – Introduction

Osteoarthritis is an affliction affecting upwards of 32.5 million people in the US with multitudes higher worldwide (“Osteoarthritis (OA) | Arthritis | CDC” 2020). There exist a variety of remedies for this malaise, depending on the severity of the problem and the pain level associated with osteoarthritis. These include physical activities and dedicated exercises, weight loss efforts, medications, injections in the affected joint space, and finally, when it becomes unmanageable, a total joint replacement (TJR) (“5 Ways to Manage Arthritis | CDC” 2023). The TJRs covered in this thesis primarily involve total hip replacement (THR) and total knee replacement (TKR) with occasional references to total shoulder replacements (TSR). A staggering 10% of men and 13% of women in the senior citizen demographic suffer from this affliction in the knee while about 20% of the population in this age group suffers from it in the hip joint (Zhang and Jordan 2010; Fan et al. 2023). These numbers are slated to only increase in the coming years with a higher share of the population needing TJRs, including in younger demographics (S. Kurtz et al. 2007).

TJRs are meant to serve as a substitute for the afflicted joint and are a combination of varied articulating mechanical elements with finite lifetimes and like any all-mechanical assemblies, they too are prone to failure through various mechanical modalities. When TJRs do fail, patients have to undertake a revision surgery and presently, the revision burden is as follows: for knee replacements, it is about 10% at the one and half decade mark whereas for hip replacements, it is around 7% at the 10-year mark (Nugent et al. 2021; “Total Knee Replacement - OrthoInfo - AAOS” 2024). Complicating matters further is the fact that full recovery spans about a year for knee and a year to year and half for hip revisions, thereby prolonging the suffering for patients (“Hip & Knee Revision Surgery Recovery Timeline” 2021).

Different material combinations are utilized as part of different TJRs (Uwais et al. 2017) although the predominant ones are ceramic or metallic counter-bearing on a polymer bearing. The polymer bearing is composed of a specialized polymer called Ultra-high molecular weight polyethylene (UHMWPE) while the counter-bearing materials include metallic alloys – CoCr/CoCrMo or ceramics like zirconia, alumina, or Oxinium. Some of the other components in TJRs such as the acetabular shell in THRs and tibial plate in TKRs are made up of a Ti alloy (Ti_6Al_4V). Differences in the material classes lead to different joint replacement systems being classified as metal-on-polymer (MoP), metal-on-metal (MoM), ceramic-on-ceramic (CoC), and ceramic-on-polymer (CoP). MoP TJRs are the predominant ones with a lion’s share followed by MoM, and then CoC & CoP (Uwais et al. 2017; Santavirta et al. 1998; Bozic et al. 2009) out of which a majority of MoP use a CoCr counter-bearing in conjunction with a UHMWPE bearing.

There are several challenges currently plaguing the two components of TJRs, i.e. the polymer bearing as well as the metallic counter-bearing. One of the historical problems arises from the issue of conventional TJR designs being meant to serve the interests of an aging demographic with a sedentary lifestyle. In the recent past, it has been observed that younger demographics with an active lifestyle are increasingly needing TJRs, thereby putting immense pressure on the previous designs of TJRs to perform under more intense environments (S. M. Kurtz et al. 2009). With regards to the polymer bearing component, it is exposed to a troika of problems including wear owing to the constant articulation between the different mechanical components in a TJR, fatigue because of the cyclic nature of biomechanical stresses at the joint sites, and oxidation given the aqueous environment of the body (Ansari, Ries, and Pruitt 2016; S. M. Kurtz 2009). Similarly, the metallic components face problems associated with corrosion, fatigue, wear, and in the process can induce secondary problems like metallosis or implant failures through osteolysis. Sudden impacts caused by intense physical activities can culminate in instantaneous fracture and these could prove detrimental to both TJR components. In sum, a variety of primary failure modalities exist including but not limited to wear, fatigue, corrosion, fracture, and secondary modalities such as fatigue-induced wear, fatigue-induced fracture, and stress-corrosion cracking.

Amongst the multitude of problems surrounding TJR components, one of the key ones is fatigue. To that effect, the second chapter of the thesis delves into the fatigue of polymers as this material class has garnered an increased share in the structural materials' pie chart. There is a push towards incorporating polymers in more and more load-bearing domains given the numerous advantages they offer including low density, chemical inertness, lubricity, specific strength and modulus, and most importantly from an industry standpoint, cost effectiveness. The 21st century has witnessed the ingress of polymers in domains ranging from automobiles, aerospace, sporting equipment, to the biomedical field. In structural applications involving cyclic loads, ascertaining the chances of fatigue failure and preempting that by enhancing the fatigue resistance of the polymer through different molecular, microstructural, and processing methods is paramount.

The molecular factors include parameters like molecular weight and its distribution, percent crystallinity, entanglement density, crosslinking density, and volume fraction and type of filler material or reinforcements in case of polymer composites. Other mechanical and environmental factors also influence the fatigue behavior of polymers such as frequency of cyclic loading, waveform applied, service conditions like chemical ambience and temperature, stress/strain amplitudes, peak cycle stress and the mean values, geometric factors causing stress concentrations like notches, undercuts, fillets, etc. These factors are compiled from several reviews published on this topic (Andrews, 1969; Beardmore and Rabinowitz, 1975; Sauer and Richardson, 1980; Sauer and Hara, 1990; Hertzberg et al., 1979; O'Connell and Mckenna, 2002; Naebe et al., 2016; Awaja et al., 2017; Hertzberg and Manson, 1980, 1986; Kausch and Williams, 1986; Ferry, 1961). Microstructural mechanisms involving both intrinsic as well as extrinsic crack-shielding and toughening mechanisms are explored. Crack deflection, particle tearing, bridging via fibers or second-phase particles, shear banding, development of voids, craze formation, zone shielding via phase transformations, fibrillation, blunting, microcracking, and more are included in the discussion.

The two design philosophies used to estimate the fatigue life of a polymeric component are discussed therein. The first one is the total life approach which assumes that a majority of the fatigue life of a component is expended in nucleating a defect from an originally defect-free material and utilizes unnotched samples to experimentally obtain the fatigue lives. The use of unnotched samples helps prevent undue stress concentrations which can bias the initiation dynamics of a flaw. The majority of the fatigue life is then spent in nucleating a flaw and a smaller segment in the propagation of this flaw to failure. On the other hand, the defect-tolerant approach begins with the assumption that all materials have inherent flaws and thus, the fatigue life can be computed based on the number of cycles needed to propagate that flaw to criticality, at which point the material fails. The latter approach is extensively applied in safety critical domains like aerospace, medical devices, etc. A sweep of the available literature on this topic is undertaken and correspondingly, the focus is on crack initiation studies for total-life vs crack propagation for defect-tolerant approaches. The former approach includes both stress- and strain-based loadings while the latter approach includes the fracture-mechanics calculations for estimation of fatigue life. Overall, a generic review of the fatigue of engineering polymers is pursued encompassing both the classical works on fatigue alongside the more-recent developments in this field over the past decade or so, thereby holistically covering the entirety of the fatigue of polymers landscape.

Once the landscape of fatigue of polymers is thoroughly covered, the thesis pivots towards a potential substitute of UHMWPE in TJRs by emphasizing on another specialized polymer called polyether ether ketone (PEEK) and its carbon-fiber reinforced composites (CFR-PEEK, hereafter referred to as PEEK composites) in the third chapter. While UHMWPE may have been the go-to material for the past six decades, it is still challenged with multiple issues as outlined previously. Briefly, these issues include wear, fatigue, and oxidation (Ansari et al., 2016; Kurtz, 2009). Therefore, PEEK and PEEK composites have been proposed as a plausible replacement for UHMWPE in this orthopedic application (Kurtz and Devine, 2007) to sustain the constant articulation at the joint space as well as aid in the load-bearing functionality.

The choice of PEEK and its composites, particularly in the context of medical devices arises from its favorable attributes like biocompatibility, chemical stability, toughness, fatigue resistance, and excellent tailorability to be in sync with the mechanical properties of bone (Kurtz, 2012b). Tailorability of PEEK and its composites' mechanical properties can be traced back to the crystalline domain size, annealing and thermal processing, and adhesion between the fibers and the matrix (Bonnheim et al., 2019; Regis et al., 2018). Amongst the various filler materials available for load-bearing applications (Abdullah et al., 2015), CFR-PEEK proves worthy of further investigation, especially PEEK reinforced using pitch- and PAN-based fillers. PEEK has the distinction of maintaining its tribo-mechanical properties despite undergoing sterilization processes used in medical device applications, for example, gamma sterilization, autoclaving, ethylene oxide, etc. (Solavy, 2017; Kumar et al., 2018). Further, there is close match between the moduli of bone and PEEK and CFR-PEEK (the tailorability factor helps immensely too) precluding the possibility of stress shielding and bone resorption and is also a potential substitute for the metallic components of TJRs (de Ruiter et al., 2021). Plus, the substitution of metallic components in TJRs with PEEK and PEEK composites could also potentially alleviate issues surrounding metal sensitivity from arising (Thyssen et al., 2009). Its radiolucency is an additional benefit for purposes of in-vivo imaging and monitoring of medical devices (Kurtz and Devine, 2007). The wear results obtained for low-stress high-conformity contact situations like in the hip joint are encouraging and justify this pursuit. The sheer number of successful biocompatibility studies concerning PEEK and its composites in both bulk and particulate form only help the cause.

The ongoing concerns around carbon fiber debris produced as a result of wear of PEEK composites warrant further query. Moreover, the lack of retrieval studies with regards to PEEK compound the problem alongside the divergence between clinical results and lab tests. The lack of standardization amongst different research groups doesn't help either, not to mention the technical difficulties in simulating real-life like lubrication regimes during tribological experiments. Unfortunately, laboratory experiments demonstrating the significantly higher wear rates for PEEK composites vis-à-vis medical grade UHMWPE under high-stress low-conformity contact situations witnessed in the knee joints have discouragingly closed the door on adopting PEEK and its composites as a potential substitute for UHMWPE in TKRs.

Given the mixed bag of results, the third chapter also points to the need for a rigorous assessment of the bio-tribo-mechanical landscape of PEEK and PEEK composites prior to any final recommendation regarding the substitution of UHMWPE with PEEK, especially in the context of orthopedic bearing devices. An immense amount of literature from the bio-tribo-mechanical literature of PEEK and its composites is condensed in this chapter with objective arguments for and against the potential substitution. The chapter is devoted to the in-depth investigation of PEEK and its composites' applicability in the orthopedic realm.

The fourth chapter thereafter reports the initial findings pertaining to a fatigue crack initiation study. Fatigue behavior is generally classified under two groups, namely, fatigue crack initiation and fatigue crack propagation tests. Given the overwhelmingly large number of studies focusing on the latter that have been reported in the literature for UHMWPE (Ansari, Ries, and Pruitt 2016; L. Pruitt, Wat, and Malito 2022; Furmanski and Pruitt 2007; Patten et al. 2011a; Ansari et al. 2016; Furmanski and Pruitt 2018; Baker, Hastings, and Pruitt 1999; 2000; Baker, Bellare, and Pruitt 2003; Bradford et al. 2004; L. A. Pruitt et al. 2005; Ries and Pruitt 2005; Simis et al. 2006), there exists a gap in the literature that forms the foundation for this chapter as the former remains rather unexplored. Suffice it to say that crack propagation behavior of UHMWPE has been fully characterized but the same can't be said about fatigue crack initiation of UHMWPE.

As covered in the second chapter more extensively, there are two philosophies to estimate the fatigue life of a polymeric component, viz. the total life and the defect-tolerant approach. Pertinently, fatigue experiments have been conducted by numerous researchers who have studied the steady-state crack propagation regime of UHMWPE, a.k.a. the Paris regime plotted as da/dN vs ΔK graphs. Within these studies, some have also focused on minimum stress intensities needed for the crack to propagate at a very slow rate of 10^{-7} mm/cycle (Baker, Bellare, and Pruitt 2003; Simis et al. 2006) which helps decipher the stress intensity inception value symbolized as ΔK_{incep}. The second approach entails utilizing the stress amplitude vs number of cycles plots (S-N data) and the parameters of the Basquin relation are calculated from these plots (Baker, Bellare, and Pruitt 2003; Michael C. Sobieraj et al. 2013).

As far as UHMWPE is concerned, it is considered as a fatigue brittle material and therefore, the fatigue life is predominantly the number of cycles to crack initiation after which fast fracture ensues, meaning that the number of cycles to failure is relatively close to the number of cycles to initiate a flaw (crack in the material). The underlying assumption being that the number of cycles to flaw initiation/crack nucleation is substantially larger than the number of cycles for that crack to propagate to a critical size to failure. Consequently, the $N_{failure}$ is almost equal to $N_{initiation}$ and highlights the paramountcy of crack initiation investigations summarized through typical S-N format plots. While traditional S-N plots were drawn by performing fatigue tests on unnotched samples, it is noteworthy to mention here that TJRs have a number of features imparting heightened stress-concentrations, such as posts, undercuts, fillets, grooves, notches, etc. by virtue of their geometry and locking mechanisms. Regions experiencing increased stress-concentrations are prone to accelerated crack nucleation/flaw initiation which can culminate in catastrophic failure eventually, given the presence of constant quasi-static and fluctuating loads in the joint space (Furmanski et al. 2009; Furmanski, Kraay, and Rimnac 2011).

Geometric features like notches, undercuts, fillets that are present inherently as part of the design of TJR components also influence the micro-mechanisms that transpire during the fatigue failure processes. It is therefore important to isolate the effect of notch geometry on the fatigue properties of UHMWPE and consequently, the severity of notching (from sharp to blunt) was varied as part of this study by testing with different notch root radii. Additionally, the stress intensity experienced at the notch root was varied by modifying the a/W ratio in the notched sample geometries. The study builds on a previously published work on crack propagation dynamics of fatigue cracks initiating from notch roots by adopting a linear-elastic fracture mechanics model (Ansari et al. 2016). While the previous work studied crack propagation as a function of notch geometry, it also paved the way for the next research iteration in the form of gauging the effect of notch geometry on crack initiation characteristics, covering both parameters of interest – notch root radii and a/W ratio. Two different formulations of medical grade UHMWPE, two different clinically relevant notch root radii, and multiple a/W ratios were brought into the scope of this work. Cracks were allowed to organically nucleate from the stress concentration-affected notch roots without any external interventions by cycling samples at different load amplitudes (in effect, different stress intensities) and the number of cycles to fatigue failure were subsequently noted. Results were analyzed in the context of correlations between the a/W ratio, the notch root radii, and the number of cycles to fatigue failure. Furthermore, the damage accumulation theory proposed by Palmgren-Miner was tested by performing fatigue tests at incrementally increasing stress cycles vis-à-vis tests at the highest stresses. The futuristic direction in this research endeavor is to develop a parametric model comprising notch root radii, a/W ratio, and material formulation on the input parameter side with crack initiation characteristics and number of cycles to fatigue failure being output parameters.

Changing gears from the UHMWPE polymer bearing to the metallic components of TJRs, the fifth chapter focusses on establishing the feasibility of incorporating Diamond-like Carbon (DLC) in TJR components as a potential coating material on the metallic components (Dearnaley and Arps 2005; Butter and Lettington 1995). The objective is to surmount the problems of wear, corrosion, and metal-ion release presently degrading the quality and performance of the metallic counter-bearing components in TJRs. Another possibility involving a monolithic Ti-alloy femoral component is also explored (Shah et al. 2021) given the challenges surrounding galvanic or crevice corrosion (Ghadirinejad et al. 2023; Urish et al. 2019) in modular systems comprising a Ti stem and a CoCr head attached through a Morse taper. This could potentially help overcome the wear and corrosion problems that have traditionally precluded the use of a monolithic Ti component in TJRs. A comprehensive examination outlining the advantages and disadvantages of incorporating DLC technology into TJRs remains the overarching theme of this chapter.

The choice of DLC for use in TJRs is attributed to its bio-tribo-thermo-mechanical excellence which makes it an ideal candidate not only for use in orthopedic bearing devices, but also underscores why it is currently used in a plethora of application domains (Bhatia et al. 1998; A. Roy, Wang, and Komvopoulos 2023; Robertson 2001; Xu and Pruitt 1999; Grill 1997; Lettington 1998; Grill 2003; Mehta and Cooper 2003; Sze and Tay 2006; Dowling et al. 1997; Casiraghi, Robertson, and Ferrari 2007; Moser et al. 1998; Cheah et al. 1998; Luo et al. 2007; Wu et al. 2013; Komvopoulos 1996; Tiainen 2001; R. K. Roy and Lee 2007). Some of the properties it exhibits which make it an interesting material worthy of exploration in this domain are its biocompatibility, wear resistance, high hardness, and low coefficient of friction, thermal stability and chemical inertness, strong adhesion to metallic substrates, as well as its through-thickness tailorability (Dearnaley and Arps 2005; Xu and Pruitt 1999; Robertson 2002; Yeo et al. 2015; Na Wang and Komvopoulos 2013; S. Wang, Roy, and Komvopoulos 2021; J. Yeo et al. 2017; Dwivedi et al. 2017). To balance out the advantages, anticipated challenges and existing concerns are highlighted, including delamination, hydrophobicity, and conflicting as well as outdated results presented in the tribology literature. Given both the qualities offered by DLC as well as the concerns that surround it, the final recommendation is to integrate DLC into TJR systems once all the challenges currently plaguing DLC technology's successful incorporation into the orthopedic bearing devices are convincingly addressed.

In sum, this thesis broadly serves as a resource for researchers, medical device professionals, designers of biomedical devices, and the orthopedic community at large.

Chapter 2 – Fatigue of Polymers

This chapter has been published in the 2nd Edition of the Comprehensive Structural Integrity book (Pruitt et al. 2023).

2.1 Introduction

Fatigue of polymers is of critical concern to the engineering community as plastics have been increasingly incorporated into load-bearing applications over the last few decades. Polymers offer a variety of unique properties including low density, chemical inertness, lubricity, good specific strength and modulus, as well as cost effectiveness. These properties have made plastic materials ideal candidates for applications in the automotive, aerospace, sporting goods, and medical industries. When designing polymeric components for structural applications involving cyclic loading conditions, understanding fatigue resistance is of paramount importance. As with other engineering materials, failure often ensues in the polymer as a result of accumulated damage, or growth of a defect to a critical dimension. The fatigue performance of polymers is extremely sensitive to the molecular structure of the polymer. Molecular variables include molecular weight, molecular weight distribution, crystallinity, chain entanglement density, crosslink density, and the presence of fillers or reinforcements. Most polymers are viscoelastic and hence are sensitive to frequency, waveform, along with service temperatures. In addition to molecular factors, the fatigue life of a polymeric component is controlled by a number of mechanical factors including the stress or strain amplitude of the loading cycle, the mean and peak stress of the cycle, and the presence of stress concentrations or initial defects in the component. All of these factors are of considerable interest and practicality for the safe design of structural polymeric components that are subjected to fatigue loading.

Characterization of fatigue behavior of an engineering polymer generally entails the use of one of two distinct design philosophies. The first of these, commonly used in applications where the majority of the fatigue life is spent in the nucleation of a flaw, is termed as the total life approach. This design methodology assumes that the component is initially defect-free and fatigue characterization is typically performed with unnotched specimens that are free of substantial stress concentrations. This methodology is based on the notion that fatigue failure is a consequence of crack nucleation and subsequent growth to a critical size. The total life philosophy is distinct from the defect-tolerant approach, in which the fatigue life of a component is based on the number of loading cycles needed to propagate a crack of an initial size to a critical dimension. The defect-tolerant philosophy is commonly employed in safety-critical applications such as medical devices. In light of this, it is important to note that the literature generally makes a clear distinction between crack initiation and propagation studies, which then go on to emulate the total-life and defect-tolerant philosophies, respectively. Over the last few decades, researchers have provided a number of detailed reviews that speak to the various factors contributing to the fatigue performance of engineering polymers (Andrews 1969; Beardmore and Rabinowitz 1975; Sauer and Richardson 1980; Sauer and Hara 1990; Hertzberg et al. 1979; O'Connell and Mckenna 2002; Naebe et al. 2016; Awaja et al. 2017; Hertzberg and Manson 1980, 1986; Kausch and Williams 1986; Ferry 1961). These reviews encompass the fatigue behavior in polymers based on both total-life and fracture-mechanics approaches.

This article first explores fatigue life estimation approaches viz. total-life philosophy which includes both stress and strain-based loadings. The defect-tolerant philosophy predicated on fracture-mechanics follows with discussion of crack shielding and toughening mechanisms in polymeric materials. The subsequent section then laboriously compiles the molecular and mechanical factors that influence the fatigue characteristics of polymers.

The aim of this chapter is to provide a general overview of the fatigue behavior of engineering polymers. To accomplish this, a number of the original pioneering works on fatigue of polymers are cited as well as the recent advances in the field are included. The chapter also qualitatively and quantitatively presents the overall fatigue landscape vis-à-vis polymers.

2.2 Total-Life Philosophy

2.2.1 Stress-Based Loading

The total-life philosophy is founded on the premise that the component is initially defect-free, and that the life of a polymeric component is based on the initiation of a flaw and subsequent growth to a critical crack size. Damage is accumulated until a flaw nucleates. Failure ensues (i.e. the sample rips in half) as the specimen accommodates a critical level of damage. The preponderance of polymer fatigue characterization based on this design philosophy is performed under stress-controlled conditions. In these tests, unnotched specimens are generally subjected to constant-amplitude load cycles until failure occurs.

In fatigue testing, the applied stress, $\boldsymbol{\sigma}_a$, is typically described by the stress amplitude of the loading cycle and is defined as:

$$\sigma_a = \frac{\sigma_{max} - \sigma_{min}}{2} \qquad \text{Eq. [1]}$$

where $\boldsymbol{\sigma}_{max}$ is the maximum stress and $\boldsymbol{\sigma}_{min}$ is the minimum stress of the loading cycle. Once many samples are tested, an S-N plot is generated by plotting the stress amplitude (S) against the number of cycles to failure (N) on a linear-log scale, each broken sample as its own data point. Starting at high stress amplitudes, samples are broken at increasingly smaller values of stress amplitude until an endurance limit is reached ($\boldsymbol{\sigma}_e$). An endurance limit is defined as the stress level that results in more than 10 million cycles without failure. The assumption is that if the device is exposed to stress amplitudes below $\boldsymbol{\sigma}_e$, then the device is safe from fatigue failure (it is noteworthy, that not all polymers have an endurance limit). S–N curves enable life to be predicted based on the stress amplitude or range of stress amplitudes that a component is expected to encounter.

Figure 1 shows the S–N behavior of several commodity plastics. Polymers such as polyethylene (PE), polypropylene oxide (PPO), polystyrene (PS), polytetrafluoroethylene (PTFE), polypropylene (PP), polymethyl methacrylate (PMMA), and epoxy (EP) clearly exhibit an endurance limit below which failure does not occur in less than 10^7 cycles. On the other hand, nylon and polyethylene terephthalate (PET) do not exhibit endurance limits (the slopes of their S-N curves do not approach zero nor do the curves become asymptotes to any line parallel to the horizontal axis). The specifics of why some polymers exhibit an endurance limit while others do not is a current area of research and has garnered significant attention in the polymer community. However, it is generally accepted that the measured endurance limit in polymeric glasses is a result of the polymer's previous stress and temperature states (Pastuhov et al. 2020). Called "progressive aging", the evolution of a polymer's properties throughout its characterization and service life affects many important mechanical attributes. It is therefore of paramount importance to understand the processing history of the polymer and the conditions under which the mechanical testing is performed, so that any design decisions based on those mechanical properties are sound.

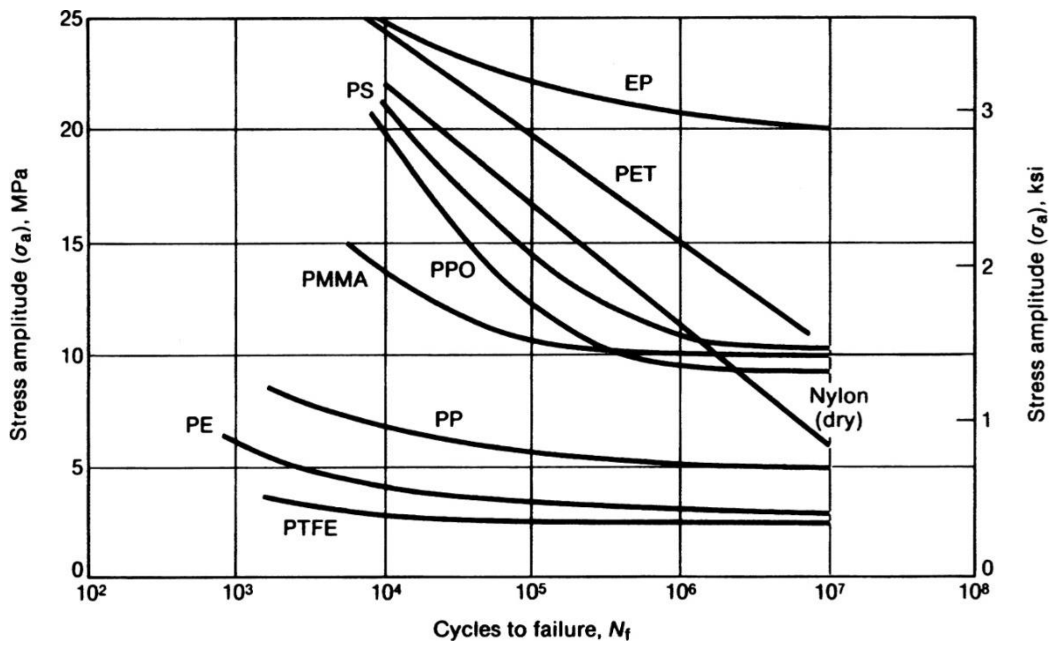

Figure 1 Stress amplitude vs. cycles to failure (S–N behavior) of several commodity plastics. (Hertzberg and Manson 1980)

The total life fatigue performance of polymers is sensitive to many experimental factors including test frequency, temperature, and mean stress. In addition, fatigue performance is also heavily influenced by molecular factors such as chemistry, molecular weight, crystallinity, and degree of crosslinking. These factors will be explored in greater detail in later sections. While there are ASTM and ISO standards (E647 and 12110-1:2013, respectively) which stipulate the specifics of the test conditions for ensuring standardization, it is essential that the fatigue test conditions closely mimic the service conditions of the polymeric component and customization is often vital for polymeric testing. In sum, the S–N approach is widely accepted in the engineering plastics community for design applications where stress concentrations are expected to be minimal or where the fatigue life of the component is likely to be dominated by the nucleation of a crack, a.k.a. crack initiation.

2.2.2 Strain-Based Loading

Strain-based tests are often utilized to characterize polymers when the structural component is likely to experience fluctuations in displacement or strain and are often utilized for components with accumulated strain or blunt notches (Hertzberg and Manson 1980). Most strain-based fatigue tests are performed using fully reversed loading conditions. In general, this is accompanied by a cyclic softening phenomenon in plastics (Ferry 1961; Beardmore and Rabinowitz 1975; Landel and Nielsen 1993; Krzypow and Rimnac 2000). Under cyclic strain conditions, the fatigue response is best characterized by the cyclic stress–strain curve. Figure 2 shows a comparison of the cyclic and monotonic (tension) stress–strain curves for nylon, polycarbonate (PC), polypropylene, and acrylonitrile butadiene styrene (ABS). An interesting attribute of these plots is that all of these polymers cyclically soften with lower yield points than their quasi-static values. Polymers generally soften under cyclic loading conditions, rather than cyclically harden as is observed in many structural metals.

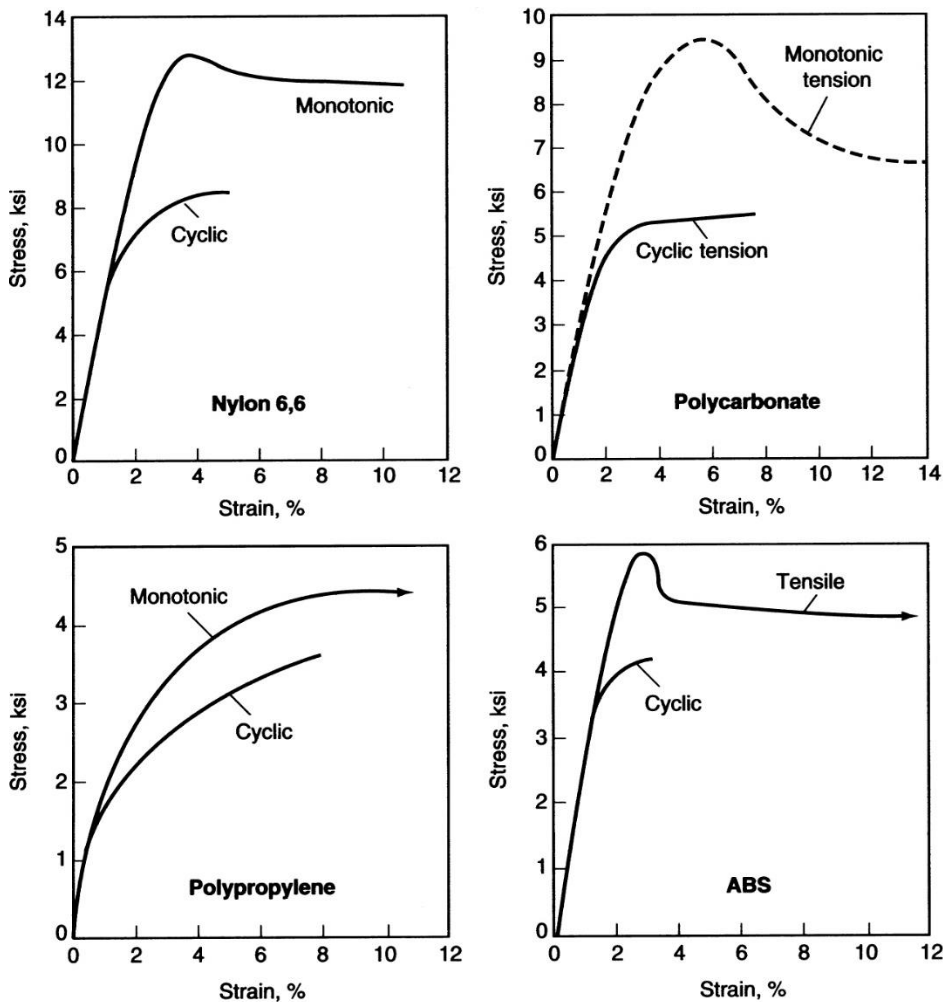

Figure 2 Comparison of the cyclic and monotonic (tension) stress–strain curves for nylon, polycarbonate, polypropylene, and acrylonitrile butadiene styrene (ABS). (Hertzberg and Manson 1980)

Cyclic strain data can also be represented in a manner that is analogous to the S–N characterization. The total strain amplitude can be divided into the elastic and plastic strain amplitude components. In these tests, the strain amplitude of the fatigue cycle is plotted against the number of cycles or load reversals to failure. This provides an empirical relationship between the strain amplitude of the fatigue cycle and the number of cycles to specimen failure (Hertzberg and Manson 1986):

$$\epsilon_a = \frac{\sigma_f'}{E}\left(2N_f\right)^b + \epsilon_f'\left(2N_f\right)^c \qquad \text{Eq. [2]}$$

Equation [2] is commonly known as the Coffin-Manson equation. Here $\boldsymbol{\varepsilon}_a$ is the strain amplitude, $\boldsymbol{\sigma}'_f$ is the strength coefficient, $\boldsymbol{\varepsilon}'_f$ is the ductility coefficient, $\boldsymbol{2N_f}$ is the number of load reversals to failure, and b and c are material constants. The first term on the right-hand side of Equation [2] represents the elastic component of the strain amplitude, while the second term signifies the plastic component of the strain amplitude. Tests dominated by small amounts of cyclic plastic strain are designated high-cycle fatigue while those with high plastic strains are termed low-cycle fatigue. The former is characterized by a large number of cycles to failure and the latter is identified by the relatively small number of cycles to failure. In between these two extremes lies the transition life $2N_t$, which marks the distinction between high-cycle and low-cycle fatigue and is ascertained by equating the elastic and plastic components of the strain amplitude and thereafter, solving for the number of cycles to fatigue failure $2N_t$:

$$\frac{\sigma'_f}{E}(2N_t)^b = \epsilon'_f(2N_t)^c \qquad \text{Eq. [3]}$$

Solving for $2N_t$, we get:

$$2N_t = \left(\frac{\epsilon'_f E}{\sigma'_f}\right)^{\left(\frac{1}{b}-c\right)} \qquad \text{Eq. [4]}$$

It is paramount to consider the attributes of the fatigue test since those guide the relative ranking of fatigue resistance amongst various polymers. For example, polymers with higher damping capacities may be less resistant to fatigue. This is due to thermal heating when tested under constant stress amplitude. Conversely, these same polymers may have enhanced fatigue resistance if tested under constant deflection conditions. Moreover, the relative placement of fatigue resistance in polymers is correlated strongly with whether the tests are performed under adiabatic or isothermal conditions (Hertzberg and Manson 1980). These factors are important considerations to make when designing fatigue tests for the evaluation of polymeric components.

2.3 Defect-Tolerant Philosophy

2.3.1 Fracture Mechanics Concepts

The defect-tolerant philosophy is based on the implicit assumption that structural components are intrinsically flawed and that the fatigue life is based on the propagation of an initial flaw to a crack of critical size (Ritchie and Liu 2021). Linear elastic fracture mechanics (LEFM) is used to analyze the propagation of fatigue cracks in advanced engineering plastics that are capable of sustaining a large amount of subcritical crack growth prior to fracture. The defect-tolerant approach is used in safety-critical applications such as aerospace, pressure vessels, and medical applications (Kurtz 2009). Fatigue crack propagation (FCP) resistance in polymers is influenced by near-tip micro-mechanisms, mean stress, frequency, and environment (Hertzberg and Manson 1983). Such factors complicate fatigue characterization as cracks may advance at different rates depending on their propensity. Understanding the effects of molecular and mechanical factors is of critical importance for the safe design of structural polymeric components subjected to repetitive loading. These influences are explored after a brief review of linear elastic fracture mechanics as it is utilized in crack propagation studies.

The stress intensity factor, K, derived from linear elastic fracture mechanics is the parameter used to describe the magnitude of the stresses, strains, and displacements ahead of the crack tip. The linear elastic solution for the normal stress in the opening mode of loading is written as a function of distance, r, and angle, $\boldsymbol{\theta}$, away from the crack tip (Sih 1973):

$$\sigma_{yy} = \frac{K_I}{\sqrt{2\pi r}} cos\frac{\theta}{2} \left(1 + \sin\frac{\theta}{2} sin\frac{3\theta}{2}\right) \qquad \text{Eq. [5]}$$

where K_I is the mode I (opening mode) stress-intensity factor. The stress-intensity parameter incorporates the boundary conditions of the cracked body and is a function of loading, crack length, and geometry. The stress-intensity factor can be found for a wide range of specimen types and is used to scale the effect of the far-field load, crack length, and geometry of the flawed component.

LEFM provides a conservative design approach for predicting the life of a cracked structural component under cyclic loading conditions. Although the fracture micro-mechanisms vary for metals, polymers, and ceramics, the fatigue crack propagation behavior of these materials shares many similar attributes at the macroscopic scale. As with other engineering materials, there are three distinct regimes of crack propagation for polymers under constant amplitude cyclic loading conditions viz. zone A: near-threshold regime, characterized by slow crack growth and below which, crack propagation doesn't occur; zone B: intermediate crack growth regime a.k.a. Paris regime; and zone C: fast crack propagation regime, commonly referred to as the unstable crack growth regime which is dominated by K_{max}. These regimes are denoted in Figure 3 which shows typical crack growth rate (velocity) plotted against the cyclic stress intensity range (illustrated on a log–log scale). Ultimately, the curve reaches a stage where it becomes an asymptote, corresponding to $K_{max} \rightarrow K_c$, where K_c is the fracture toughness of the material under study (Dowling 1993). The velocity of a moving fatigue crack subjected to a constant stress amplitude loading is determined from the change in crack length, *a*, as a function of the number of loading cycles, *N*. This velocity represents the fatigue crack growth per loading cycle, *da/dN*, and is found from experimentally generated curves where *a* is plotted as a function of *N*. Paris and co-workers suggested that the stress-intensity factor range, $K= K_{max} - K_{min}$ which itself captures the far-field stress, crack length, and geometry, should be the characteristic driving force parameter for fatigue crack propagation (Paris et al. 1961). This is known as the Paris Law, and it states that *da/dN* scales with ΔK through the following power-law relationship:

$$\frac{da}{dN} = C\Delta K^m \qquad \text{Eq. [6]}$$

where C and m are material constants. The Paris equation is valid for intermediate ΔK levels spanning crack propagation rates from 10^{-6} to 10^{-4} mm/cycle, which is considered the universal range for the Paris regime (Suresh 1998). The Paris regime is most often used for life prediction, although the fatigue threshold is key for designing against the inception of crack growth where components are expected to have long service lifetimes or where intermittent inspections may be difficult, such as in the medical device industry.

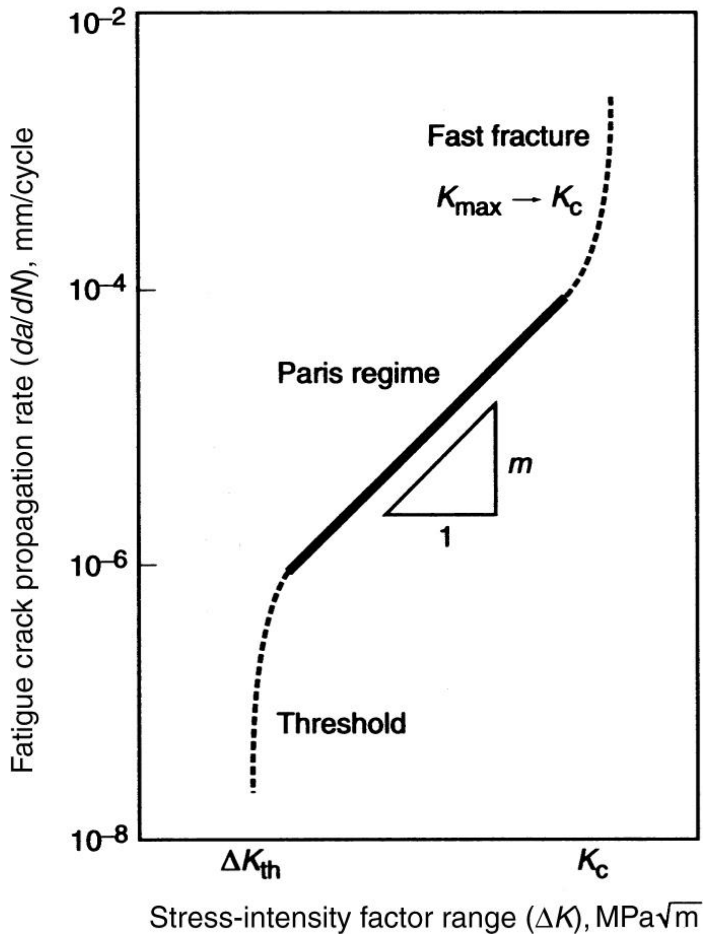

Figure 3 Illustration of the sigmoidal curve that captures the crack growth rate as a function of stress-intensity range (illustrated on a log–log scale).

The Paris Law is commonly employed for fatigue-life prediction of polymer components that have known stress concentrations and for which small scale yielding conditions prevail. It is worth noting that not all polymers lend themselves to the use of linear elastic fracture mechanics, some ductile thermoplastics lend themselves better to assessment through elastic-plastic fracture theories or viscoelastic models (Hertzberg and Manson 1983). It is implied in the use of an LEFM defect-tolerant approach that the device or component contains an initial defect or crack size, a_i. This can be determined from non-destructive evaluation (NDE), and if no defect is found, an initial defect whose size is the limit of resolution of the NDE method is assumed to exist. Assuming that the fatigue loading is performed under constant stress amplitude conditions, that the geometric factor, $f(\boldsymbol{\alpha})$, does not change within the limits of integration, and that fracture occurs when the crack reaches a critical value, a_c, one can integrate the Paris equation to predict the total fatigue life of the component:

$$N_f = \frac{2}{(m-2)C\, f(\alpha)^m (\Delta\sigma)^m \pi^{\frac{m}{2}}} \left(\frac{1}{a_i^{\frac{m-2}{2}}} - \frac{1}{a_c^{\frac{m-2}{2}}} \right) \text{for m} \neq 2 \qquad \text{Eq. [7]}$$

2.3.2 Crack-Shielding Mechanisms in Polymers

Crack shielding occurs when the crack driving force near a fatigue crack tip, ΔK_{tip}, is lower than the 'applied' crack driving force, ΔK_a, and this phenomenon is also known as extrinsic toughening (Ritchie and Liu 2021). Extrinsic toughening mechanisms shield the crack tip from the full effect of the applied crack driving force and hence, lower the crack growth rate. While extrinsic toughening mechanisms work behind the crack tip, intrinsic toughening mechanisms take place ahead of the crack tip and occur in the form of dissipative processes, redirecting the additional energy from crack growth to some form of microstructural alteration such as crazing, fibrillation or blunting (Pippan and Hohenwarter 2017). There are several shielding/toughening mechanisms that may be activated in polymers or polymer blends, both intrinsic and extrinsic and these include: (1) crack deflection; (2) particle tearing; (3) bridging by fibers, ligaments, or second-phase particles; (4) massive shear banding; (5) plastic void growth; (6) multiple craze formation or microcracking; (7) zone shielding through phase transformations; or (8) contact shielding from surface asperity contact or plasticity induced closure (Lampman 2003). The extrinsic crack-tip shielding effect has been expressed (Ritchie 1988) as:

$$\Delta K_{tip} = \Delta K_{\boldsymbol{a}} - K_S \qquad \text{Eq. [8]}$$

where K_S is the stress-intensity factor due to shielding. There are three general classes of shielding mechanisms that operate under cyclic loading conditions: crack deflection, zone shielding, and contact shielding. Crack deflection results in improvements in the fatigue crack propagation behavior over all ranges of ΔK. Contact shielding mechanisms are more effective at low ΔK levels, while process-zone shielding mechanisms operate more effectively at high ΔK levels (Ritchie 2000).

The crack-tip shielding process that results in crack path deflection has been previously modelled (Suresh 1998). He derived the effective fatigue crack driving force and subsequent crack growth rates by analyzing a small segment of the crack with an out-of-plane deflection:

$$\Delta K_{tip} = \frac{b \cos^2\left(\frac{\theta}{2}\right) + c}{b + c} \Delta K_a \qquad \text{Eq. [9]}$$

and

$$\frac{da}{dN} = \frac{b \cos\theta + c}{b + c} \left(\frac{da}{dN}\right)_n \qquad \text{Eq. [10]}$$

where θ is the deflection angle, b is the deflected distance, c is the undeflected distance, and $(da/dN)_n$ is the propagation rate of a straight crack subjected to the same effective driving force.

The amount of shielding due to process-zone mechanisms depends on the size of the process zone and micro-mechanisms activated ahead of the crack tip. For polymers, these may include lamellar reorientation, phase transformations, crazing, or shear banding (Evans et al. 1986; Bucknall and Stevens 1978; Hertzberg 1996; Anderson 1995; Argon 1989; Plummer and Kausch 1996; Ansari 2015). The yielding in front of the crack due to far-field tensile loading results in the formation of a plastic or permanent deformation zone. For example, in a crazeable polymer, amorphous chains are reorganized into load-bearing fibrils ahead of the crack tip, that are aligned with principal tensile stress. For this micro-mechanism, a Dugdale or strip yield approximation

(Estevez and Van der Giessen 2005) is used to estimate the size of this plastic zone (Suresh 1998):

$$r_d = \frac{\pi}{8}\left(\frac{K_I}{\sigma_y}\right)^2 \qquad \text{Eq. [11]}$$

For an elastic, perfectly plastic material behavior, the plastic zone, r_p, can be estimated as (Suresh 1998):

$$r_p \approx \frac{\mathbf{1}}{\boldsymbol{\pi}}\left(\frac{K_I}{\sigma_y}\right)^2 \qquad \text{Eq. [12]}$$

In equations [11] and [12] above, $\boldsymbol{\sigma}_y$ depicts the craze stress or yield stress, respectively and K_I is the mode I stress intensity factor. Qualitatively, it is easy to see that the size of the plastic zone increases with ΔK. Therefore, process-zone shielding mechanisms are most effective at high ΔK levels.

Contact shielding involves the physical contact between mating crack surfaces due to the presence of asperities, second-phase particles, and/or fibers. Premature contact between the crack surfaces occurs during unloading at a stress-intensity level known as K_{cl}, which is often referred to as the closure stress intensity. The amount of shielding due to closure effects can be calculated from:

$$\Delta K_{tip} = K_{max} - K_{cl} \qquad \text{Eq. [13]}$$

where K_{max} is the maximum stress intensity of the fatigue cycle (Ritchie 2002). Additionally, fiber bridging has been shown to be a viable shielding mechanism in short fiber composites (Lang et al. 1984).

2.3.3 Toughening Mechanisms in Polymers

Toughening mechanisms are often divided into two categories: those involving the process zone ahead of the crack tip and those which occur behind the crack tip as illustrated in Figure 4. Some polymeric structures such as rubber-toughened polymers can activate both mechanisms to obtain synergistic toughening (Pearson and Pruitt 1999). The process-zone mechanism of toughening is typically described using crack-tip energetics (Kinloch and Guild 1996; Clark et al. 1991; Kramer and Berger 1990; Azimi et al. 1996; Quaresimin et al. 2015).

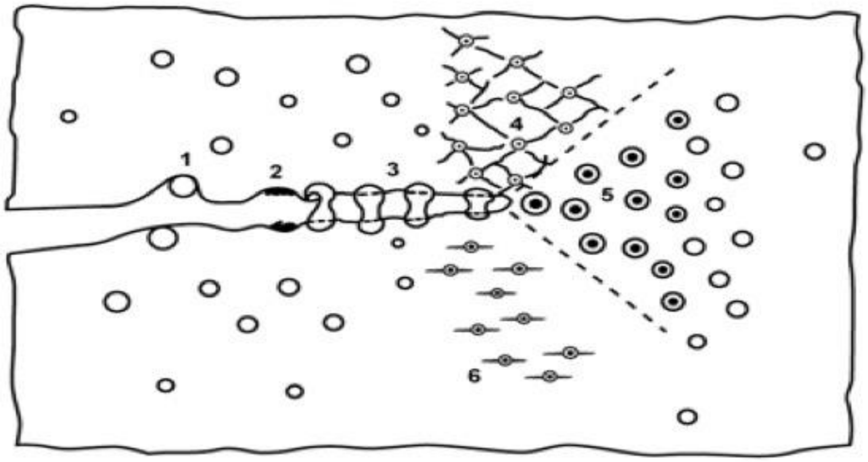

Figure 4 Schematic showing a range of micro-mechanisms that may be activated in polymers or reinforced polymer systems. These include (1) crack deflection; (2) particle tearing; (3) bridging by fibers or second phase particles; (4) massive shear banding; (5) plastic void growth; and (6) multiple craze formation or microcracking (Pearson and Pruitt 1999).

The energy release rate, G, characterizes the release in potential energy with advancement of the crack front. The energy release rate is related to the stress-intensity parameter under linear elastic conditions (plane strain) and can be written as $G = K^2/E$, where E is the elastic modulus and K is the stress intensity factor (Suresh 1988). If one considers a polymeric material that generates a process zone of width equal to $2w$ at its crack tip, then as the crack advances through the material, it leaves a wake behind the crack tip. The change in toughness due to energy changes in the strip is given as (Anderson 1995):

$$\Delta G_c = 2\int_0^w \int_0^{\varepsilon_{ij}} \sigma_{ij}\boldsymbol{\varepsilon}_{ij} dy \qquad \text{Eq. [14]}$$

where the second integral represents the strain energy density. The critical energy release rate for propagation is then equal to the work required to advance the crack from a to $a+da$ (normalized by the new crack area, da (for unit thickness)):

$$G_c = \Delta G_c + G_i = 2\int_0^w \int_0^{\varepsilon_{ij}} \sigma_{ij}\boldsymbol{\varepsilon}_{ij} dy + 2y_e \qquad \text{Eq. [15]}$$

where G_i is the intrinsic toughness and ΔG_c is the energy to generate new crack surfaces under elastic conditions. An analogous form can be developed for non-linear deformations by using the J-integral approach (Evans et al. 1986): $J_C = \Delta J_C + J_i$.

If the reinforcing particles are responsible for all of the energy dissipation, one can assume the strain energy does not depend on y (the normal direction to the crack plane). For f particles per unit volume, one can write the toughness as (Anderson 1995):

$$G_c = 2wf \int_0^{\varepsilon_{ij}} \sigma_{ij} \varepsilon_{ij} dy + 2y_e \qquad \text{Eq. [16]}$$

Particle bridging provides another mechanism of toughening. Here, an advancing crack leaves second phase particles intact behind the crack tip as it advances through the polymeric material. It was shown that rubber particle bridging and tearing could lead to improvements in toughening (Ahmad et al. 1986). Many toughened polymer systems utilize second phase additions capable of non-linear deformation and in such instances non-linear elastic fracture mechanics may be utilized (Evans et al. 1986; Kinloch and Guild 1996).

Many of these toughening mechanisms are activated in rubber-toughened polymers through rubber particle bridging and cavitation as well as matrix plasticity resulting in the nucleation of multiple crazes and shear bands (discussed above). Numerous theories are postulated on the predominance, ordering and synergistic effect of these mechanisms (Argon 1989; Evans 1986; Kinloch and Guild 1996). In summary, extrinsic and intrinsic shielding and toughening mechanisms can be synergistically and efficiently utilized in order to improve fatigue crack propagation resistance in engineering polymers as demonstrated from the aforementioned sub-sections. Together, they shield the crack tip from the driving force trying to open the crack front as well as induce microstructural changes which prevent the crack from propagating further, both behind and in front of the crack tip.

2.4. Factors Affecting Fatigue Performance of Polymers

2.4.1 Molecular Variables

The fatigue behavior of polymers is strongly affected by their molecular structure. Polymers with the same backbone chemistry can still vary immensely in their structure owing to a broad range of molecular variables. These include molecular weight, crystallinity, chain entanglement density, degree of crosslinking, as well as the contributions of fillers or reinforcements (Sauer and Richardson 1980; Hertzberg and Manson 1980; Lang et al. 1984; Kinloch and Guild 1996; Clark et al. 1991; Ansari 2015; Kishi et al. 2021). As a general rule, polymers with higher molecular weights and crystallinity exhibit an increased resistance to fatigue damage. Figure 5 shows a comparison of fatigue crack propagation behavior for several amorphous and semicrystalline polymers. From this figure it can be deduced that semi-crystalline polymers exhibit the greatest resistance to crack propagation.

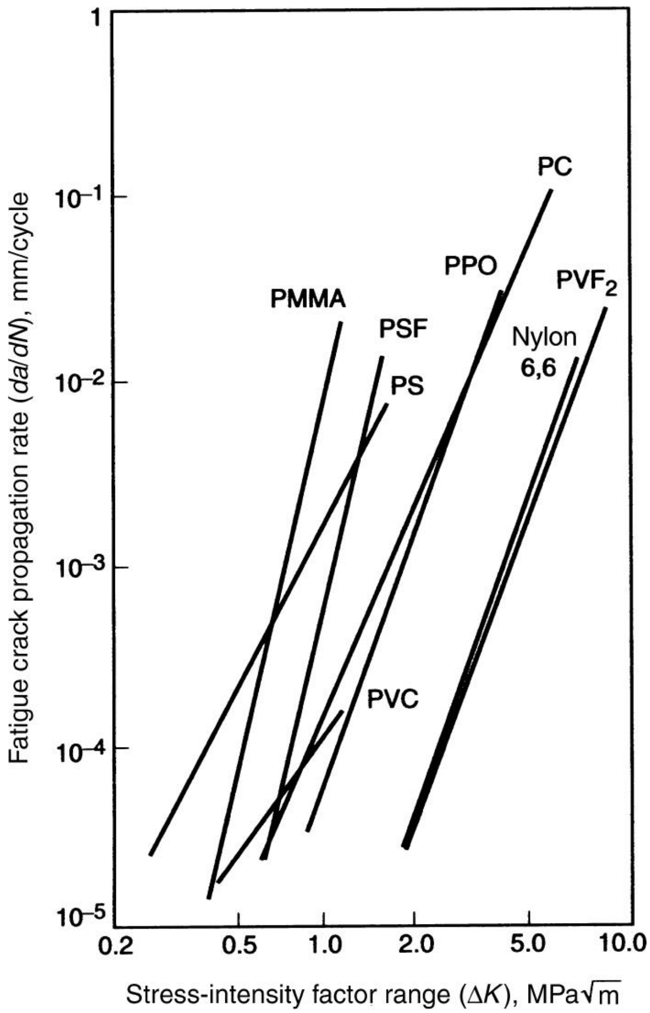

Figure 5 Comparison of fatigue crack propagation behavior in the Paris regime for several amorphous and semi-crystalline polymers. Note the enhanced fatigue resistance of the semicrystalline polymers (Hertzberg and Manson 1980).

The fatigue characteristics of ultra-high molecular weight polyethylene (UHMWPE) across various formulations has been investigated in previous studies (Pruitt et al. 1992; Pruitt 1993; Baker et al. 2003, Atwood et al. 2011; Ansari 2015; Pruitt et al. 2013; Ansari et al. 2016). For UHMWPE resins of equivalent molecular weight, an increase in crystallinity results in a proportional increase in the crack inception stress-intensity values ($\Delta K_{inception}$). Similar trends are observed with molecular weight. Higher molecular weight formulations provide the greatest toughness and resilience to crack growth. However, resistance to fatigue crack growth can be diminished through crosslinking. Figure 6 shows the effect of crosslinking on the fatigue crack propagation resistance of UHMWPE. It is pertinent to note here that increasing the amount of radiation dosage concomitantly increases the amount of crosslinking in UHMWPE. Crosslinking restricts flow of the amorphous chains and lamellar plasticity, resulting in a diminished resistance to crack growth (Baker et al. 2003; Atwood et al. 2011; Pruitt et al. 2013; Ansari et al. 2016).

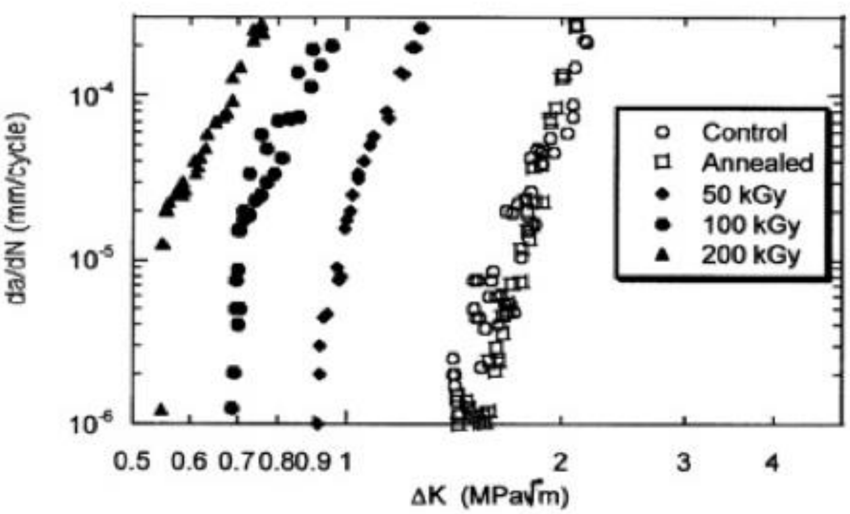

Figure 6 Plot showing the effect of crosslink density on the fatigue crack propagation resistance of UHMWPE. The radiation dose is directly related to the amount of crosslinking present in the UHMWPE microstructure (Baker et al. 2003).

Many amorphous polymers are susceptible to craze nucleation in the presence of hydrostatic stress states (Sauer and Richardson 1980; Kramer and Berger 1990). Under cyclic tension, crazes can lead to subsequent crack growth and fatigue failure. Mechanistically, this occurs after a critical amount of damage has accumulated, advancing the crack advances through rupture of the leading fibrils in the craze zone (Hertzberg and Manson 1980; Argon 1989). This process often occurs through a void growth mechanism that can be exacerbated by temperature, chemical environment, or rupture of the highly stressed fibrils; crazes often advance in an intermittent manner and can results in discontinuous fatigue crack growth (Hertzberg and Manson 1980).

It has been shown that the craze stability depends on numerous factors, including the molecular weight and chain entanglement density of the polymer (Kramer and Berger 1990). The stability or strength of the craze is generally improved by increasing the molecular weight of the polymer. In fact, numerous studies indicate that increasing the molecular weight of the polymer increases craze strength, creep rupture strength, and endurance limit under cyclic loading conditions (Sauer and Richardson 1980; Hertzberg and Manson 1980; Argon 1989; Kramer and Berger 1990; Sánchez-Valencia et al. 2017). It is noteworthy to mention here that while amorphous polymers are more inclined towards crazing (which is a nanometer scale phenomena) under fatigue loads, semi-crystalline polymers tend to exhibit fibrillation (which happens to be more of a sub-micron scale event) as the primary mode of fatigue failure.

As mentioned above, semicrystalline polymers, on the whole, provide improved fatigue resistance over glassy amorphous polymers. One premise is that the composite, two-phase structure, consisting of crystalline and amorphous constituents, offers enhanced toughness. Improved yield strength is provided by the crystalline phase and ductility is provided by the compliant amorphous phase (generally above its glass transition temperature) along with post-yield mechanisms for lamellar plasticity.

2.4.2 The Effect of Reinforcements

The most common reinforcements for polymers include rubber particles, glass spheres, organic fillers, and fibers (continuous and chopped). Fibers have long been used to strengthen polymer resins and many composites offer enhanced mechanical attributes including increased elastic modulus, fatigue resistance, and fracture toughness. Composites provide a milieu of toughening mechanisms through crack bridging, fiber pull-out, kink-banding, and crack-tip shielding processes (Lang et al. 1984; Teoh 2000; Mortazavian and Fatemi 2015).

Organic fillers are often used to enhance tribological characteristics or to enhance thermal properties of the polymer; yet many of these systems benefit from augmented fatigue resistance through crack deflection processes. The presence of rubber particles can initiate a process-zone shielding mechanism involving massive shear banding of the matrix and leading to improved fatigue crack propagation resistance. The role of crack-tip shielding mechanisms on the crack growth rate regime has been modeled previously (Ritchie 1988). According to this model, the occurrence of a process-zone shielding mechanism should change the slope *m* in the Paris regime but should not affect crack growth behavior in near-threshold regimes. Experimental support of this model in polymers has also been given (Azimi et al. 1996) by demonstrating that the fatigue crack propagation characteristics are strongly influenced by the size of the rubber particles as well as the blend morphology.

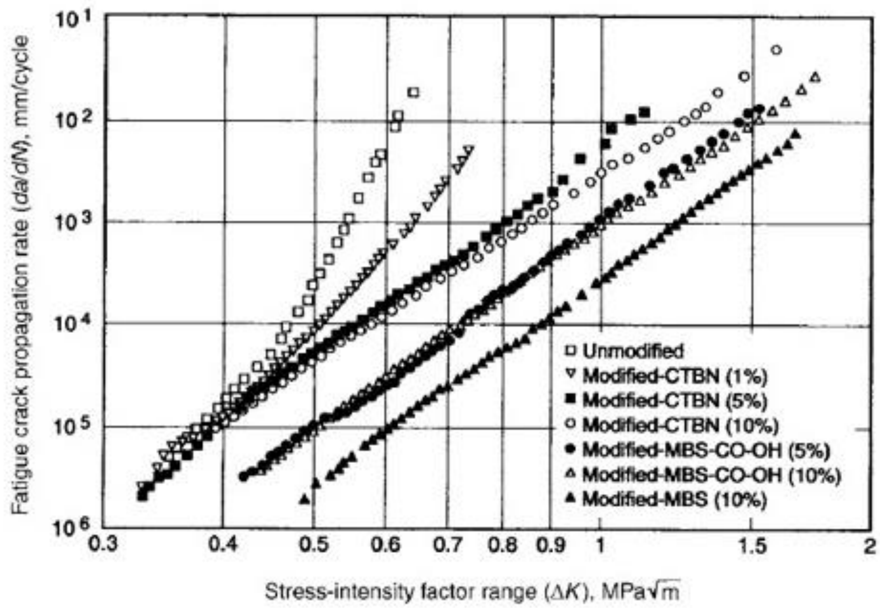

Figure 7 Fatigue crack propagation plot which shows that the addition of rubber decreases the slope, *m*, and retards crack growth at high crack growth rates (Azimi et al. 1996).

Figure 7 reveals that the addition of rubber in epoxy decreases the slope, *m*, and retards crack growth at high crack growth rates, thereby establishing that the modifiers' volume fraction can affect the Paris regime. Nonetheless, the power law remains independent of the particle size and blend morphology for this polymeric system. It is noteworthy that at low values of stress-intensity range, where the process zone in front of the crack tip is small, the crack growth rates for these rubber-toughened epoxies are nearly identical to the neat resin. In this realm, the rubber reinforcements are not highly stressed and crack growth occurs with minimal plasticity. The mechanism changes at higher ΔK levels where the process zone becomes larger than the size of the particles. Within this highly stressed region, particle cavitation causes significant plasticity in the matrix and the crack propagation rate is reduced.

A study has shown that glass-filled, rubber-toughened blends offer improvements to fatigue crack growth resistance in epoxy resins (Azimi et al. 1996). It is believed that the improved fatigue crack propagation resistance is the result of a synergistic interaction between the hollow glass filler at the crack tip and the plasticity triggered by the presence of rubber particles. In the process of cavitation, the creation of new surfaces dissipates energy from the crack tip. This process is thought to relieve the triaxial state of tension existing in the matrix in the vicinity of the rubber particles, leading to a local state of plane stress and an increased plastic zone size (Yang and Liu 2001). Cavitation is not without mechanical penalty to these polymer systems as void formation promotes debonding between the rubber particles and the matrix.

The effect of carbon nanotube (CNT) inclusion on total life fatigue behavior of polyurethane (PU) composites has been studied extensively (Loos et al. 2013). It was found that the incorporation of CNTs increased the fatigue life of PU in the high-stress amplitude (low-cycle regime) by up to 248%. An interesting observation in reinforced polymers is that the second phase addition typically improves resistance to crack propagation; yet these same polymer systems can exhibit a decreased resistance to fatigue crack initiation or flaw inception. The second-phase addition serves as a nucleation site for crazes, voids, or shear bands and these mechanisms dissipate energy away from an advancing crack but serve as flaw initiation sites. An increased resistance to crack propagation but a degraded resistance to crack inception in rubber-modified polystyrene when compared to the unmodified resin has also been noted (Hertzberg and Manson 1980).

Reinforcements such as carbon-fibers are usually beneficial for enhancing the fatigue crack propagation resistance of polymers; yet, it has been found that this principle does not apply universally to all polymers. For instance, owing to poor interfacial adhesion, carbon-fiber reinforced UHMWPE performed poorly under *in-vivo* cyclic loading conditions in comparison to unmodified UHMWPE (Connelly et al. 1984; Wright et al. 1988; Medel et al. 2009). The choice of the reinforcement-matrix couple and interfacial bond strength greatly affect fatigue resistance of polymers. Thus, designers need to have a clear understanding of the component design and loading environment when making their polymer selection.

2.4.3 Viscoelastic Effects

Most polymers are viscoelastic, and a portion of their strain energy is dissipated under cyclic loading conditions in the form of heat generation. A consequence of hysteretic heating is that the specimen temperature increases until the heat generated per cycle is equal to the heat dissipated through mechanisms of conduction, convection, and radiation. The amount of temperature elevation depends strongly on the frequency of the test, the amplitude of the applied stress or strain, and the damping properties of the polymer. This is especially predominant in unnotched specimens, where the temperature of the polymer specimen can locally surpass the glass transition or the flow temperature of the polymer. The energy dissipated per second, $\dot{E}$, is given as (Ferry, 1961):

$$\dot{E} = \pi \nu J''(\nu, T, \sigma) \sigma^2 \qquad \text{Eq. [17]}$$

where $\boldsymbol{\nu}$ is the frequency, J'' is the loss compliance, and $\boldsymbol{\sigma}$ is the peak stress of the fatigue cycle. The rate of change of temperature for adiabatic heating conditions in which the heat generated is transferred into temperature rise is given as:

$$dT/dt = \dot{E} / \rho\, c_p \qquad \text{Eq. [18]}$$

where ρ is the mass density and c_p is the heat capacity of the polymer. As a general rule, the increase in temperature is proportional to the increase in frequency, stress amplitude, and internal friction of the polymer (Movahedi-Rad et al. 2019). In many polymer systems, the thermal work brought about by high damping and low thermal conductivity contributes to micro-mechanisms of permanent deformation, including craze formation, shear bands, voids, or even microcracks. The temperature rise in the specimen can be monitored with a thermocouple or an infrared sensor and many researchers limit test frequency or impose external cooling mechanisms to limit thermally driven fatigue mechanisms.

Under cyclic loading conditions, dissipative losses in viscoelastic polymers appear as hysteresis loops and provide useful insight into the micro-mechanisms of fatigue damage. Figure 8 shows the hysteresis loops after various numbers of fatigue cycles in both high-impact polystyrene (HIPS) and acrylonitrile butadiene styrene (ABS). A distinction can be made between the two polymer systems, owing to differences between micro-mechanisms of deformation. In the ABS polymer blend, the hysteresis loops are symmetrical through the compression–tension cycle, while in HIPS, the hysteresis loops become much larger for the tensile portion of the fatigue cycle as the fatigue test progresses. These events are rationalized by the fact that ABS undergoes shear-yielding mechanisms, while the HIPS undergoes crazing, which requires a tensile component of stress. Crazing results from the fibrillation or polymeric drawing ahead of the fatigue flaw. The advancement of the craze zone is associated with damage accumulation in the leading fibrils and thus, the tensile portion of the hysteresis loop grows as damage accumulates in the specimen.

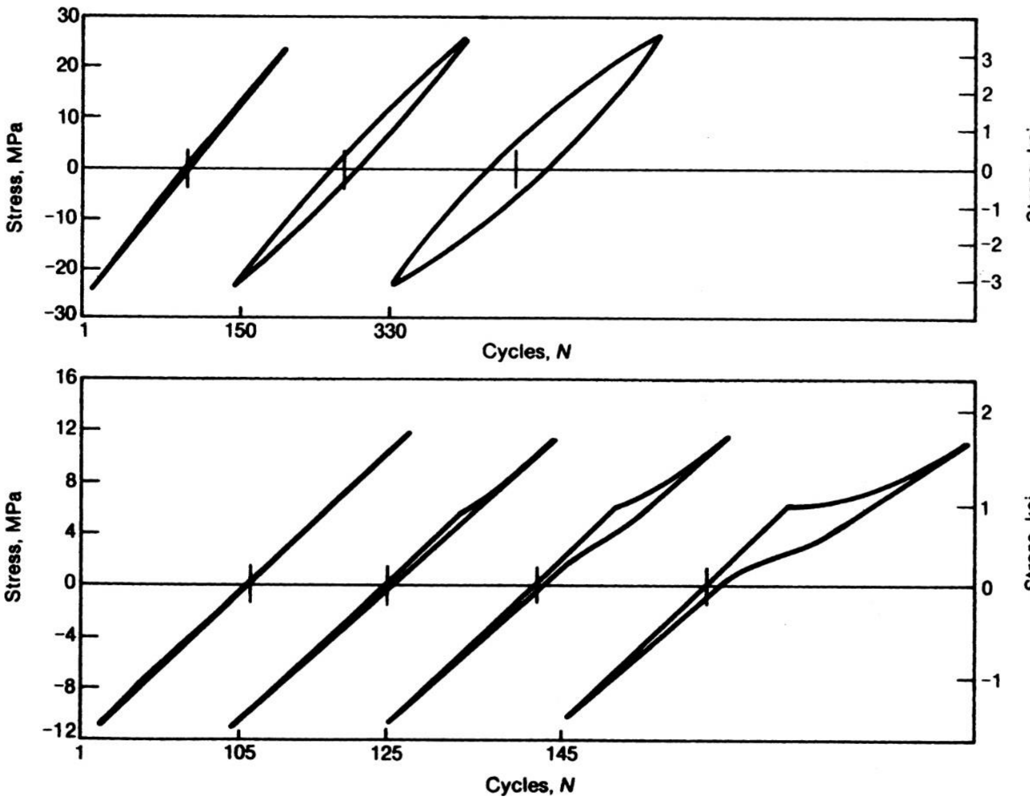

Figure 8 Hysteresis loops after various numbers of fatigue cycles in both high impact polystyrene (HIPS) (bottom) and acrylonitrile butadiene styrene (ABS) (top). Note the lack of symmetry in the HIPS due to crazing mechanisms (Hertzberg and Manson 1980).

2.4.4 Mean Stress Effects

The fatigue response of a polymeric material is highly sensitive to the mean stress of the fatigue cycle. An interesting finding for engineering polymers is that, depending on the structure of the polymer and the micro-mechanisms of deformation, there are two distinct responses to an increase in mean stress. For a nominal stress-intensity range, certain classes of polymers exhibit an increase in crack propagation rate, while others show a decrease in crack growth rate. The published research on the effects of mean stress and R-ratio covers a broad range of polymer classes, including amorphous, semicrystalline, crosslinked, and rubber-modified polymers (Pruitt et al. 1992; Pruitt 1993; Pruitt and Suresh 1994; Pruitt and Rondinone 1996; Mukherjee and Burns 1971; Zhou and Brown 1992; Arad et al. 1971; Moskala 1991; Argon and Cohen 1990; Manson et al. 1981; Takemori 1982; Mills and Walker 1976; Scholz et al. 2018; Amjadi and Fatemi 2020; Klimkeit et al. 2011; Zheng et al. 2019). Table 1 provides a summary of the effect of mean stress for several polymers.

Table 1 Effect of increasing mean stress on polymer fatigue behavior.

Increasing crack propagation rate with increasing mean stress
High-density polyethylene
Nylon
High-molecular-weight PMMA
Polystyrene
Epoxy
Polyethylene copolymer
UHMWPE
Decreasing crack propagation rate with increasing mean stress
Low-density polyethylene
Polyvinyl chloride
Low-molecular-weight PMMA
Rubber-toughened PMMA
High-impact polystyrene
Acrylonitrile-butadiene-styrene
Polycarbonate
Toughened Polycarbonate Polyester

The fatigue crack growth rates could be scaled to the stress-intensity factor with the following relationship (Arad et al. 1971):

$$da / dN = \beta \lambda^{n} = \beta (Kmax^{2} - Kmin^{2})^{n} \qquad \text{Eq. [19]}$$

where β depends on the loading environment, frequency, and material properties, n is a material constant, and $\boldsymbol{\lambda}$ is a parameter dependent on K_{mean} and ΔK. A micro-mechanistic explanation for this response to an increase in stress ratio or mean stress is also possible. Polymers that become more prone to fracture with increasing mean stress are most likely to be affected by the monotonic fracture process associated with the maximum portion of the loading cycle as it approaches a critical stress-intensity level. In general, these polymers are susceptible to crazing, chain scission, or crosslink rupture. For these polymer types, an increase in mean stress results in faster crack propagation rates as seen in polymers such as HDPE, Nylon, epoxies and PS.

Several polymers offer improved resistance to crack propagation as the mean stress is increased, for instance, such phenomenon is observed in LDPE, PVC, HIPS, ABS, PC, and toughened PC. Many of these polymeric systems also demonstrate a marked improvement of fracture toughness with increasing mean stress (Hertzberg and Manson 1980). They postulated that the strain energy normally available for crack extension is consumed through deformation or structural reorganization ahead of the crack tip. The use of strain energetics to describe fracture processes in polymers is formulated as (Andrews 1969; Manson et al. 1981):

$$T = T_o\, [\, C / (C - f(\Psi))]\qquad \text{Eq. [20]}$$

where T is the total energy used by the polymer to create a new unit area of surface through crack advance, T_0 represents the elastic strain energy, C is a material constant that depends on the strain state of the polymer, and Ψ is the hysteresis ratio. Here, Ψ captures the energy lost due to inelastic energy expenditure. If the energy loss is large, the amount of energy needed to cause fracture increases. Thus, the crack growth rate is reduced with increasing Ψ. Moreover, the effect of mean stress on the fatigue crack propagation resistance of the polymer is directly linked to the parameter Ψ. Hence, polymers with a molecular structure susceptible to hysteretic losses, or capable of structural reorganization, are likely to be more resistant to fatigue crack propagation as the mean stress is increased. These polymers have near-tip processes that dissipate elastic energy ahead of the crack tip.

2.4.5 Variable Amplitude Effects

The effect of variations in the load cycle can have a profound effect on polymeric materials (Mars and Fatemi 2004; Teoh 2000). Understanding the variable amplitude behavior is also important for the design of polymeric components where stresses are expected to vary throughout the life of the device. Additionally, this is a concern for components that are likely to experience tensile or compressive overloads, and such effects are quite prevalent in the sporting and orthopedics applications of polymers. It is common to model the effect of variable amplitude loading using a cumulative damage approach, whereby the Palmgren-Miner's rule (Miner 1945; Palmgren 1924) is employed to predict the life of the device. The incremental damage d_i accrued owing to a certain stress amplitude $\boldsymbol{\sigma}_i$ is formulated as

$$d_i = N_i / N_{fi} \qquad \text{Eq. [21]}$$

where N_i is the number of cycles experienced with stress amplitude $\boldsymbol{\sigma}_\mathrm{i}$ and N_{fi} is the number of cycles to failure if only $\boldsymbol{\sigma}_\mathrm{i}$ was applied from start till end when the sample finally fails due to fatigue. Hereafter, the total damage D can be ascertained by summing all these individual incremental damages as formulated below-

$$D = \Sigma\, d_i = \Sigma\, N_i / N_{fi} \qquad \text{Eq. [22]}$$

It should be noted here that the total damage D a material can sustain until fatigue failure is always 1.0.

Nevertheless, the aforementioned approach predicated on damage accumulation cannot capture the subtle effects of the nature (compressive or tensile) or position of the overload in the loading sequence, and its subsequent effect on a propagating crack. For example, it is well known that the application of a single tensile overload can extend the life of a cracked component by retarding the rate of crack advance (Suresh 1998). This transitory behavior is often dictated by several mechanisms including crack closure (Elber 1970), residual compressive stresses (Suresh 1983; Pruitt and Suresh 1993), and crack tip blunting (Rice 1967). Crack closure justifies the retardation of crack velocity in terms of residual compressive stresses left in the plastically deformed wake of the advancing crack. This results in premature contact between the crack faces while the specimen is still in the tensile portion of the fatigue cycle. Crack closure effectively reduces the stress-intensity range driving the crack advance. This mechanism has been initially proposed to describe crack retardation in PMMA (Pitoniak et al. 1974) and PC (Murakami et al. 1987). Blunting has been proposed by others to describe the reduced crack velocity following tensile overloads (Banasiak et al. 1977). Although crack-tip blunting can affect the crack velocity subsequent to the overload, it does not provide a basis for the prolonged regime of crack retardation. The zone of residual compressive stresses sustained at the crack tip upon unloading in amorphous polymers increases in size and magnitude as the far-field tensile load increases (Pruitt and Suresh 1994). These residual compressive stresses sustained at the crack tip are believed to decrease the crack propagation rate following the tensile overload. The crack has to then grow through this zone of enhanced residual compression before it can return to its initial crack propagation rate for the ΔK sustained prior to overload. Many current life-prediction models are formulated based on residual compressive stresses for the rationalization of crack retardation effects.

2.4.6 Waveform and Frequency Effects

Many polymers, due to their viscoelastic nature, are highly sensitive to the waveform or frequency of cyclic loading (Eftekhari and Fatemi 2016; Mars and Fatemi 2004). For instance, some crazeable polymers such as PS, PMMA, and HIPS exhibit decreased crack propagation as the test frequency is increased, while materials such as PC, nylon, and polysulfone exhibit no sensitivity (Hertzberg and Manson 1980). In such polymers, the increased test frequency can diminish chain disentanglement effects at the crack tip, resulting in a reduction in the rate of crack advance.

Crack propagation in a polymer could be described as the sum of the elastic and viscoelastic contributions (Wnuk 1974):

$$da/_{dN} = C_1 \left(\Delta K/_{K_{IC}}\right)^{n_1} + C_2 \left(\Delta K/_{K_{IC}}\right)^{n_2} \left(\frac{1}{\nu}\right) \qquad \text{Eq. [23]}$$

where the first term is the elastic contribution, and the second term is the time-dependent contribution (viscoelastic component) and includes a creep compliance term, C_2, and the test frequency, $\boldsymbol{\nu}$.

The strain rate can also play a critical role in the fatigue response of time-dependent polymers. Strong sensitivity to the waveform parameter was found in several polymers such as PVC, PS, PMMA, and vinyl urethane (VUR) (Hertzberg et al. 1975). For instance, the square wave provides a high strain rate in ramp up and then subjects the specimen to a longer period of peak load than a triangular waveform with the same stress amplitude. The difference in load function can cause major differences in fatigue crack propagation (FCP) behavior. For example, the fatigue crack propagation rate in VUR is reduced by nearly an order of magnitude when changing from a triangular to a square wave loading function (Harris and Ward 1973). This behavior is attributed to the higher strain rate that dominates in the case of very flexible polymers, such as VUR. Another important factor is the amount of creep sustained in the peak loading portion of the fatigue cycle.

Consequently, polymers that are susceptible to creep damage will generally perform poorly when tested under the square waveform loading due to creep at peak load (Harris and Ward 1973).

2.4.7 Environmental Factors

Environmental factors play a critical role in the fatigue performance of engineering polymers (Teoh 2000; Scholz et al. 2018). Such factors can include ambient temperature, chemical environment, exposure to ionizing radiation, oxidative embrittlement, or stress cracking. The ambient temperature relative to the glass transition temperature (T_g) is important for predicting how the polymer is going to behave. At temperatures above T_g, many polymers will be susceptible to viscous effects. Well below T_g, the polymers will behave in a glassy manner. The chemical environment surrounding the polymer is also of paramount importance. Many ester-based polymers undergo scission in aqueous environments, while others are affected by the environmental pH. Some amorphous polymers are known to be susceptible to chemically induced crazing (Hertzberg and Manson 1980). In such cases, the crack inception values can be substantially reduced in the presence of aggressive media (Hertzberg and Manson 1980). For example, PC is known to nucleate surface crazes in the presence of acetone vapor. Many rubbers are susceptible to oxidation-induced embrittlement (Kurtz et al. 1994). Many medical polymers, such as orthopedic grade UHMWPE or bone cement (PMMA), degrade due to oxidation embrittlement and chain scission. These degradative mechanisms are induced by ionizing modes of sterilization and subsequent aging (Dawes and Glover 1996; Kurtz et al. 1994; Connelly et al. 1984; Wright et al. 1992; Goldman and Pruitt 1998; Goldman et al. 1998; Rimnac et al. 1988). In order to accurately predict the fatigue behavior of polymers, fatigue tests must closely mimic not only the stress variations but also the chemical and aging environments that are most likely to be encountered in the device's lifetime.

A compilation of several key studies which investigated the fatigue characteristics of different polymers and polymer composites has been presented in Table 2.

Table 2 Novel polymer fatigue studies (2009–2016)

Researcher	**Key research takeaways**
Krause 2016	Characterized epoxy resin system Araldite LY564/Aradur22962 and proposed a novel physically based fatigue failure criterion for polymers under multiaxial loading.
Kanters et al. 2015	Compared and contrasted the compliance method with that of optical tracking method of fatigue crack propagation in polymers and it was reported that the nonlinear and viscoelastic behavior of polymer proves to cause a strong loading condition and time dependency of calibration curve and as a result no unique relation could be found for crack length as a function of dynamic compliance.
Garcea et al. 2015	Studied the fatigue behavior of toughened and untoughened matrices. It was found that for the toughened systems, damage does not propagate evenly and in contrast untoughened material is characterized by more uniform crack progression.

Garcea et al. 2014	Evaluated fatigue damage micro-mechanisms in [90/0]s carbon fiber reinforced epoxy double-edge notched specimens using in situ synchrotron radiation computed tomography and the damage was found to be quantified in terms of crack opening and shear displacements.
Klimkeit et al. 2011	Conducted an experimental evaluation of the multiaxial fatigue behavior of PBT–PET GF30 (polybutylene terephthalate–polyethylene terephthalate with 30% mass short glass fibers) and PA66 GF35 (Polyamide 66 with 35% mass short glass fibers) under constant amplitude force loading and analyzed the experimental results using a through process modeling.
Berrehili et al. 2010	Explored the multiaxial fatigue behavior of polypropylene pipes under tension and fatigue loadings. A multiaxial fatigue criterion was proposed and it depicted that the fatigue behavior of semi-crystalline polymer seems to be governed by the von Mises maximum stress.
Charles et al. 2010	Investigated the Rolling Contact Fatigue (RCF) behavior of polyamide 6 nanocomposites. RCF behavior at different normal loads (P) (150, 175, 200, and 225 N) and rolling speeds (V) (1000, 1500, and 2000 rpm) was investigated to understand the pressure–velocity (PV) parameter effects. It was found that the RCF life of PA 6 organo-clay reinforced nanocomposite is the function of rolling speed and applied load.
Tao and Xia 2009	Probed the biaxial fatigue behavior of an epoxy polymer under cyclic shear and proportional axial-shear combined loadings with mean strains and multiaxial fatigue life prediction models were established upon stress-, strain-, and energy-based approaches with consideration of mean stress/strain effect, where better agreement was achieved in stress-based and energy-based approaches.
Zenkert and Burman 2009	Carried out quasi static tests in tension, compression, and shear on a closed cell foam of poly-metacrylimide (Rohacell) with three different densities. It was found that the fatigue life for different load types exhibit different failure mechanisms.

2.5 Concluding Remarks

The fatigue performance of engineering systems that incorporate polymeric constituents is quite complex. Many theoretical models exist which can be utilized for attaining a reasonable estimate of the fatigue life without conducting prolonged experiments. These include the total-life and the defect-tolerant philosophes. The total-life philosophy is generally employed to predict the fatigue life of a polymeric component that is likely to be free of significant defects or stress concentrations and that is expected to spend the majority of its lifetime in the initiation stage of crack growth. In contrast, the fracture mechanics approach adopted in the defect-tolerant philosophy is used for fatigue prediction of polymeric structural components that have initial flaws or significant stress concentrations and which are likely to sustain a large degree of stable crack growth prior to fracture. However, these models have a lot of underlying assumptions which might not necessarily hold true during the entire service life of an actual polymeric component. For instance, the fatigue characteristics of polymers are affected by not only mechanical variables but also microstructural attributes, as well as the intricacies of the fatigue test. For safe design of polymeric devices, it is imperative that appropriate test conditions are used that best mimic the service conditions of the component under investigation. Parameters like frequency, strain rate, waveform, temperature, and environment can impact fatigue behavior. Similarly, tests should utilize specimens with a structural composition that replicates the polymeric component as molecular factors such as molecular weight, crystallinity, and crosslinking strongly influence fatigue micro-mechanisms. This chapter compiles the relevant literature, encompassing both the classical studies as well as the relatively new findings pertaining to the fatigue of polymers and is intended to assist researchers, designers, and technical professionals by acting as a centralized repository on polymer fatigue behavior.

Chapter 3 – Bio-tribo-mechanical properties of PEEK and CFR-PEEK for use in total joint replacements

This chapter has been published in the Journal of the Mechanical Behavior of Biomedical Materials (Arevalo et al. 2023).

3.1 Introduction

With an increase in life expectancy, patients demand orthopedic devices implanted into the body through total joint arthroplasty (TJA) surgeries, to last several decades in the body to minimize the number of revision surgeries over the patient's lifetime (Kurtz et al. 2009; Kremers et al. 2015). While a ten-year implant lifetime was the standard at the inception of these devices (Kurtz et al. 2005), patients are now expecting more mobility and more cycles on their joints as the age demographics of patients is trending towards younger populations (Kurtz et al. 2009). This puts the implant at risk for premature failure since the original designs and selection of materials were for sedentary populations, but for the past few decades these implants have catered to a more active population.

In total joint replacement (TJR) surgery, a damaged joint is removed and replaced with a metal, plastic, or ceramic device. However, TJA designs can have the following material couplings: metal-on-metal (MacDonald 2004), metal-on-ceramic (Bal et al. 2006), metal-on-polymer, ceramic-on-polymer (Bal et al. 2006), and ceramic-on-ceramic (Clarke 1992). Additionally, the fixation stem is usually composed of titanium or cobalt-chrome. While these materials are commonly found in TJA, they are far from being the perfect material. For instance, the go-to polymeric material is Ultra High Molecular Weight Polyethylene (UHMWPE), but it is challenged by wear, oxidation, and fatigue failures in the body (Ansari et al. 2016; Kurtz 2009). Moreover, the metallic load bearing components are prone to stress shielding, resulting in bone resorption from the modulus mismatch between the surrounding bone and implant. Alongside, there is an ongoing concern of metal particles inside the body due to wear, corrosion, or fatigue failure of components as well as metal ion release culminating in metallosis (Kerner et al. 1999; Archibeck et al. 2000; Willis-Owen et al. 2011).

Therefore, materials such as carbon fiber reinforced (CFR) Poly-ether-ether-ketone (PEEK) have been proposed to replace the articulating and the load bearing portion of the device (Kurtz and Devine 2007). PEEK is a polymer widely used in medical applications due to its biocompatibility and chemical stability, high toughness, fatigue resistance, and ability to tailor its mechanical properties to match those of bone (Kurtz 2012b). There are several ways for designers to tailor the mechanical properties such as: thermal treatments (e.g. annealing) and adding a filler material (e.g. carbon fibers, β-tricalcium phosphate, titanium (Ti), calcium silicate (CS), hydroxy-apetite (HA), strontium containing hydroxyapatite, and nano-fluorohydroxyapetite (nano-FHA)) (Regis et al. 2017; Monich et al. 2016). Only certain fillers are appropriate for load-bearing orthopedic applications (Abdullah et al. 2015). In this chapter, the main focus will be on PEEK and PEEK reinforced with pitch-based and PAN-based carbon fibers for use in load bearing and articulating surfaces of TJRs. Unless otherwise specified, the aforementioned will be referred to as PEEK and PEEK composites in this chapter.

There are notable advantages to using CFR-PEEK over UHMWPE and metal-based biomaterials in TJRs, for instance, PEEK is able to maintain its mechanical properties during commonly employed sterilization processes such as gamma, steam autoclave, vaporized hydrogen peroxide, and ethylene oxide up to a certain number of cycles (Solavy 2017; Kumar et al. 2018). Furthermore, using CFR-PEEK as a load bearing material to replace metallic components, may reduce stress shielding and bone resorption since the modulus will be a closer match to bone (de Ruiter et al. 2021), while also addressing long- term concerns of metals in the body. Using PEEK can mitigate allergic reactions in those patients with metal sensitivity (Thyssen et al. 2009). Lastly, the radiolucency of CFR-PEEK may enable in vivo imaging and monitoring of devices (Kurtz and Devine 2007). It is noteworthy to mention here that PEEK composites behave differently from their cross-linked counterparts. Thermoset systems may abrade but offer limited plastic deformation. Bio-active glass fiber-reinforced thermosets have been successfully employed in cranial implants (Aitasalo et al. 2014; Posti et al. 2016; Piitulainen et al. 2015). These thermosetting systems offer improved stiffness and osseointegration but have not been utilized in orthopedic bearing systems owing to their greater propensity for higher contact stresses and fractures. PEEK resins offer tailorable plasticity though the overall mechanical properties are linked to crystalline domain size, annealing conditions, and the degree of adhesion with reinforcing fibers (Bonnheim et al. 2019; Regis et al. 2018). It also comes with the caveat that there are still ongoing concerns surrounding carbon fiber debris from CFR-PEEK (Stratton-Powell et al. 2016), which warrants more research in this domain.

PEEK and PEEK composites have mechanical properties that can become an alternative material in TJRs. However, stringent assessment of the mechanical, biological, and tribological properties is needed to ensure its efficacy and suitability to serve in articulating and load bearing applications. Therefore, this chapter collects and critically assesses the existing research on mechanical, tribological, and biocompatibility research of PEEK composites to verify the validity of using these materials as articulating or load bearing applications and aims to bring PEEK and PEEK composites to the forefront of orthopedic bearing devices. The existing literature reviews in this domain have been summarized in Table 3. This chapter undertakes a deep dive into the biological and tribo-mechanical characteristics of PEEK and PEEK composites and in the process, generating a centralized resource to aid researchers, medical device engineers, and designers, who can then make informed decisions on orthopedic device-related matters. This chapter is exclusively devoted towards the compilation and in-depth analysis of the bio-tribo-mechanical property landscape of PEEK and CFR-PEEK, as a means to evaluate their feasibility in TJRs.

Table 3 Table highlighting the relevant review articles discussing Poly-ether-ether-ketone (PEEK) for use in medical applications.

Researcher	Aim of literature review
Li et al. 2015	Assesses the performance of carbon fiber reinforced-PEEK, specifically as an implant material for arthroplasty systems.
Abdullah et al. 2015	The review discusses the biomechanical and bioactivity challenges for utilizing PEEK and PEEK composites in orthopedic implants.
Monich et al. 2016	Reviews the mechanical and biological behavior of PEEK composites for biomedical applications.
Lvhua et al. 2017	Reviews the research progress and status in the aspects of preparation, mechanical properties, and biological performance of these PEEK matrix with bio-active ceramics for hard tissue implant, and predicts its future development.
Liao et al. 2020	Reviews recent advances in the development, preparation, biocompatibility, and mechanical properties of PEEK and its composites for hard and soft tissue engineering.
Verma et al. 2021	Documents the development of PEEK as a biomaterial and highlights the major advancement and breakthroughs.
Ma et al. 2021	Reviews research progress of performance requirements, material development, and material surface modification of PEEK as an orthopedic implant and discusses future advancement of medical PEEK materials.

3.2 PEEK and PEEK composites overview

PEEK is a dominant member of the polyaryletherketones (PAEK) family, which was introduced in the 1980s for use in trauma, orthopedic, and spinal implants (Kurtz and Devine 2007). Prior to that, PEEK was already commercially used in aircraft and turbine blades (Kurtz and Devine 2007). The arrival of PEEK coincided with the development of isoelastic hip stems and fracture fixation plates with stiffness comparable to bone (Kurtz and Devine 2007). By the 1990s, PEEK emerged as the leading thermoplastic candidate for replacing metal implants, with an emphasis in orthopedics and trauma application. Shortly after, in 1998, PEEK was commercially offered as a biomaterial for implants (Kurtz and Devine 2007). The wide range of applications PEEK has to offer is a testament to the microstructure of PEEK, enabling desirable mechanical behavior, manufacturability, resistance to chemical and radiation damage, and biocompatibility (Blundell and Osborn 1983).

3.2.1 Material overview - structure and morphology

PEEK is a semicrystalline polymer, whose chemical structure consists of an aromatic molecular backbone, along with combinations of ketone and ether functional groups between the aromatic rings (Blundell and Osborn 1983) as shown in Figure 9 (a). The large aromatic units inhibit chain mobility, thereby requiring large amounts of thermal energy for chain motion (Kumar et al. 1986). Thus, PEEK has a high glass transition temperature of 143˚C, a high melting temperature (343˚C) and is stable at room and body temperature (Bonnheim et al. 2019).

Through this distinct chemical structure, PEEK exhibits stable chemical and physical properties: chemical as well as wear resistance and stability at high temperatures, resistance to structural degradation resulting from sterilization. The mechanical properties of PEEK depend on the crystalline structure, chemical architecture, and morphology (Kurtz 2012a). PEEK has a phase separated microstructure consisting of an amorphous and a crystalline phase (Kumar et al. 1986). The crystallinity content of PEEK can be controlled through thermal processes. Depending on the processing conditions, it can be up to 43% crystalline, but 30%–35% crystallinity is more common in medical devices (Kurtz 2012a; Blundell and Osborn 1983; Reitman et al. 2012). The crystalline domains are generally lamellar in structure and organize into spherulites (Kumar et al. 1986). Techniques to enhance crystallinity are usually done by slow cooling from the molten state and annealing. Fillers, such as carbon fibers, affect the morphology by altering the geometry of crystalline domains of the PEEK matrix (Reitman et al. 2012). Figure 9 (b) illustrates the microstructure of PEEK reinforced with carbon fiber, imaged by scanning electron microscopy (SEM).

The fiber type in CFR-PEEK has an impact on the elastic modulus (pitch-based ~12.5 GPa and PAN-based ~18.5 GPa) and on ultimate tensile strength (pitch-based ~145 MPa and PAN-based ~192 MPa) for equivalent weight percent of fiber (Bonnheim et al. 2019). These can be adjusted by changing the weight percent of fiber, among other things. Additionally, PAN-based PEEK composites show better wear and friction properties than pitch-based at high pressures and low speeds (1 m/s) in a pin-on-disc wear experiment (Flöck et al. 1999). A schematic evincing the differences between the microstructures of the two different types of CFR-PEEK composites (i.e. pitch- vs. PAN-based) has been sketched in Figure 9 (c).

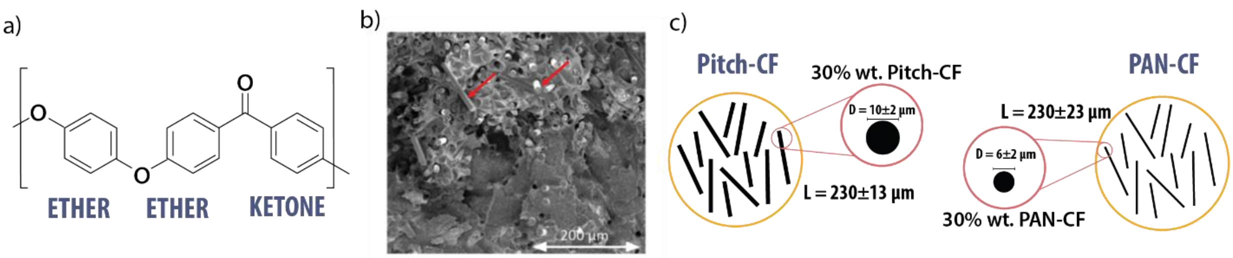

Figure 9 (a) Chemical structure of PEEK molecule. (b) SEM image of a fractured surface of a CFR-PEEK composite (Arevalo and Pruitt 2020). The white colored fibers are carbon fiber reinforcements, marked by the red arrows in the diagram. (c) A schematic demonstrating the differences between pitch-based and PAN-based CFR-PEEK microstructures.

3.2.2 Applications

The majority of current applications of PEEK within medical treatments are for orthopedic trauma internal fixation devices (Ma et al. 2021). The first medical use of PEEK, and now widely accepted, was for use as spinal implants (Kurtz and Devine 2007; Kurtz 2012b). CFR-PEEK has also been used as fracture fixation plates with promising results (Kurtz and Devine 2007; Rotini et al. 2015; Schliemann et al. 2015). CFR-PEEK has the potential to eliminate stress shielding in applications such as femoral stems but is still undergoing research (Bonnheim et al. 2019). PEEK is also starting to be adopted in dental medicine and is a growing field of research (Rahmitasari et al. 2017; Schwitalla et al. 2015; Schwitalla and Müller 2013). For example, PEEK composites are undergoing further study for use in implant abutments and implant body (Rahmitasari et al. 2017).

3.3 Tribo-mechanical properties

Carbon fiber type, volume fraction, and thermal history inform the mechanical and tribological properties of PEEK and PEEK composites. Literature in this section demonstrates how wide-ranging testing methodologies and a lack of standardization lead to conflicting results. The literature highlights the need for tailoring testing conditions towards the specific type of joint being studied, i.e., knee, shoulder, or hip. The conformity differences and similarities are highlighted in Figure 10. Most notable are the differences in rotational and translational motion between joint types. In general, the design requirements of a material used in a specific orthopedic application vary depending on the location. This is because there is significant variation in the loading pattern experienced in each joint space. Regardless of the location however, a good candidate material for orthopedic joint replacement must meet certain basic requirements such as biocompatibility, wear resistance, low friction, and high impact toughness. This section will delve into the mechanical properties (monotonic, fatigue, nanoindentation) and tribological properties (wear) of PEEK and PEEK composites.

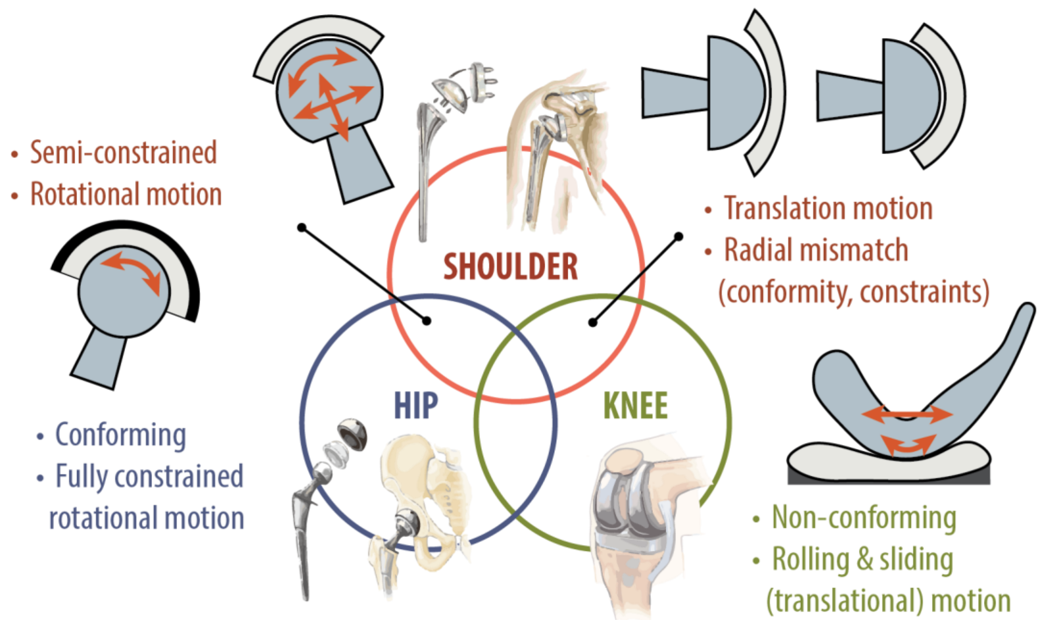

Figure 10 The stresses and conformity variations across TJRs; and the biomechanical differences and similarities between the shoulder, hip, and knee joints. Hip joints are the most constrained while the knee is the least constrained. Knee and shoulder display translational motion and a radial mismatch. Shoulder and hip display rotational motion. The knee joint is the least conforming joint and thus displays a sliding motion.

3.3.1 Mechanical properties

This section focuses on the mechanical properties of interest for TJR applications, and the results obtained by numerous researchers, using different testing methodologies (Dworak et al. 2017; Bonnheim et al. 2019; Kim et al. 2013; Arevalo and Pruitt 2020; Regis et al. 2017; Qin et al. 2019). A summary of the experiments performed in these studies is detailed in Table 4. For instance, the dynamic performance of layered PEEK composites has been reported (Dworak et al. 2017) and no signs of degradation induced by the simulated body fluid were found, suggesting that this was potentially due to the cyclic load frequency used (50 Hz and 1 Hz). Furthermore, the dynamic test to failure conducted in bending and compression modes did not show a significant difference in the material's performance, with the exception of the case where all fibers are aligned, which decreased the mechanical strength after 106 fatigue cycles by about 10%. However, for all the composites tested under dry ambient conditions, the bending strength ranged from 416.8 to 780.6 MPa, with the upper value being similar to that of the titanium-based alloys used in TJR. Flexural and compression modulus (both ranged from 19 to 38 GPa) are similar to that of cortical bone, making these composites an ideal candidate for structural implants in orthopedic applications.

Table 4 Summary of mechanical experiments.

Material	Type of test	Conditions	Reference
Layered PEEK composites (CF) (cross ply 0/90, +/−45, multidirectional and 1D fibers)	Static (3-point- bending, axial compression) and 10^6 cycles under cyclic flexural or compression loads	Dry and simulated body-fluid (pH 6.5, 37˚C)	Dworak et al. 2017
PEEK (unfilled) and PEEK composites (PAN and Pitch)	Monotonic and cyclic loading	Ambient	Bonnheim et al. 2019
PAN PEEK with different CF-orientations and thermal pre-treatments vs CFR/Epoxy	Tension, compression, and short beam	Ambient	Kim et al. 2013
PEEK and composites (thermally pretreated and untreated)	Nanoindentation	Ambient	Arevalo and Pruitt 2020

The elastic properties and fatigue crack propagation (FCP) behavior of PEEK and PEEK composites has been investigated (Bonnheim et al. 2019). In addition, the effect of annealing on the FCP behavior has been looked into. Their experimental results demonstrated the superiority of PAN-based PEEK over pitch-based PEEK in terms of the monotonic elastic modulus and the ultimate tensile strength (UTS) as shown in Figure 11. In terms of FCP, PAN-CFR-PEEK exhibited a higher resistance compared to the unfilled and pitch-based PEEK composite as illustrated in Figure 12. Moreover, the annealed versions of PAN-CFR-PEEK showed further improvements in FCP resistance compared to the unfilled and pitch-based annealed samples. To propagate a crack at a $da/dN = 2 \times 10^4$ mm/cycle, ΔK for pitch-based and unfilled samples were 4.7 vs. 4.8 MPa$\sqrt{m}$ respectively, compared to 7.0 MPa$\sqrt{m}$ for PAN-based samples. These differences in the results were attributed to the cumulative effect of the following factors: (1) PAN-based CFR is stiffer than pitch-based CFR, (2) more PAN-based CFR are present compared to pitch-based CFR for the same wt.%, and (3) potentially the presence of more CFR surface area for bonding in case of PAN-based CFR-PEEK. The mechanical behavior of heat-treated PAN-based CFR-PEEK and CFR-Epoxy as alternative materials for artificial hip replacement has been an interesting topic of study (Kim et al. 2013). The composites had different ply configurations ranging from (0), (+/−45) (0/90) (+/−45) to (+/−45). The [(0)6] configuration exhibited considerably higher strength than the other configurations for both the matrix materials tested. The CFR-PEEK composites showed higher tensile strength (~800 MPa) and compressive strength (~600 MPa) when juxtaposed against the epoxy composites and its heat-treated versions.

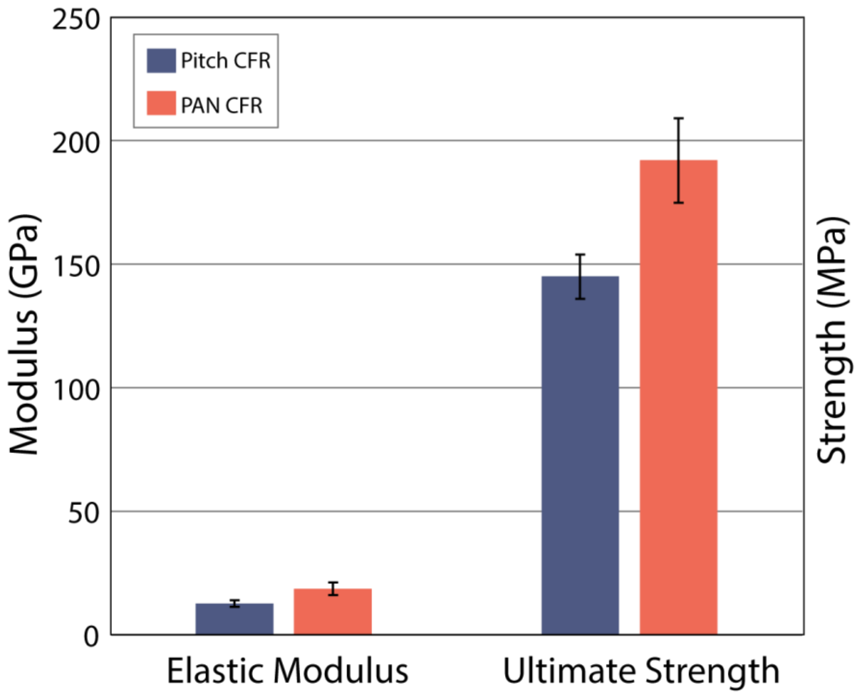

Figure 11 Elastic modulus and ultimate tensile strength comparison of pitch-based and PAN-based CFR. *Source:* Data from literature (Bonnheim et al. 2019).

Understanding the nanoscale behavior of these materials as they interact within the body at all possible length scales is paramount since the nanoscale phenomena affect the long-term integrity and biocompatibility of the implant as well as influence the macro-scale behavior. Although there is a dearth of research in this realm, the mechanical behavior of PEEK and PEEK composites in their untreated and thermally treated forms has been thoroughly evaluated (Arevalo and Pruitt 2020). The methodology they adopted involved conducting nanoindentation using conospherical tips of two different diameters, in order to determine the nanoindentation modulus at different length scales and thereafter, establish a correlation to previously gathered micro-indentation data (Regis et al. 2017; Arevalo and Pruitt 2020). The results unequivocally showed that nanoindentation using a smaller spherical tip is an effective characterization tool to understand small scale fiber–matrix interactions and to optimize the composite properties for eliciting the desired behavior for orthopedic implant applications. In that study, the PAN-based composite exhibited higher nanoindentation elastic modulus in its heat treated and untreated versions compared to the unfilled and pitch-based PEEK composite samples tested, thereby reaffirming the superiority of PAN-based CFR-PEEK vis-a-vis pitch-based PEEK composites.

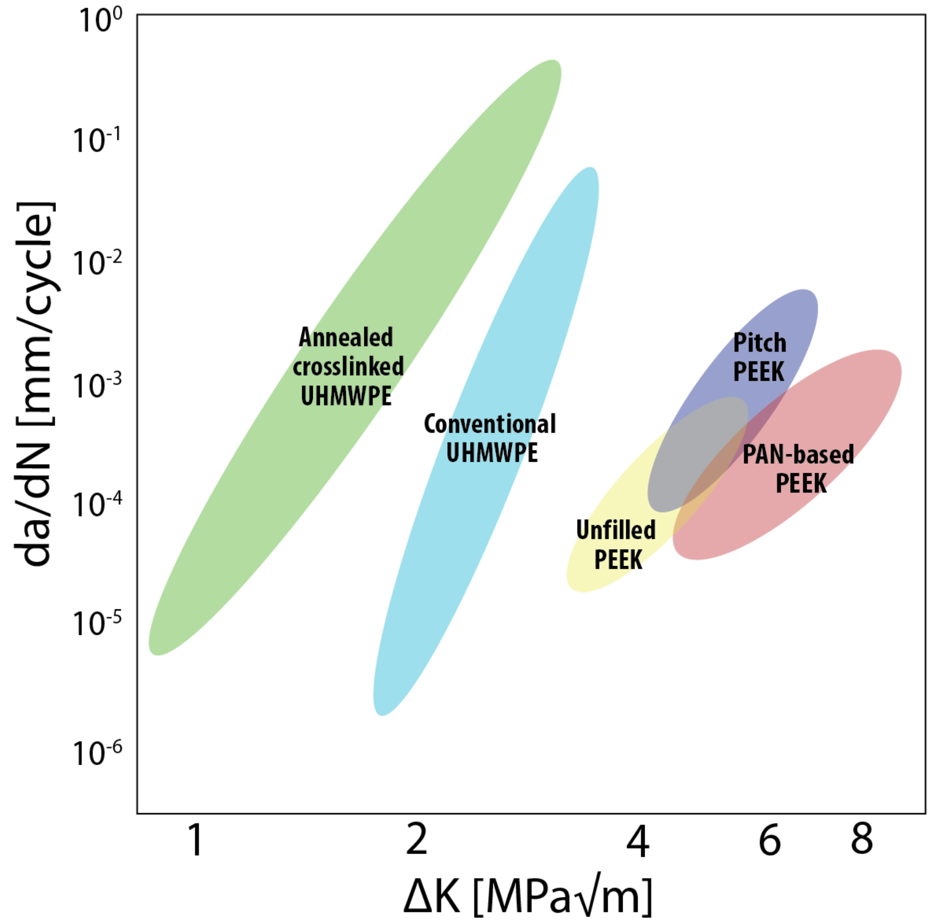

Figure 12 FCP plot of PEEK and PEEK composites compared with UHMWPE. *Source:* Data compiled from literature (Bonnheim et al. 2019; Gencur et al. 2006).

3.3.2. Tribological properties

It is evident from the literature that there exists a correlation between the results (wear performance, coefficient of friction (COF), other tribological parameters of interest) and the type of tribological testing methodology employed, best illustrated through Figure 13. For instance, the wear rate obtained using linear reciprocating or unidirectional pin-on-plate wear testing equipment was radically different when the same material (UHMWPE) was tested under the same test conditions using a modern hip joint simulator predicated on multi-axial motion (Wang et al. 1997). The literature also highlights the limitations of the conventional wear testing (i.e. pin-on-plate) technique. In-vitro pin-on-plate wear testing is not representative of the intricate joint bearing/sliding material interactions. Particularly when the in-vitro tests or joint simulators use only unidirectional linear motion, which radically alters the wear mechanism and is significantly different from the in-vivo experience (Wang et al. 1998a), where cross-shear and multi-directional motion dominate. Hence, different custom equipment have been created by different groups without standardization to simulate the knee joint and the hip joint.

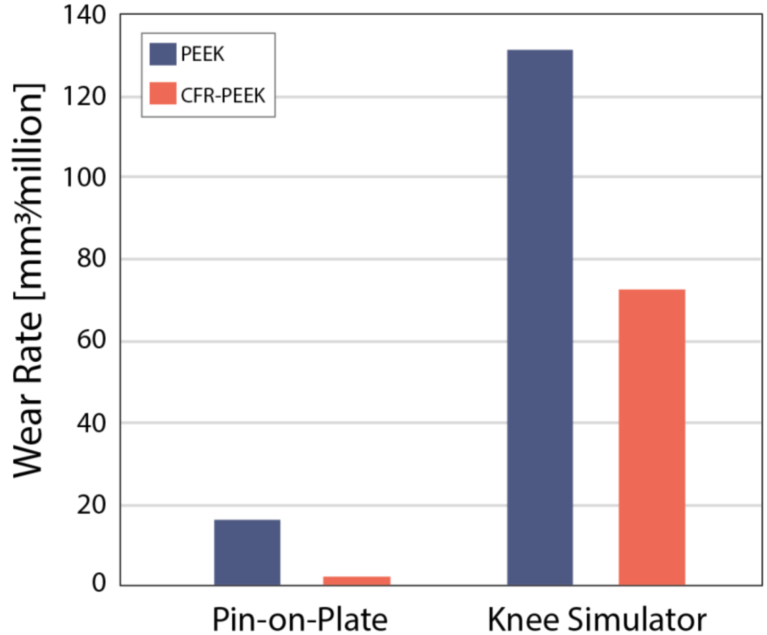

Figure 13 Comparison of wear rate results obtained with pin-on-plate and knee simulator for PEEK and CFR-PEEK. *Source:* Adapted from literature (Koh et al. 2019).

An array of in-vitro tribological tests conducted on PEEK and PEEK composites has been compiled in this chapter. Given the wide diversity of testing parameters involved and the lack of uniformity between them, there is an urgent need to standardize these tests, which implies establishing a set protocol involving the material against which PEEK or PEEK composites articulate in the tribological test, the lubricant used and its composition, test temperature, load, frequency of testing, sliding distance or number of wear cycles tested, amongst many other parameters of interest. The lack of standardization across different research groups and medical-device organizations also drives home the need for more uniformity in equipment. Having more uniform standards for tribo-testing equipment as well as testing parameters would make it easier to compare the tribological performance of different sets of material couplings utilized for orthopedic bearing applications.

It has been observed that for PEEK and PEEK composites articulating against zirconia-toughened alumina, low carbon and high carbon cobalt-chromium-molybdenum, UHMWPE, and self-mating couples (i.e. PEEK on PEEK), there is evidence to suggest that PEEK composites' wear rates are comparable to that of the conventional configurations with UHMWPE (Scholes and Unsworth 2007, 2009; Evans et al. 2014; Koh et al. 2019; Cowie et al. 2020; Scholes and Unsworth 2010; Joyce 2005). Additionally, a few studies have reported other polymers (i.e. highly cross-linked polyethylene a.k.a. HXLPE) that demonstrate better wear resistance when articulating against PEEK (East et al. 2015). While the aforementioned tribological trends have initially pointed towards utilizing PEEK and PEEK composites as a potential substitute for UHMWPE in TJR applications, several studies have suggested otherwise. Testing PEEK and PEEK composites against Co-Cr in low conformity knee simulators (which are more representative of the real-life in-vivo experience) resulted in higher wear rates. Furthermore, there have been reports of PEEK and its composites' mechanical failure (delamination and cracking) vis-a-vis UHMWPE's performance under similar testing conditions. This has led to the inference that PEEK and PEEK composites would not be suitable candidates for replacement of UHMWPE under these low-conformity total knee replacement (TKR) applications (Brockett et al. 2017; Grupp et al. 2010).

It is interesting to note here that conflicting results have been found in hip simulator investigations as well. Lower wear rates were observed in PEEK composites articulating against Co-Cr and zirconia ceramic heads with and without lubrication (Wang et al. 1998b; Brockett et al. 2012; Polineni et al. 1998) with specific configurations like 30 wt.% pitch-based CFR PEEK against zirconia ceramic head, having wear rates nearly two orders of magnitude lower than UHMWPE/metal and UHMWPE/ceramic couplings. In addition, there is no significant difference in wear rates when PEEK composites are tested under different contact stresses (similar to that of natural hip joints) with a pin-on-flat scenario (Kandemir et al. 2019), although there are definitely reservations concerning the use of a pin-on-disk setup to evaluate the true tribological performance for reasons explained previously. Moreover, it was observed that the Co-Cr discs articulating against PEEK composites experienced a reduction in weight, pointing towards metallic wear. In the long run, this could potentially culminate in metallosis.

The effect of ambient test conditions was investigated by attempting to simulate the joint's biological environment, i.e. under dry vs. wet conditions (Polineni et al. 1998; Regis et al. 2018). For instance, PEEK and annealed PAN- and pitch-based PEEK composites were articulated against alumina spheres on a pin-on-flat test in two lubrication regimes, i.e. dry and bovine serum (Regis et al. 2018). Under dry ambient conditions, the experiments revealed that PEEK composites have improved wear resistance in comparison to the unfilled formulation. The wear rate reduction under lubricated conditions is much higher in the unfilled formulation vis-a-vis the CFR-PEEK composites. However, the wear rate is still substantially higher for the unfilled formulation in comparison to the composites. Additionally, the annealed versions of the materials under-performed in terms of wear resistance with respect to the non-annealed versions. This can be attributed to the increase in crystallinity and material strength resulting in deleterious effects on the wear rate; a hardened structure obtained through annealing (annealing increases crystallinity and consequently hardness and strength) enhances the second-body abrasion, generating more wear debris and in turn, culminating in higher wear volume. Further, it was observed that these effects were diminished in the samples tested with bovine serum.

In terms of the effect of CFR content, it was found that when testing PEEK composites on a pin-on-disc wear machine at two different sliding velocities, the 10% pitch-based CFR and 10% PAN-based CFR exhibited outstanding friction and wear characteristics, except at high sliding velocities (Flöck et al. 1999). Moreover, they noticed that with an increase in the weight percentage of the fiber reinforcements, there was a concomitant increase in the abrasive wear rate, applicable to PEEK composite formulations. However, when probing the wear behavior in a high-stress line-contact reciprocating wear machine, it was observed that the smaller wear rates resulted for CFR content of 30% and that they were lower in pitch-based CFR PEEK (against alumina) than in the PAN-based counterpart at 10% and 50% (Wang et al. 1999). Despite the initial success with pitch-based CFR PEEK composites against alumina, their wear rates were still an order of magnitude higher than those of UHMWPE articulating against CoCr (control), reiterating the caveat concerning using CFR-PEEK composites as a substitute to UHMWPE in high-stress non-conforming situations such as those experienced in TKR. On the other hand, when tested in a ball-in-socket hip simulator, the best material combination was 30% pitch-based CFR PEEK and zirconia femoral head, for which the wear rates were one to two orders of magnitude lower than those of PAN-based composites, unfilled PEEK, and UHMWPE sliding against CoCr and alumina heads.

PEEK behaves like many thermoplastic polymers and is capable of plastic deformation, delamination, adhesion, and abrasive wear mechanisms. Plastic deformation of the polymer matrix within the PEEK composites has been reported (Regis et al. 2018). Debris formation and delamination were noted when wear tests were performed in bovine serum. For CFR-PEEK, researchers noted some evidence of fiber rupture; yet fibers remained embedded within the polymer matrix. Differences in crystallization mechanisms between PAN- and pitch-based CFR-PEEK contribute to differences in interfacial bond strength as a function of annealing, even for similar crystallinity (Regis et al. 2017). Similar findings were observed under crack propagation conditions where PAN fibers offered significantly improved fatigue resistance owing to improved interface adhesion (Bonnheim et al. 2019).

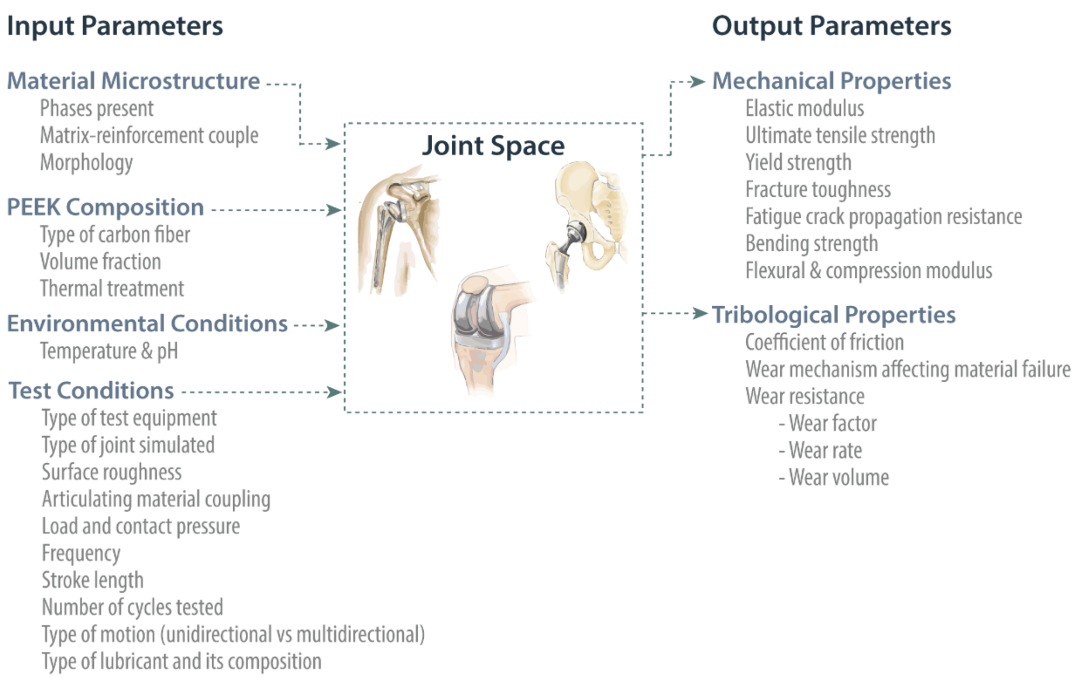

Figure 14 Illustration to demonstrate the key input and output parameters of interest in the tribo-mechanical landscape of PEEK and PEEK composites.

A useful way to visualize the tribo-mechanical landscape of PEEK and PEEK composites is through a parametric table, illustrated in Figure 14. All the parameters of interest in the design space have been classified into either input or output parameters. The tribo-mechanical properties of PEEK and PEEK composites (output parameters) cannot be altered directly, but can be affected indirectly by tailoring other parameters of interest (input parameters) such as the material's microstructure, its composition, the articulating material coupling, as well as the testing and environmental conditions under which the experiments are performed (Flöck et al. 1999; Scholes and Unsworth 2007, 2009; Evans et al. 2014; Cowie et al. 2020; Scholes and Unsworth 2010; East et al. 2015; Brockett et al. 2017; Grupp et al. 2010; Wang et al. 1998b; Brockett et al. 2012; Polineni et al. 1998; Kandemir et al. 2019; Regis et al. 2018; Wang et al. 1999; Chamberlain et al. 2019; Brockett et al. 2016). The definitions are as follows: input parameters (also known as control parameters) are the ones which can be controlled directly during experiments while the output parameters can be indirectly influenced by adjusting the input parameters but there exists no way to alter them through a direct route. Therefore, to optimize the tribo-mechanical performance of the material, there is a need to repeatedly undertake parametric studies to decipher not only the individual but also the synergistic effect of the input parameter(s) and to optimize the performance from the vantage of tribo-mechanical behavior of PEEK and PEEK composites. It is equally important to emphasize that Figure 14 attests to the multi-factorial nature of PEEK's tribo-mechanical landscape. The multi-factorial (multiple input-multiple output) system implies that each input parameter influences a majority of, if not all the output parameters. On a similar note, to optimize any of the tribo-mechanical properties, one can circle back to any or all input parameters and tailor them accordingly.

3.4 Biocompatibility and toxicity

In this chapter, the biocompatibility literature pertaining to PEEK and PEEK composites is explored at various length-scales and the different modalities for evaluating biocompatibility of a material are presented. A biocompatible material will be stable in the biological ambience prevalent inside the body and will not exhibit cytotoxicity, mutagenicity, or carcinogenicity. Literature has shown that PEEK is neither cytotoxic nor mutagenic (Katzer et al. 2002; Wenz et al. 1990; Morrison et al. 1995). This has been demonstrated using tests, such as, hypoxanthine–guanine–phosphoribosyl-transferase test (HPRT) test, direct contact cell culture evaluation (ASTM F813 American Society for Testing and Materials, 2012), tetrazolium dye-based colorimetric assay (MTT assay) (Sgouras and Duncan 1990), the Ames test (Ames et al. 1975), etc. Furthermore, PEEK is biocompatible in the bulk form (Williams et al. 1987; Scotchford et al. 2003; Wenz et al. 1990; Jockisch et al. 1992; Morrison et al. 1995; Cook and Rust-Dawicki 1995; Toth et al. 2006; Nieminen et al. 2008; Petillo et al. 1994) and demonstrates the ability to stay relatively inert in other aggressive media, for instance, aerospace and high moisture environments (Cogswell and Hopprich 1983).

However, the biocompatibility of a material is dependent on the length scale of the foreign particles, not just their presence in the bulk form. Thus, a material that is biocompatible in bulk might not be at the micron or sub-micron level, particularly in the phagocytozable size range (~0.1–10 μm). More so for particles in the size range <1 μm which tend to exhibit the maximum biological reactivity (Glant and Jacobs 1994; Green et al. 1998, 2000; Matthews et al. 2000a,b; Shanbhag et al., 1995; Stratton-Powell et al. 2016). An immunological response is nonetheless elicited for any foreign particle irrespective of its size, with a stronger response being provoked by smaller particles (<2 μm) (Zysk et al. 2005). This immunological response is often also accompanied by inflammation (Zysk et al. 2005). In light of this, biocompatibility tests need to consider the entire spectrum of particles' sizes before a material can be certified as biocompatible and consequently used in an implant for a medical device application.

The biocompatibility of any implant material is influenced by wear particles' size (Green et al. 1998, 2000; Gelb et al. 1994), mass distribution (Ingram et al. 2002), material type (Hallab et al. 2012; Rader et al. 1999; Shanbhag et al. 1995; von Knoch et al. 2004; Glant and Jacobs 1994), dosage/concentration of wear particles at the implant site (Green et al. 2000; Ingram et al. 2002; Matthews et al. 2000a), surface area and volume of the wear debris formed (Shanbhag et al. 1994; Gelb et al. 1994), their morphology (Gelb et al. 1994), composition (Glant and Jacobs 1994), and volume fraction of carbon fiber reinforcement particles (pitch and PAN) (Lorber et al. 2014;

Utzschneider et al. 2010). Numerous studies support PEEK and PEEK composites as biocompatible (Scotchford et al. 2003; Wenz et al. 1990; Katzer et al. 2002; Williams et al. 1987; Rivard et al. 2002; Jockisch et al. 1992; Hallab et al. 2012; Howling et al. 2003; Morrison et al. 1995; Cook and Rust-Dawicki 1995; Cunningham et al. 2013; Utzschneider et al. 2010; Latif et al. 2008; Grupp et al. 2014; Bao et al. 2007; Toth et al. 2006; Nieminen et al. 2008; Petillo et al. 1994). However, a couple of studies have concluded otherwise (Lorber et al. 2014; Khonsari et al. 2014). The aforementioned biocompatibility investigations have inherent methodology variations such as testing in-vivo (Cunningham et al. 2013; Grupp et al. 2014; Latif et al. 2008) or in-vitro (Scotchford et al. 2003; Hallab et al. 2012; Howling et al. 2003; Morrison et al. 1995; Katzer et al. 2002; Petillo et al. 1994). Even within in-vivo explorations, biocompatibility can be evaluated via animal studies such as in rats (Williams et al. 1987; Latif et al. 2008; Petillo et al. 1994), rabbits (Williams et al. 1987; Rivard et al. 2002; Jockisch et al. 1992; Cunningham et al. 2013; Grupp et al. 2014), mice (Lorber et al. 2014; Utzschneider et al. 2010), sheep (Toth et al. 2006; Nieminen et al. 2008), dogs (Jockisch et al. 1992; Cook and Rust-Dawicki 1995), baboons (Bao et al. 2007) or via clinical trials in humans (Pace et al. 2004; Khonsari et al. 2014; Pace et al. 2008, 2005a,b). Another classification for in-vivo biocompatibility tests arises from whether the material being evaluated was used directly as a bulk implant/ fixation device at the specific site (Jockisch et al. 1992; Cook and Rust-Dawicki 1995; Bao et al. 2007; Pace et al. 2004, 2008) or through the use of a subcutaneous implantation such as a pouch inside an animal's body (Latif et al. 2008; Williams et al. 1987), in which wear is not taken into consideration.

The most pertinent classification for biocompatibility is based on the length scale, i.e. biocompatibility in bulk form vs at the particulate level. As mentioned previously, PEEK and PEEK composites have long been established as biocompatible in the bulk form (Williams et al. 1987; Scotchford et al. 2003; Wenz et al. 1990; Jockisch et al. 1992; Morrison et al. 1995; Cook and Rust-Dawicki 1995; Toth et al. 2006; Nieminen et al. 2008; Petillo et al. 1994). Therefore, their presence in the macro-form inside the human body is less likely to cause adverse effects than in the sub-micron form. More recently, studies have delved deeper into the micron and sub-micron length scales (Hallab et al. 2012; Grupp et al. 2014; Cunningham et al. 2013; Lorber et al. 2014; Utzschneider et al. 2010; Rivard et al. 2002). The biocompatibility literature for PEEK suggests a lack of research devoted exclusively towards particles at the nanoscale. Since PEEK and PEEK composites are often modeled as a substitute for other polymeric materials of interest such as UHMWPE, results from PEEK's biocompatibility tests are often reported in relative terms. In this regard, parameters like cytotoxicity (Howling et al. 2003; Morrison et al. 1995), cellular (Jockisch et al. 1992) and macrophage responses (Hallab et al. 2012), histopathological responses (Cunningham et al. 2013), cytokine expression (Lorber et al. 2014; Hallab et al. 2012), inflammation (Latif et al. 2008; Utzschneider et al. 2010), growth of osteoblasts and fibroblasts (Morrison et al. 1995), histological parameters (Jockisch et al. 1992; Utzschneider et al. 2010; Grupp et al. 2014), alkaline phosphate activity (Scotchford et al. 2003), percent LDH activity per unit surface area (Wenz et al. 1990), number of secreted cells (Petillo et al. 1994), bone contact and interface shear strength (Cook and Rust-Dawicki 1995), immunocytochemical characteristics (Cunningham et al. 2013) are compared between PEEK and the current standard polymer, Ultra High Molecular Weight Polyethylene (UHMWPE).

Table 5 Biocompatibility literature compiling tests performed in the bulk form.

Composite formulation	Type of study	Biocompatibility	Potential application	Reference
PAN (30%)	In-vitro	Yes	Replace metal alloys in orthopedic applications	Wenz et al. 1990
30% chopped PAN CFR-PEEK	In-vivo, Animal study (rabbits and dogs)	Yes	Fracture Fixation Plates	Jockisch et al. 1992
PEEK	In-vivo, Animal study (sheep)	Yes	Spinal Implants	Toth et al. 2006
PEEK	In-vivo and in-vitro, Animal study (sheep)	Yes	Spinal Implants	Nieminen et al. 2008
PEEK	In-vivo, Animal study (rats)	Yes	Monolithic Implants	Petillo et al. 1994
mix of PEEK, tricalcic phosphate (-TCP) and titanium dioxide (TiO_2)	In-vivo, Human Study (three cases)	No	Dental Implants	Khonsari et al. 2014
PEEK	In-vivo and in-vitro, Animal study (baboons)	Yes	Disc arthroplasty device	Bao et al. 2007

Any material that is used in TJR applications will invariably produce wear particles in the long run. Therefore, to find a suitable substitute for UHMWPE, the material must outperform or at the very least, be at par with the current gold standard on the biocompatibility front. PEEK and PEEK composites have demonstrated that they are on par or better than UHMWPE in a majority of studies (Hallab et al. 2012; Jockisch et al. 1992; Howling et al. 2003; Cunningham et al. 2013; Utzschneider et al. 2010; Latif et al. 2008; Grupp et al. 2014). Comparative biocompatibility tests have not been limited to only PEEK vs UHMWPE, but rather include PEEK's biocompatibility being juxtaposed against that of Ti6Al4V (Scotchford et al. 2003), polysulfone composite (Wenz et al. 1990), epoxy resin polymer (Morrison et al. 1995), Ti-coated PEEK (Cook and Rust-Dawicki 1995), carbon–carbon composites (Howling et al. 2003), and polyetherurethane ureas (PEUU), polydimethylsiloxane (PDMS) and polyetherimide (PEI) (Petillo et al. 1994) with mixed results.

The literature overwhelmingly supports the biocompatibility claim for PEEK and PEEK composites, both in the bulk form (Table 5) as well as in the particulate form (Table 6) while clearly pointing to the need for more targeted studies aimed at ascertaining their biocompatibility at the nano-level. This paves the way for future researchers to explore the biocompatibility of nanoparticles produced by PEEK and PEEK composites.

Table 6 Biocompatibility literature compiling tests performed in the particulate form.

Composite formulation	Type of study	Biocomp atibility	Potential application	Reference
Both 30% Pitch and 30% PAN	In-vivo and in-vitro, Animal study (mice)	No	Knee implants	Lorber et al. 2014
PEEK	In-vitro	Yes	metal-on-polymer, bearing surfaces	Hallab et al. 2012
PEEK	In-vivo, Animal Study (Rabbits)	Yes	Spinal Implants	Rivard et al. 2002
PAN	In-vitro	Yes	Load Bearing Surfaces for Artificial Hip Joints	Howling et al. 2003
Both (30% Pitch and 30% PAN CFR-PEEK)	In-vitro, knee simulator and in-vivo, Animal study (mice)	Yes	Load Bearing for Orthopedic Application	Utzschneider et al. 2010

3.5 Conclusions

This chapter highlights the numerous limitations, and a deep divide between, clinical studies and mechanical testing of PEEK and PEEK composites. A major limitation to bringing PEEK and PEEK composites for orthopedic applications is the lack of retrieval studies. Further, the lack of mechanical testing standard and inability to replicate in-vivo conditions, makes it challenging to definitively recommend as a replacement to current TJR materials. While simulating in-vivo conditions could improve development time of implants, a few challenges arise: matching the behavior of bodily fluids to dynamically react to changes in loads, pH, viscosity, and temperature. Hence, making it difficult to replicate the dynamic lubrication regime observed in a human body within a laboratory without the use of a test subject. This reveals a gap in the existing literature pertaining to the complex parameters impacting the lubrication regime.

This is especially critical for assessing wear as conflicting literature complicates design decisions. While there are conflicting results from different testing methodologies, the fiber content does affect the wear rate. Additionally, a vast majority of the literature has shown that CFR-PEEK has a higher wear rate than UHMWPE under high-stress nonconforming contact conditions as is the case of the knee joint. On the other hand, although a reduction of wear rate of the polymeric material is desirable, even more problems arise when the metallic couplings are worn. This can lead to a whole different type of biological reaction. Hence, a final decision on PEEK composite suitability also depends on the study of material coupling combination.

This chapter aggregates the expansive number of studies that assess the biocompatibility of PEEK and PEEK composites, both in the bulk and particulate form (micron and sub-micron ranges). Simultaneously, this chapter identifies the need for more detailed investigations into the biocompatibility of PEEK and its composites at the nano-level, which remains rather unexplored. It can also be observed that there are innumerable variables impacting biocompatibility test conditions such as testing environment (in-vivo vs in-vitro), the use of animal vs human studies, the site of implantation, the potential application, and the biological parameters that are being used to assess the biocompatibility of the said materials.

A majority of experiments indicate that PEEK composites are more appropriate for hip rather than knee implants. But the lack of research regarding clinical trials or retrieval analysis makes it challenging to definitively state that PEEK composites will be the new go-to material in the future. Based on the limitations presented (Li et al. 2015), the present chapter cannot present a final recommendation for PEEK or PEEK composite knee implants. While research findings and studies remain inconclusive, PEEK and PEEK composites warrant further exploration as candidate biomaterials for enhanced longevity in orthopedic devices.

Chapter 4 –Study of crack initiation phenomena in orthopedic grade UHMWPE from clinically relevant notches: Initial Findings

4.1 Introduction

Total joint replacement (TJRs) is one of the solutions for a severely degraded osteoarthritic joint such as the hip, shoulder, or knee (“5 Ways to Manage Arthritis | CDC” 2023). TJRs impart relief from pain and much-needed mobility to osteoarthritis-afflicted patients. A specialized polymer called Ultra-high molecular weight polyethylene (UHMWPE) is used as the bearing material in TJRs and has been in use since the 1960s (Charnley 1961; S. M. Kurtz 2009). The choice of UHMWPE arises from a volley of attributes including but not limited to wear resistance, energetic toughness, and biocompatibility.

Despite its excellent bio-tribo-mechanical performance, UHMWPE is subjected to large cyclic contact stresses and must endure loading for 20-30 million cycles in-vivo. Such extensive biomechanical demand can result in the generation of sub-micron sized wear debris, ultimately leading to osteolysis, implant loosening, and failure of the TJR. There is an ongoing effort to develop formulations of UHMWPE that resist the troika of challenges faced in the body – wear, fatigue, and oxidation (Atwood et al. 2011; S. M. Kurtz and Oral 2016; Ansari, Ries, and Pruitt 2016). The optimal microstructure remains that of moderately cross-linked UHMWPE which has been remelted alongside vitamin E added to protect it from oxidation while balancing fatigue and wear properties (Atwood et al. 2011; Bracco and Oral 2011).

4.2 Background

Fatigue behavior can be divided into two categories, namely, fatigue crack initiation and fatigue crack propagation. The latter has been extensively studied and there is a plethora of crack propagation studies which have comprehensively characterized UHWMPE (Ansari, Ries, and Pruitt 2016; L. Pruitt, Wat, and Malito 2022; Furmanski and Pruitt 2007; Patten et al. 2011a; Ansari et al. 2016; Furmanski and Pruitt 2018; Baker, Hastings, and Pruitt 1999; 2000; Baker, Bellare, and Pruitt 2003; Bradford et al. 2004; L. A. Pruitt et al. 2005; Ries and Pruitt 2005; Simis et al. 2006).

One approach to study the fatigue life of a polymer component is using the defect-tolerant philosophy which utilizes the fracture mechanics formulation to assess the crack growth dynamics. Numerous studies report the steady-state crack propagation in the Paris regime in the form of da/dN vs ΔK curves across clinically relevant formulations of UHMWPE. When it comes to the study of crack growth initiation, researchers have reported crack initiation in terms of $\Delta K_{inception}$ which is the minimum stress intensity that needs to be applied for the crack to propagate at the rate of 10^{-6} mm/cycle (Baker, Bellare, and Pruitt 2003; Simis et al. 2006). Exacerbating the problem is the insight into the crack propagation behavior that cracks, once initiated, can propagate under static and/or marginal or no stress fluctuations, with the crack propagation being dependent primarily on the peak stress intensity and not the stress intensity range (Furmanski and Pruitt 2007; 2018; P. A. Sirimamilla, Furmanski, and Rimnac 2013; 2011). This implies that a concerted effort needs to be made towards precluding the nucleation/ initiation of cracks so that the subsequent issues with propagation never transpire.

Another approach is the total life fatigue data whereby the S-N route (stress amplitude vs number of cycles) is adopted and formulated using the Basquin relation (Baker, Bellare, and Pruitt

2003; Michael C. Sobieraj et al. 2013). Total life philosophy presumes that the fatigue life is a sum of the time/cycles to initiate a flaw and the time/cycles for it to grow to a critical crack size. For fatigue-brittle polymers, the first component is rather predominant, implying that the time/cycles to nucleate a flaw (crack) is substantially higher than the time/cycles for it to grow to a critical size and for fatigue failure to ensue. Therefore, it is safe to presume that once a flaw initiates, that can be approximated to be the fatigue life of the specimen, ignoring the second component. That underscores the importance of crack initiation studies. These are usually conducted in the classic S-N style format by loading specimens at constant-amplitude stresses and observing when the specimen fails.

It is of paramount importance to factor in notches and their effects on the fatigue behavior of medical-grade polymers like UHMWPE. The reason to focus on notches can be traced back to the design of TJRs which have stress-concentration features (posts, undercuts, grooves as well as various locking mechanisms) by virtue of their clinical requirements. These regions of heightened stress-concentrations often act as sites of crack initiation from which fatigue cracks then propagate through the material, leading to the catastrophic failure of the TJR inside the patient (Furmanski et al. 2009; Furmanski, Kraay, and Rimnac 2011).

In one study, fatigue testing was conducted using cylindrical dog-bone specimens with notches present centrally while a smooth cylindrical geometry was the control sample (Michael C. Sobieraj et al. 2013). Their experimental results demonstrated that conventional UHMWPE (ram extruded GUR 1050, sterilized at 30kGy in inert nitrogen environment) strongly follows the S-N curve-based Basquin relation but for other formulations of UHMWPE (such as moderately or highly cross-linked) with notches, the results exhibit significant variance in their S-N distribution data or don’t follow the Basquin relation at all. On the other hand, another study also used small dog-bone specimens for their fatigue behavior investigation but had no notches machined into the samples (Baker, Bellare, and Pruitt 2003). Both of the aforementioned studies also had varying definitions for the N value (number of cycles) as one of them used the number of cycles to the onset of yielding (Baker, Bellare, and Pruitt 2003) while the other opted for fracture (Michael C. Sobieraj et al. 2013) as the definition of failure of the specimens. The current study is predicated on the initiation of crack(s) at/near the vicinity of the notch root as the failure criteria but given the very marginal difference between $N_{initiation}$ and $N_{failure}$, the N value is experimentally determined as the number of cycles to fatigue failure incorporating both the predominant initiation plus the numerically insignificant propagation cycles. Moreover, while both studies (Baker, Bellare, and Pruitt 2003; Michael C. Sobieraj et al. 2013) incorporated different formulations of UHMWPE, neither utilized the current-day vitamin E-added formulation for their fatigue tests in the presence of notches, which is one of the material groups explored in the current work.

Other peripheral studies conducted by groups investigating fatigue of UHMWPE contributed to better comprehension of the effects of notches and varied notch root radii. For instance, Rimnac and co-workers found that the axial yield stress increased in the presence of notches incorporated into the tensile specimens while observing a reduction in the ultimate properties (both stress and strain) vis-à-vis unnotched specimens and reported a ‘notch-strengthening and hardening’ phenomenon that depended on the severity of the notching (Michael C. Sobieraj et al. 2013; M. C. Sobieraj, Kurtz, and Rimnac 2005; Michael C. Sobieraj et al. 2008). This was attributed to the triaxial state of stress that exists in the region surrounding the notch in comparison to the uniaxial state of stress observed in unnotched specimens. Typically, fracture in UHMWPE starts with microvoids coalescing into a ‘crack’, followed by slow fracture up until it reaches a critical dimension after which fast fracture occurs (Gencur, Rimnac, and Kurtz 2003). This is the case for unnotched specimens where a standard axial force is applied. However, as the state of stress transforms to a triaxial one in the presence of notches, it inhibits chain alignment and subsequently, the cascade of void formation, coalescence, and crack growth to fast fracture is interrupted (M. C. Sobieraj, Kurtz, and Rimnac 2005). It is pertinent to mention here that just like notches culminate in a triaxial state of stress and inhibit chain alignment, crosslinking of UHMWPE also has a similar microstructural effect on the lamellar alignment prevention (Klapperich, Komvopoulos, and Pruitt 1999; Zhou and Komvopoulos 2005). The key takeaway is that geometric features like notches significantly modify the micro-mechanisms of void formation and crack growth to fracture, and drastically reduce the critical stress intensity or threshold needed for failure. These findings have strong implications for the notch-based fatigue tests and interpretation of the results obtained therein.

While it is known that cracks in UHMWPE can propagate once initiated, under static loads with minimal or no fluctuations (Furmanski and Pruitt 2007), it is even more concerning to learn that cracks can initiate under static loads from notches in UHMWPE of similar root radius as the design features (like fillets) inherently present in TJR components (P. A. Sirimamilla, Furmanski, and Rimnac 2011; 2013). Crack initiation under quasi-static loads was preceded by non-uniform material de-cohesion at the notch surface followed by a tortuous crack front, after which the crack propagated at velocities that could be correlated to the magnitude of static loads being applied to the compact tension samples, hereafter referred to as C(T) samples. Single-layer and multi-layer crack initiation was also noted. The former occurred when the crack front erupted on the line of the notch root while the latter was seen in some cases whereby the crack initiated simultaneously at multiple parallel planes in the vicinity of the notch root. A positive correlation was obtained between the time for crack initiation and the type of crack initiation, i.e. single-layer or multi-layer, and the time for crack initiation also correlated with the distance between the different layers in the multi-layer crack initiation. Furthermore, increased crosslinking (a product of increased gamma radiation dosage) was found to reduce the crack initiation resistance and detrimentally increase the crack propagation velocities. Noteworthy to mention here that the researchers behind these studies employed a video measurement apparatus and quantified crack initiation in terms of initiation time (t_i) and proved that the viscoelastic fracture model developed by Williams (Williams 1977) can be successfully used to predict crack initiation in crosslinked formulations of UHMWPE.

A parametric study demonstrated the relationship between notch root radii and the crack initiation dynamics under quasi-static loading conditions (P. A. Sirimamilla, Rimnac, and Furmanski 2018). Two highly cross-linked formulations of UHMWPE and three different notch root radii were included in the scope of this investigation and it again went to prove that the Williams' viscous fracture model (Williams 1977) governs crack initiation in these UHMWPE formulations. Reaffirming previous results, this study again evinced that increased crosslinking density resulted in decreased crack initiation resistance in the presence of notches. Therefore, increasing crosslinking density reduced the resistance to fracture for UHMWPE, given the quasi-static nature of the loads. For the sharp notch case, crack initiation was almost instantaneous for all the static loads that were applied in those experiments but for the same static loads, the blunter the notch (larger notch root radii) the longer it took to initiate a crack. This has been explained using the Williams fracture model whereby the J_0 (energy available at the notch front) is substantially reduced in the case of the blunter notches, making it harder to initiate a crack front from the notch tip. In addition, the work specified that a decrease in the applied quasi-static load came with a concomitant increase in the crack initiation time.

While the previous parametric study explored the notch root radii effect on crack initiation under quasi-static loading conditions, a follow-up study expanded into the crack initiation dynamics under cyclic loading conditions for only one clinically relevant notch root radius (0.25 mm) in highly cross-linked and remelted UHMWPE (A. Sirimamilla and Rimnac 2019).

Interestingly, for the same set of experimental parameters (such as same maximum load), the crack initiation time (t_i) decreased by an order of magnitude for the cyclic loading case vis-à-vis the static one. Additionally, cyclic loading parameters like frequency, loading rate, and waveform had a strong effect on crack initiation alongside the J_0 parameter. Unlike the previous study (P. A. Sirimamilla, Rimnac, and Furmanski 2018), no multi-layer crack initiation was detailed in their results.

The current study is predicated on pertinent research published a few years ago whereby crack propagation dynamics for cracks originating from notches of different root radii was probed using a linear-elastic fracture mechanics approach (Ansari et al. 2016). Three relevant UHMWPE formulations were considered: conventional UHMWPE, highly cross-linked and remelted UHMWPE, and vitamin E blended and highly cross-linked UHMWPE. The stress intensity factor K (driving force) is markedly influenced by the notch geometry, yet the inherent mechanisms driving crack growth in UHMWPE in the presence of notches are not significantly affected by whether the crack is propagating through the elasticity or plasticity-affected zones in the vicinity of the notch. Another key finding was that crack growth rate was irrespective of the notch root radii and that crack growth was predominantly determined by the microstructure of UHMWPE with highly crosslinked formulations exhibiting fast crack growth rates while the conventional UHMWPE showed the slowest. Therefore, crack growth dynamics weren't affected by notch geometry once a crack initiated. But then, crack initiation as a function of notch geometry becomes worthy of further enquiry. This forms the foundation of the current study.

Another point worthy of being noted here is that the former study purposefully added a razor-sharp crack edge at the notch root for ease of crack growth inception, which foregoes any significant finding from the crack initiation standpoint. Building on the insight of previous research, the present study examines crack initiation from the notched regions. Thus, cracks nucleate from inherent material flaws or machining features rather than any artificial interventions in this particular study.

4.3 Objectives

The current investigation presents some initial findings related to the effect of different notch root radii, UHMWPE formulations, as well as different a/W ratios on crack initiation phenomenon from clinically relevant notches. Different load amplitudes are applied on the samples, in essence, applying different stress intensities, and consequently, the number of fatigue cycles to crack initiation (experimentally measured here as fatigue failure) are noted. This chapter also includes failed endeavors as part of the study, which could potentially help future researchers as lessons learnt, for preparing their research plans to study crack initiation from clinically relevant notches in UHMWPE or other orthopedic-grade polymers in general.

4.4 Materials and Methods

Two clinically relevant notch root radii (0.25 mm and 3 mm) and two formulations, namely, virgin UHMWPE as well as 0.1 wt.% vitamin E-blended highly crosslinked UHMWPE, both derived from GUR 1020 resin originally, are included in the scope of this work. The former formulation is hereby referred to as UHMWPE and serves as the control group whereas the latter formulation with vitamin E and 100 kGy crosslinking dosage is referred to as VXLPE, following a convention set in a previous work (Ansari et al. 2016). C(T) samples were machined from blocks of UHMWPE and VXLPE sourced from Orthoplastics located in Lancashire, UK (Malito et al. 2018) and the dimensions were based on the recommendations from the ASTM Standard ASTM

E647-15€1 ("ASTM E647-15e1 - Standard Test Method for Measurement of Fatigue Crack Growth Rates" 2015; Patten et al. 2011b). It is important to state here that while ASTM E647 prescribes a set of dimensions and dimensional ratios and proportions for the specimens used for fatigue testing, the standard was originally developed keeping ductile metals and metallic alloys in mind. Consequently, some of the prescriptions do not necessarily translate to the polymer material class. This necessitates an upgrade to the ASTM E647 standard for ensuring that it can be meticulously utilized for fatigue testing of polymeric materials.

The following dimensions (all reported in mm unless specified otherwise) were chosen for the specimen geometry: W = 25, L = 31.25, h = 1.5, B = 5, ϕ = 6.25, initial notch length a = a_n = 6.25, 8.75, 12.5, 15, and notch root radius ρ = 0.25, 3. The other relevant dimensions have been labelled in the diagram below, all of which are based on the ASTM standard cited earlier. It is to be noted here that all dimensions remain the same as the ones reported in Figure 15 except the notch root radius ρ varying between 0.25 and 3 mm (as marked on the figure) and also the initial notch length 'a' varying between 6.25 to 15 mm. The initial notch lengths were determined based on different a/W ratios of 0.25, 0.35, 0.5, and 0.6.

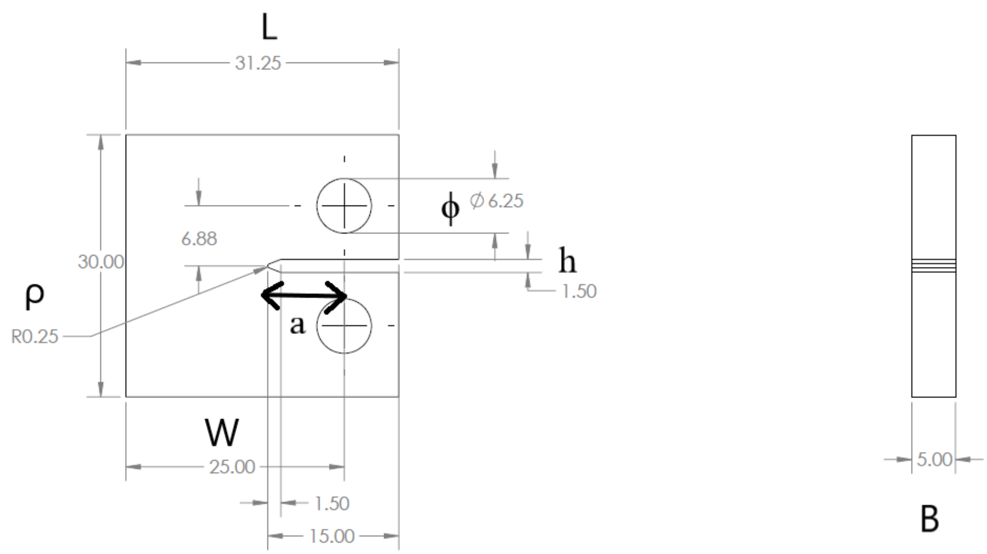

Figure 15 Dimensions of a typical C(T) sample used for the crack initiation fatigue studies based on ASTM Standard ASTM E647-15€1. Dimensions shown are given in mm.

Tension-tension loading based fatigue tests were conducted on MTS Elastomer Test System Model 831 machine. The R-ratio was kept constant (R=0.1) across all fatigue experiments with the increasing loads adjusted accordingly. The following loads were used: 10-100N, 15-150N, 18-180N, 20-200N, 22-220N, 25-250N, 28-280N, 30-300N, and 80-800N. Fatigue tests were performed at room temperature using a load-controlled sinusoidal waveform applied at a frequency of 5 Hz. Additionally, an air coolant system was utilized to reduce the possibility of hysteretic heating (M. C. Sobieraj and Rimnac 2009). Tests were stopped at N = 25000 cycles periodically to inspect crack initiation on the notch surface or in its vicinity. The notch tip was examined using a Zeiss AX10 microscope with a magnification of 50x. If a crack didn't initiate after 25000 cycles, the loading was increased to the next step (say 20-200N followed by 22-220N and so on). This process of incrementally increasing the load after a preset number of cycles continued until the sample failed via fatigue failure. Any atypical deformation in the samples post-loading was also closely monitored and if found, the test was immediately discontinued. Two samples were tested for each material group and the details of the sample geometries, material formulation, test conditions, are comprehensively tabulated in Table 7.

The stress intensity values (ΔK) were calculated using the formulation provided in Equation A1.3 of the ASTM standard ("ASTM E647-15e1 - Standard Test Method for Measurement of Fatigue Crack Growth Rates" 2015), also stated below-

$$\Delta K = \left({\Delta P}/{B\sqrt{W}}\right)\left({2+\alpha}/{(1-\alpha)^{3/2}}\right)(0.886 + 4.64\alpha - 13.32\alpha^2 + 14.72\alpha^3 - 5.6\alpha^4) \quad \text{Eq. [24]}$$

Where ΔK is the stress intensity at the crack tip (notch root in this case), ΔP is the load applied, and B, W, and α = a/W are sample dimensions. Thereafter, ΔK values were plotted against the number of cycles to failure ($N_{failure}$) for samples P7-P10 which were only tested at the highest loads and were fatigued to failure therein. Samples P5 and P6 were deliberately removed from the analysis since these two samples were incrementally loaded and there isn't a way to merge the fracture mechanics-based ΔK values with the Palmgren-Miner's rule. These values of ΔK obtained from the study were then compared to $\Delta K_{threshold}$ values obtained from other experiments performed in a different unpublished study.

Table 7 Compilation of fatigue crack initiation specimen- geometries, material formulations, test conditions, and results.

Sample	Material	Cycles	Load in N	a/W ratio	Notch root radius (mm)	Final outcome
P1	VXLPE	6881	25-250	0.25	Sharp notch tip	Sharp C(T) sample showed noticeable crack initiation of 0.198 mm within 6881 cycles
P2	UHMWPE	0	80-800	0.25	3	Sample was loaded to setpoint (440N) and sample broke at one of the pin holes
P3	UHMWPE	>35,000	30-300	0.25	3	A crack didn't initiate at the notch, but the sample deformed at one of the holes
P4	UHMWPE	>100,000	20-200	0.25	3	No crack initiated on or in the vicinity of the notch
P5	VXLPE	75000 50000 25000 50000	18-180 20-200 22-220 25-250	0.35	0.25	Sample broke into two parts at the highest load.

		9315	28-280			
P6	VXLPE	340 117000 1561	10-100 15-150 20-200	0.5	0.25	Sample broke into two parts at the highest load.
P7	VXLPE	86	20-200	0.6	0.25	Sample broke into two parts at the highest load.
P8	VXLPE	3849	20-200	0.5	0.25	Sample broke into two parts at the highest load.
P9	VXLPE	71	20-200	0.6	0.25	Sample broke into two parts at the highest load.
P10	VXLPE	12539	28-280	0.35	0.25	Sample broke into two parts at the highest load.

4.5 Results and Discussion

This section includes the results from the initial trial and error with the fatigue testing parameters and C(T) specimen geometries, encompassing all the ‘failed’ tests (not to be confused with fatigue failure of a component) and the technical learnings along the way as well actual fatigue-failure results. The results are reported with the samples indexed as P1, P2…P10. Specifics of the sample geometry, loading conditions, and visuals of failures (or lack thereof) have been presented in Table 7 and figures in this section.

Figure 16 shows the samples P1-P4 after completion of testing. The red circles demarcate the area of interest where crack initiated (P1) or failure ensued (P2) or abnormal deformations were observed (P3). The instantaneous failure and abnormal deformations noticed in samples P2 and P3 respectively (both with a/W ratio of 0.25) provided impetus to discard this particular a/W geometry, course correct, and increase the a/W ratio and/or reduce the load. This was attributed to the stress-concentrations near the hole-notch interface regions that were causing the samples to fail upon loading or deform abnormally around that area. The load was reduced to 20-200N for P4, yet no crack initiated even after 100,000 cycles at which point the fatigue test was stopped. Therefore, a/W = 0.25 was proving to be detrimental to the sample geometry and reliable fatigue crack initiation data was not possible from the notches with lower loads or high notch root radius (at this specific a/W ratio).

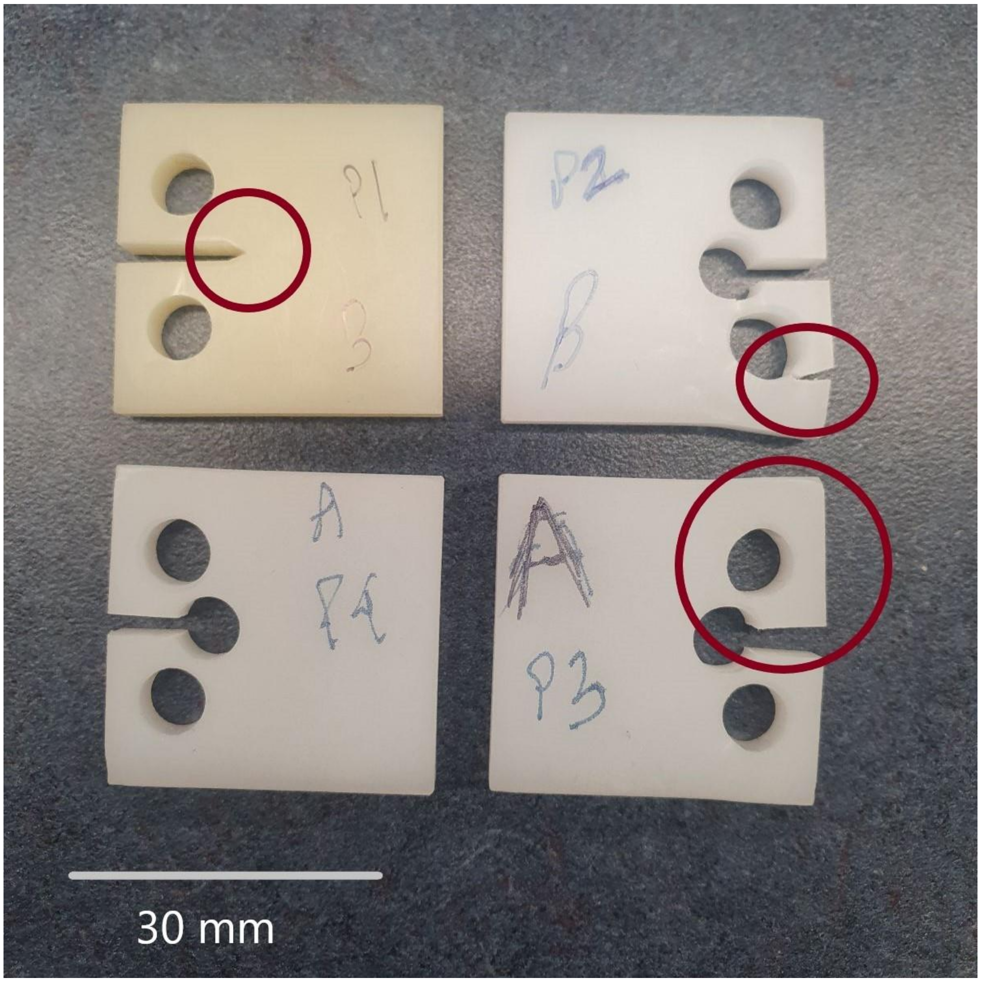

Figure 16 Samples P1-P4 (displayed clockwise from top-left) post completion of fatigue tests.

To enhance the possibility of crack initiation and eventual fatigue failure, the next set of samples (P5-P10) were made from a block of VXLPE which is known to have a reduced fatigue resistance vis-à-vis UHMWPE (Baker, Bellare, and Pruitt 2003; Medel et al. 2007), the a/W ratio was increased to 0.35, 0.5, and 0.6, and the notches were made sharper with a notch root radius of 0.25 mm.

Figure 17 shows the samples P5-P10 after each of them failed through fatigue testing. Experiments were restarted on sample P5 at the load range of 18-180N and tested for a total of 75000 cycles and then incrementally increased through 20-200N, 22-220N, 25-250N, till a load range of 28-280N when it broke into two parts symmetrically after limited cycles (9315 cycles). Since sample P6 had a higher a/W ratio of 0.5 vis-à-vis P5 (a/W ratio 0.35), the stress intensity experienced at the crack tip (notch root in this case) would be higher. Consequently, the load was reduced prior to the next series of fatigue tests with higher a/W ratio, given the direct correlation between stress intensity experienced at the crack tip with the load range as formulated in Equation A1.3 of the ASTM standard ("ASTM E647-15e1 - Standard Test Method for Measurement of Fatigue Crack Growth Rates" 2015). Sample P6 was fatigued at 10-100N initially. However, given the inaccuracies in the load control system of the machine, the minimum load often went lower than 10N culminating in one of the pins loosening and falling out time and again. To surmount this, the loading was slightly increased to 15-150N and finally to 20-200N after which the sample failed through fatigue at a limited number of cycles (1561 cycles). Next, sample P7 with an a/W ratio of 0.6 was loaded at 20-200N and the experiment failed within moments of initiation. The fatigue cycles on P7 were recorded as 86 cycles at failure. In the three aforementioned samples P5-P7, the crack initiation was traced back to the notch root region, akin to the crack tip in a conventional C(T) sample.

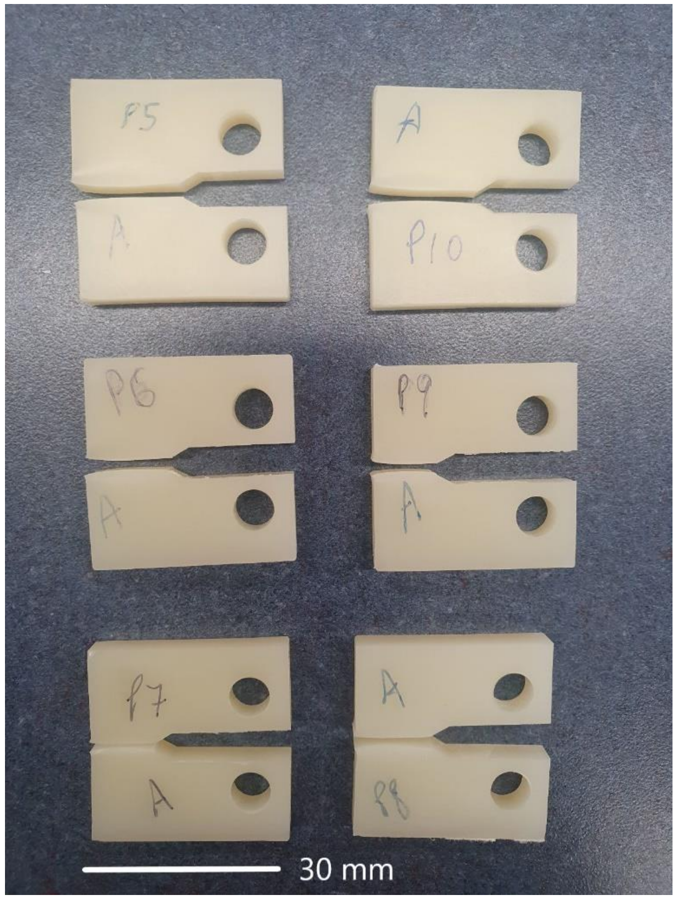

Figure 17 Samples P5-P10 (displayed anti-clockwise from top-left) after they failed via fatigue.

To examine the damage accumulation effect of the lower loads or lack thereof, the next series of samples P8-P10 were fatigue cycled at the highest load at which their counterparts (P5-P7) failed. Sample P8 (same family as P6) was fatigue cycled at 20-200N and it failed at 3849 cycles, which marks a 146% increase in fatigue life. Sample P9 (same family as P7) was tested at 20-200N, and it broke at 71 cycles, very close to the original sample P7's 86 cycles fatigue failure value. Here, the damage accumulation concept is not applicable since the samples were tested at the same load range. Finally, for sample P10 (same family as P5), loading was initiated at 28-280N and it failed at 12539 cycles, a 34% increase from sample P5. The significant addition in the fatigue lives of samples P8 and P10 in comparison to P6 and P5 respectively, holds testament to the damage accumulation at the lower load cycles and attests to the additive effect formulated in Palmgren-Miner's rule (Palmgren 1924; Miner 1945).

Table 8 Compilation of a/W ratio, stress intensity values, and number of cycles to fatigue failure for samples P7-P10.

Sample	a/W ratio	ΔK (MPa√m)	$N_{failure}$
P7	0.6	3.1915	86
P8	0.5	2.2356	3849
P9	0.6	3.2071	71
P10	0.35	2.0404	12539

Given that UHMWPE is a fatigue brittle polymer, the crack initiation length couldn't be determined during fatigue experiments. The samples P7-P10 fatigued to failure catastrophically, precluding any observation of the crack's initiation or its measurement thereof. Consequently, all calculations reported herein are based solely on the a/W ratio. An increase in a/W ratio enforces a stronger stress intensity at the notch root. Table 8 compiles the ΔK values, number of cycles to failure, and a/W ratio for samples P7-P10 which are of interest in this study. Further, Figure 18 clearly shows how increasing stress intensity at the crack tip (increased a/W ratio) leads to a reduction in the fatigue life, as is theoretically expected and also, experimentally confirmed. The data from samples P7-P10 (fatigued at highest loads only) is plotted herein. The values of ΔK obtained in this study are higher than the threshold ΔK values obtained in another study, whereby $\Delta K_{threshold}$ = 1.08 MPa√m was obtained. Noteworthy to add here that the threshold data was collected in a radically different manner which involved running $\Delta K_{decreasing}$ tests up until the point where the crack growth rate was less than 10^{-7} mm/cycle. This may also be attributed to the fatigue brittle nature of UHMWPE and its sensitivity to peak stress intensity.

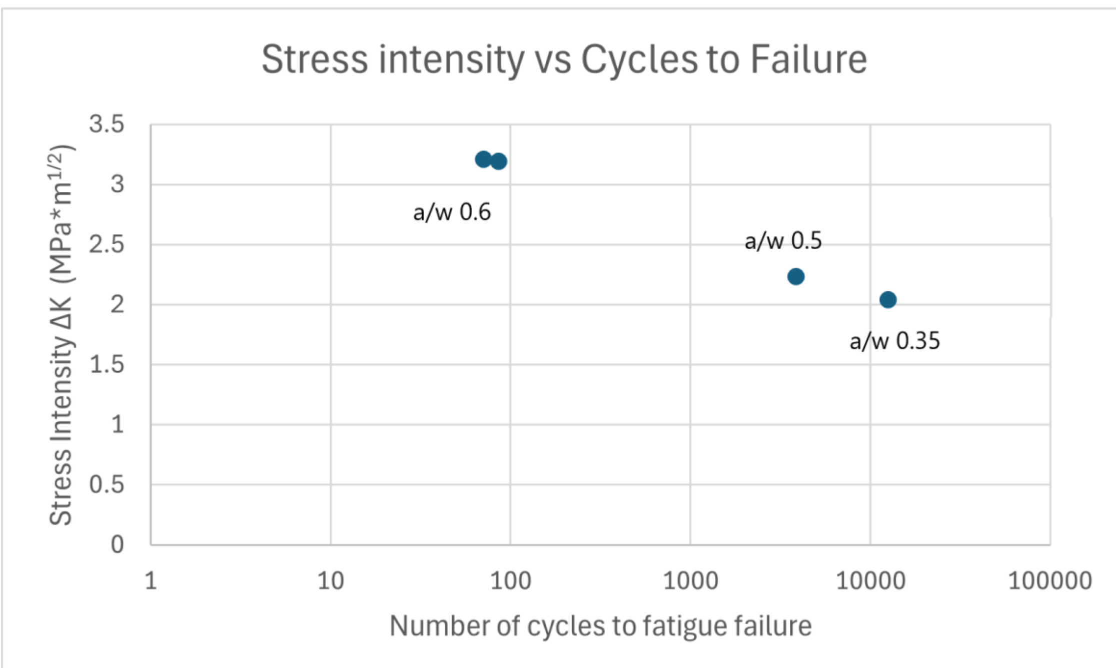

Figure 18 Stress intensity ΔK vs Number of cycles to failure (N) for the material type VXLPE.

Going forward, the a/W ratio of 0.6 may be discarded due to the excessively high stress intensity it imparts at the notch root and the extremely low number of fatigue cycles noted. Similarly, the a/W ratio of 0.25 should be avoided, especially for samples with higher notch root radii of 3mm as they might jeopardize the experiments by inadvertently creating undue stress concentrations in the region between the notch and pin holes. Future experiments must therefore work within the optimal window of a/W ratios spanning 0.35 to 0.5. Moreover, future parametric studies to be conducted can encompass different notch root radii including but not limited to 0.25, 1, and 3 mm, and different a/W ratios (range 0.35-0.5) as well as both sets of materials (UHMWPE and VXLPE) and decipher their individual and synergetic effects on the fatigue life. A parametric model with notch root radii, a/W ratio, and UHMWPE formulation as input parameters and fatigue life as the output parameter can be systematically developed thereafter. Efforts towards monitoring the moment of crack initiation can be undertaken by precisely syncing the frame rate of the optical camera for observing the fatigue test specimen and the frequency of the fatigue testing (5 Hz). That way, the sample would appear stationary and the exact moment a crack nucleates at or in the vicinity of the notch root, can be easily monitored. Crack initiation criteria could then be modified to $N_{initiation}$ instead of $N_{failure}$, even if the difference between the values is very marginal for a fatigue brittle polymer like UHMWPE.

4.6 Conclusions

This chapter summarizes some of the preliminary findings concerning the crack initiation behavior of UHMWPE with different a/W ratios, studied by fatiguing the samples to failure. The key results reaffirm the inverse relation between a/W ratio and the number of fatigue cycles to failure, which can be explained on account of the increased stress intensity experienced at the crack tip (notch root) for samples with higher a/W ratios. Additionally, the damage accumulation theory of Palmgren-Miner is evident by virtue of the significantly increased lifetime of samples from the same family (geometry, material formulation) when tested only at the highest load vis-à-vis the incremental increase in load. Future work could use multiple samples across different material formulations and aim to develop a parametric model encompassing three parameters of interest, viz. material formulation, a/W ratio, notch root radii and their relationship to the crack initiation behavior as well as fatigue life of UHMWPE.

Chapter 5 – Feasibility of using Diamond-Like Carbon films in total joint replacements

5.1 Societal Challenge: Osteoarthritis

Osteoarthritis is increasingly afflicting more and more people with as many as 32.5 million people suffering from it in the US alone ("Osteoarthritis (OA) | Arthritis | CDC" 2020). While initial remedies may include engaging in more physical activities and exercise, attempts to lose weight, medications, or even regular injections, a severely degraded osteoarthritic joint ultimately needs a total joint replacement (TJR) ("5 Ways to Manage Arthritis | CDC" 2023). This is especially important given the preponderance of osteoarthritic knees in the general population, afflicting as many as 10% of men and 13% of women above the age of 60 years (Zhang and Jordan 2010). An osteoarthritic hip afflicts about 20% of people above the age of 65 years (Fan et al. 2023). Further, the market demand for TJRs, which is the ultimate solution to extreme cases of osteoarthritic joints, is predicted to grow at staggering rates in the upcoming years (S. Kurtz et al. 2007). While TJRs substitute the original joint function, they too are an assembly of articulating mechanical components which are prone to failure and thus, have a finite lifetime. Consequently, the revision burden for total knee replacements (TKRs) stands at ~10% at the 15-year mark while that of total hip replacements (THRs) is at ~7% at the decade mark (Nugent et al. 2021; "Total Knee Replacement - OrthoInfo - AAOS" 2024). An additional complication is the duration of full recovery spanning over a year after knee revision surgeries and between 12-18 months for hip revisions ("Hip & Knee Revision Surgery Recovery Timeline" 2021).

5.2 Total Joint Replacements: types, components, and materials

The TJRs of interest in this chapter encompass the total hip replacement (THR) and total knee replacement (TKR), which act as artificial substitutes for the natural hip and knee joints respectively. Figure 19 (a) shows images of a healthy hip, an osteoarthritic hip, and a contemporary total hip replacement alongside the location where they are implanted. Similarly, Figure 19 (b) demonstrates the same set of images for the healthy knee, osteoarthritic knee, and total knee replacement. In Figure 19 (c) and (d), the individual components constituting the total hip and total knee replacements are illustrated. While different material combinations (Uwais et al. 2017) have been used for these individual components, the predominant materials of interest are as follows:

THR: Femoral head comprising CoCr (CoCrMo) alloy, zirconia, alumina, or Oxinium. Plastic liner made from Ultra-high Molecular Weight Polyethylene (UHMWPE) and acetabular shell composed of a Ti alloy (Ti_6Al_4V). Femoral stems utilize Ti_6Al_4V or CoCrMo alloys.

TKR: Femoral component prepared from CoCr alloy, the plastic spacer comprising UHMWPE, and the underlying tibial component utilizing a Ti-alloy as aforementioned.

There exist varied kinds of joint replacement systems including metal-on-polymer (MoP), metal-on-metal (MoM), ceramic-on-ceramic (CoC), and ceramic-on-polymer (CoP). The primary focus in this chapter will be on MoP given their predominant use in orthopedics (51%) followed by MoM (35%) and the rest being CoC and CoP (Uwais et al. 2017; Santavirta et al. 1998; Bozic et al. 2009). The MoP gold standard remains CoCr articulating against UHMWPE.

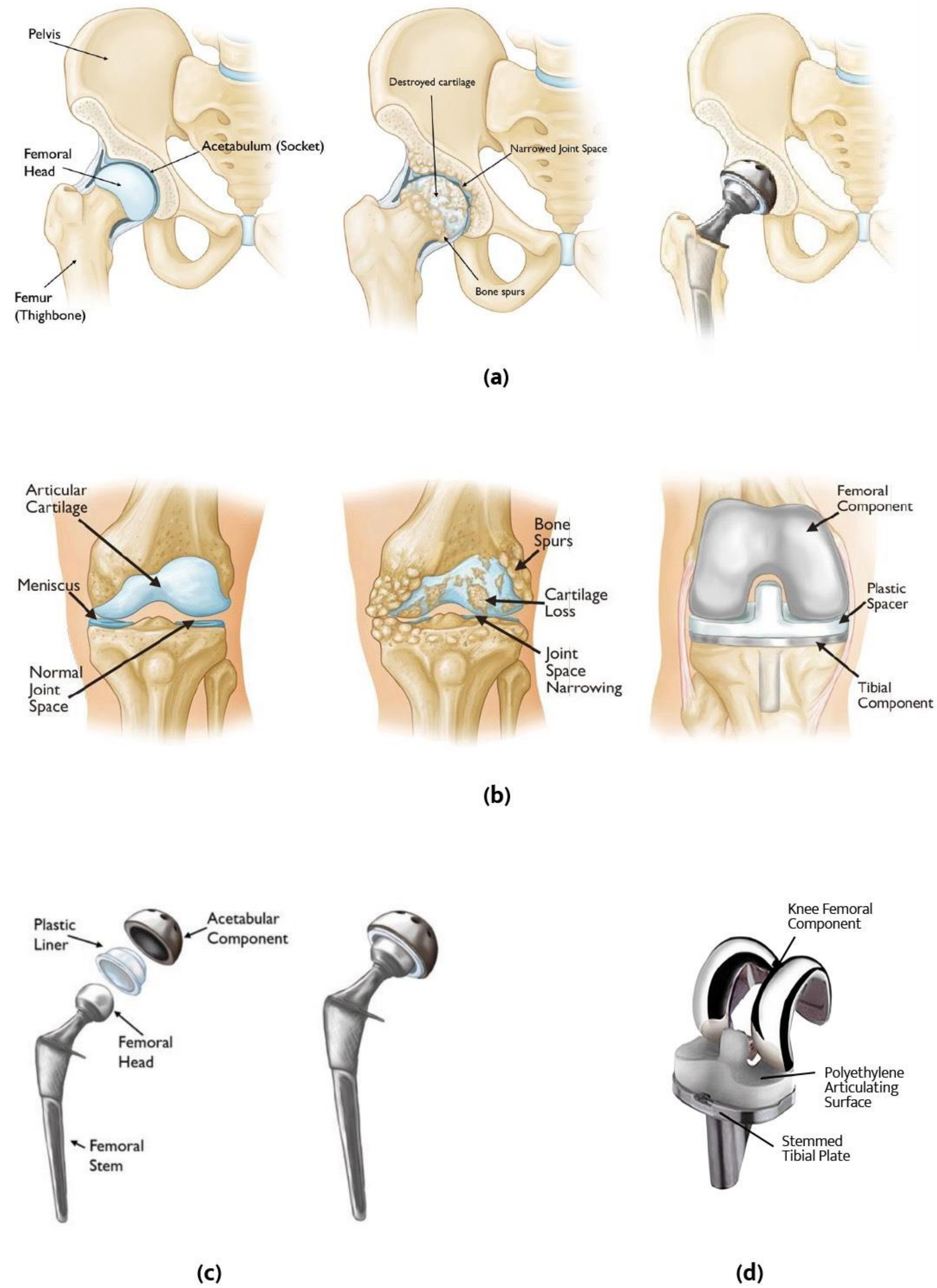

Figure 19 Healthy and unhealthy hip and knee joints, THR and TKR, and their individual components. Adapted from ("Total Knee Replacement - OrthoInfo - AAOS" 2024; "Total Hip Replacement - OrthoInfo - AAOS" 2024; Randive, Kumar, and Goyal 2015).

5.3 Challenges plaguing present-day TJRs

One of the main challenges to the current designs and materials arises from the fact that conventional designs and materials for TJRs were originally meant for an older demographic with a majorly sedentary lifestyle. Yet, the trend in orthopedics across hip and knee replacement is toward younger demographics with more active lifestyles (S. M. Kurtz et al. 2009). This puts additional loading demands on the TJR and affects performance requirements.

Another problem originates from the years of usage after the implantation of metallic components inside the aqueous environment of the body (making them prone to corrosion) and the variable loading on the joint space (inducing fatigue damage), continuous articulation during any locomotion (causing wear), and sudden impacts during physical activities (leading to possible fracture). Thus, the chances of mechanical failure through any of these modalities is greatly enhanced, i.e. through corrosion, fracture, fatigue, and wear (Ansari, Ries, and Pruitt 2016; S. M. Kurtz 2009). There are also secondary failure modalities combining these, such as fatigue-induced wear, fatigue-induced fracture, and stress-corrosion cracking.

In this chapter, the primary focus is confined to solving the challenges of corrosion and metal ion release associated with wear of the metallic component used in TJRs. Metal debris and ion release leads to metallosis, inflammation, hypersensitivity, and the possibility of pseudo tumors inside the body (Willis-Owen, Keene, and Oakeshott 2011; Archibeck, Jacobs, and Black 2000; Di Puccio and Mattei 2015).

A specific clinical challenge is related to metallic components in the femoral side of total hip replacements. Ti-alloy is generally used for the femoral stem owing to its excellent fatigue resistance as well as its propensity to mitigate stress shielding while affording mechanisms for osseointegration. Unfortunately, Ti alloys suffer from poor wear performance and fretting corrosion. For these reasons, the Ti alloy is not used as a bearing surface in a TJR space and instead the Ti stem is often coupled to a Co-Cr head through a Morse taper (S. M. Kurtz 2009). Such modular systems offer mechanical advantages but render the system prone to local galvanic or crevice corrosion processes (Ghadirinejad et al. 2023; Urish et al. 2019). However, with a robust coating applied on its surface, Ti potentially becomes a candidate for the femoral head (Shah et al. 2021). This would enable the use of a monolithic Ti-alloy femoral component that could mitigate wear and corrosion mechanisms.

5.4 Potential Solution: Diamond-like Carbon overcoats

One plausible solution to the aforementioned problems is the utilization of Diamond-like Carbon (a.k.a. DLC) (Dearnaley and Arps 2005; Butter and Lettington 1995) coatings on the metallic component of the orthopedic bearing system. This would entail its application as an overlay on CoCr to potentially solve the corrosion and metal-ion release problems as well as potential to make Ti a candidate for articulating elements such as the femoral head. A holistic assessment of DLC technology for creating a protective overlay that mitigates wear, corrosion, and metal ion release is the overarching theme of this chapter.

The interest in DLC for TJR applications arises from its unique bio-tribo-thermo-mechanical performance in multiple application domains (Bhatia et al. 1998; A. Roy, Wang, and Komvopoulos 2023; Robertson 2001; Xu and Pruitt 1999; Grill 1997; Lettington 1998; Grill 2003; Mehta and Cooper 2003; Sze and Tay 2006; Dowling et al. 1997; Casiraghi, Robertson, and Ferrari 2007; Moser et al. 1998; Cheah et al. 1998; Luo et al. 2007; Wu et al. 2013; Komvopoulos 1996; Tiainen 2001; R. K. Roy and Lee 2007). This combination of attributes includes biocompatibility; wear resistance, high hardness and low coefficient of friction; thermal stability and chemical inertness; strong adhesion to metallic substrates; as well as the ability for tailored, through-thickness microstructures (Dearnaley and Arps 2005; Xu and Pruitt 1999; Robertson 2002; Yeo et al. 2015; Na Wang and Komvopoulos 2013; S. Wang, Roy, and Komvopoulos 2021; J. Yeo et al. 2017; Dwivedi et al. 2017). Figure 20 summarizes the favorable features exhibited by DLC films for use in TJR.

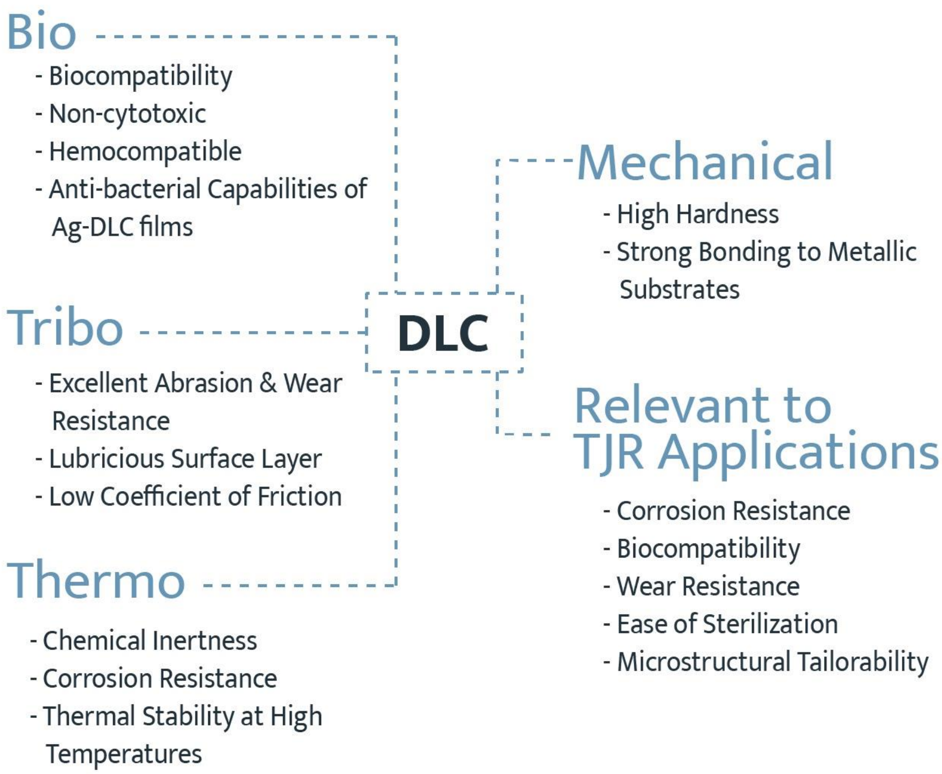

Figure 20 DLC's bio-tribo-thermo-mechanical characteristics, which make it an ideal candidate for use in TJR applications. Adapted from (A. Roy, Wang, and Komvopoulos 2023)

5.5 DLC's applicability to TJR systems

For materials being considered for TJRs, it is paramount that they be biocompatible and can be implanted inside the body without causing any adverse effects in patients. DLC coatings are generally considered to be bioinert and biocompatible. Studies addressing cytotoxicity, hemocompatibility, thrombogenicity, and cell-growth indicate that DLC coatings are viable candidates for implantable biomaterial applications (Dearnaley and Arps 2005; Butter and Lettington 1995; Grill 2003; Ma et al. 2007; Anne Thomson et al. 1991; Allen, Law, and Rushton 1994; Steffen, Schmidt, and Gonzalez-Elipe 2000; Allen, Myer, and Rushton 2001; Singh et al. 2003; Hauert 2003; Gutensohn et al. 2000).

DLC coatings show promise for the mitigation of corrosion processes in the body. Notably, DLC films on orthopedic grade CoCrMo in a simulated body fluid environment have been shown to corrode at a rate of 4-5 orders of magnitude lower than an uncoated counterpart (Sheeja et al. 2001). Other tribo-corrosion studies using DLC on CoCrMo or Ti alloy substrates in biological environments have also affirmed their corrosion resistance (Sheeja et al. 2001; J. Liu et al. 2013; Reijo Lappalainen et al. 1998; Tiainen 2001).

Further, positive research results on DLC coatings for orthopedic and maxillofacial screws as well as coronary artery stents gives further credence to their potential as an overlay to preclude metal ion release and corrosion along with chronic inflammatory response spanning prolonged durations (Butter and Lettington 1995; Gutensohn et al. 2000; Mitura et al. 1994; Olborska et al. 1994). The addition of Ag to form composite Ag-DLC films enhances the films' anti-bacterial capabilities, which favor the possibility of it being used in TJRs (Chekan et al. 2009; Marciano et al. 2009).

DLC-coated CoCr and Ti alloys have performed well tribologically against UHMWPE and evince a significant reduction in wear in TJRs (Xu and Pruitt 1999; Tiainen 2001; Oñate et al. 2001; Affatato, Frigo, and Toni 2000; R. Lappalainen, Anttila, and Heinonen 1998; Dong, Shi, and Bell 1999). DLC-coated metallic components could reduce metal ion release into the body and thereby prevent complications arising from the adverse biological reactions they elicit as there would be no direct contact between the polymer bearing and the metallic components of the TJRs. Thus, it is hypothesized that DLC would reduce the severity of the ongoing challenge with metal-ion release in orthopedic devices.

The thermal stability of DLC coatings assures that sterilization will not be cause for concern in orthopedic components. Nanoscale films of DLC maintain their thermo-mechanical properties and structural integrity up to temperatures of 250˚C (S. Wang and Komvopoulos 2020). Given that autoclaving (121˚C) and ethylene oxide (EtO) sterilization (~60˚C) transpire at much lower temperatures, it can be safely presumed that these treatments will not cause thermal deterioration of the DLC coatings. In that same vein, given the exceptional chemical inertness of DLC films (Robertson 2002), it is unlikely to be affected by the chemical agents used during EtO sterilization.

5.6 Multilayered structure of DLC

One particularly interesting facet of DLC films is their microstructural tailorability (Na Wang and Komvopoulos 2013; J. Matlak, Rismaniyazdi, and Komvopoulos 2018; J. Matlak and Komvopoulos 2018). This is especially applicable to DLC films deposited using two specialized techniques, namely, filtered cathodic vacuum arc (FCVA) and plasma-based immersion methods (PBIIID). In both cases, the films exhibit a multi-layered structure. A typical DLC film produced through these two methods is comprised of three layers: a surface layer with a higher percentage of sp^2 hybridized carbon (more graphite-like) followed by a bulk layer which is extremely hard owing to a predominantly sp^3 hybridized state (more diamond-like), and an intermixing layer (Na Wang and Komvopoulos 2013; J. Matlak, Rismaniyazdi, and Komvopoulos 2018).

The soft and lubricious surface layer is responsible for the low coefficient of friction and smooth articulation against the counter-surface in tribologically challenging applications, such as bearing surfaces in TJRs. On the other hand, the core bulk layer provides thermal stability, chemical inertness, hardness, as well as wear and corrosion resistance. The intermixing layer acts as a transition layer between the bulk of the carbon film and the underlying substrate, aiding interfacial adhesion, and precluding delamination by reducing the adverse effect of sharp stress-strain gradients at the interface (A. Roy, Wang, and Komvopoulos 2023). Instead, the intermixing layer provides a smooth gradient between the two radically different layers, i.e., carbon and metal. The multilayered structure of DLC films is best visualized in Figure 21.

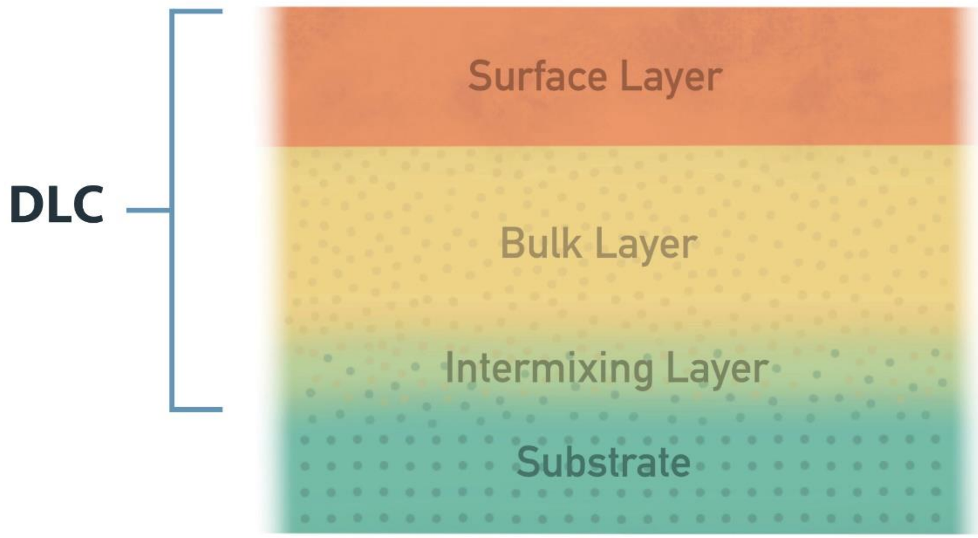

Figure 21 DLC's multilayered structure.

5.7 DLC synthesis

There is a plethora of synthesis techniques to deposit DLC coatings atop metallic substrates, such as sputtering, ion beam-assisted deposition, plasma-enhanced chemical vapor deposition, plasma-based immersion methods, and filtered cathodic vacuum arc. Roy et al. provide a comprehensive review of the specialized coating techniques applicable to DLC film synthesis (A. Roy, Wang, and Komvopoulos 2023). Two techniques stand out for the exceptionally hard and dense coatings they produce concomitant with precise microstructural control of the DLC film. These are the plasma-based immersion ion implantation and deposition (PBIIID) and filtered cathodic vacuum arc (FCVA). Sputtered films are commonly utilized owing to their quality, functionality, and cost efficiency.

FCVA and PBIIID are strikingly similar from the deposition physics standpoint. The difference between them is that the physical object is placed on the path of a plasma stream in FCVA (thereby coating a plane surface) rather than being immersed in a plasma cloud as is the case with PBIIID (3D object coating). The 3D coating ability offered by PBIIID makes it the technique of choice over FCVA, since most TJR components have 3D geometries. However, FCVA offers the ability to co-deposit carbon along with other metal ions to form DLC composite coatings with enhanced functionalities which is not possible in PBIIID. An illustration conveying the subtle differences in the setups for FCVA and PBIIID is presented in Figure 22. The best deposition method would be a PBIIID chamber that sources the individual plasma streams from multiple sides using multiple FCVA-systems adjoining the PBIIID chamber, thereby integrating FCVA with PBIIID to maximize the synergistic benefits of both these specialized DLC coating methods. This integrated setup could be applied for coating TJR components with DLC as discussed in this chapter.

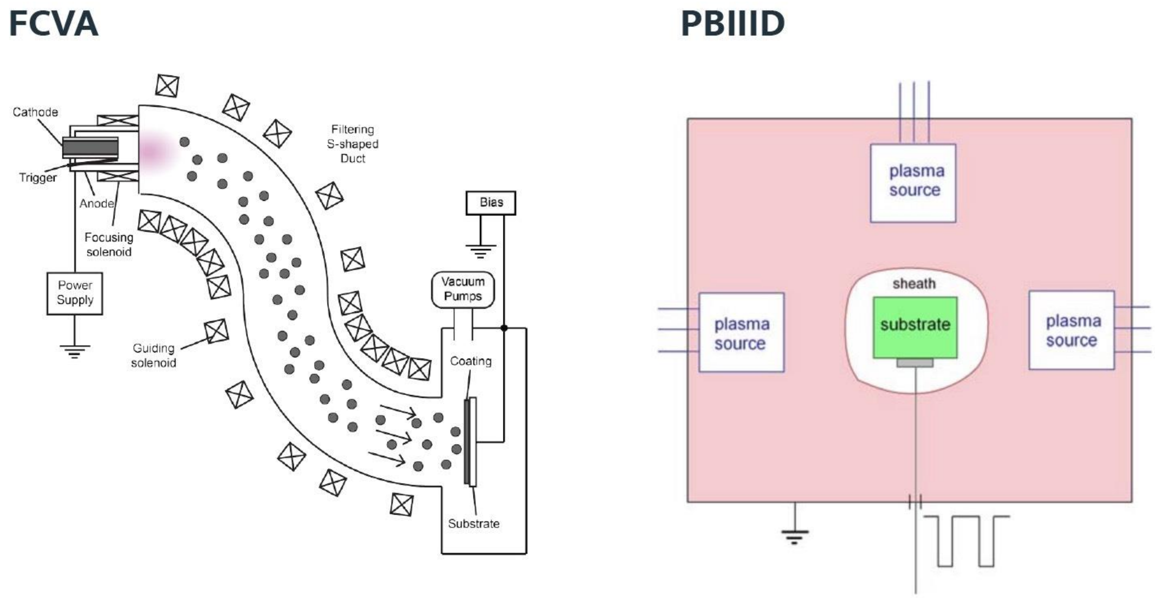

Figure 22 Coating of 2-D substrates supported by FCVA and 3-D components by PBIIID (Jozef Matlak 2017; Anders 2008).

5.8 Tribo-material characterization of DLC on TJRs

The tribo-material landscape of DLC overcoats on metallic components must be fully explored before making a final recommendation concerning TJRs. Material characterization should include visualization of the cross-section of the coating-substrate interface using Scanning Electron Microscopy (SEM) or High-Resolution Transmission Electron Microscopy (HRTEM). These techniques help identify key morphological attributes of the films such as uniformity, conformity, continuity, and surface roughness (S. Wang, Roy, and Komvopoulos 2021; Robertson 2003; Bhatia et al. 1998).

Electron Energy-Loss Spectroscopy (EELS) (S. Wang, Roy, and Komvopoulos 2021; J. Matlak, Rismaniyazdi, and Komvopoulos 2018; J. Matlak and Komvopoulos 2018; J. Xie and Komvopoulos 2016; Jun Xie and Komvopoulos 2016b) is typically utilized to characterize the intermixing layer which is intrinsic to FCVA- and PBIIID-deposited DLC films. EELS provides a chemical fingerprint of the elements present at specific locations on the cross-section and is beneficial in ascertaining the extent of carbon penetration into the underlying metallic substrate. The depth of carbon penetration into the underlying matrix defines the intermixing layer thickness and correlates with the adhesion strength as well as reduction in the possibility of delamination at the coating-substrate interface (A. Roy, Wang, and Komvopoulos 2023).

Tribological characterization is broadly classified into three categories: a) wear and friction tests, which include both pin-on-disk (PoD) bench tests as well as joint simulator testing, b) post-wear fractography, and c) surface roughness measurements.

5.8.1 Wear and friction tests

Historically, tribological wear evaluations were performed on simple PoD bench setups using a circular unidirectional motion test. However, this method fails to emulate the multidirectional cross-shear motion that is commonly experienced in TJRs (A Wang et al. 1998). Rudimentary PoDs therefore remain constrained to preliminary material assessments and exploring simple wear behavior of material systems.

Joint simulators were developed to emulate the complex kinematics and loading of the gait cycle. Such systems allow for assessment of various combination of designs, materials, and lubrication schemes for TJRs (A. Wang 1997; Bragdon 1997; A. Wang et al. 1996; Edidin et al. 1999; Saikko and Calonius 2002; Aiguo Wang et al. 2013; Brockett et al. 2016; de Villiers and Shelton 2016; Dalli et al. 2022). Complex joint simulators combine multiple motions and multidirectional loads, making them more pertinent for final-stage design and material selections but these expensive and time-consuming tests fail to isolate the fundamental mechanisms of wear at the constituent level.

Alternatively, multi-directional tribometers capture a wide variety of motions and loadings, starting from simple pin-on-disk in planar sliding to complex rolling and rotation motions in ball-on-flat contacts under clinically relevant conditions (Patten et al. 2013; Atwood et al. 2011; Chyr, Sanders, and Raeymaekers 2013). The tribo-couple of relevance is UHMWPE articulating against DLC-coated metallic TJR components (CoCr or Ti alloy) in all tribological experiments.

Tribological tests enable characterization of coefficients of friction as well as the adhesion behavior of the DLC coatings. Thicker intermixing layers inherent in certain deposition techniques such as FCVA and PBIIID lead to stronger adhesion at the coating-substrate interface (Dwivedi et al. 2017; N. Wang and Komvopoulos 2014; Dwivedi et al. 2016). Enhanced adhesion of the coating reduces the likelihood of delamination and premature failure in TJRs. Moreover, precluding delamination mitigates metal ion release from the underlying substrate and its consequent toxic effects in the body.

5.8.2 Post-wear fractography

Fractography provides insight into coating failure modality and mechanisms of wear. Post-articulation SEM of worn components has revealed a number of wear mechanisms including abrasive, adhesive, surface fatigue, and delamination (A Wang et al. 1998; Oñate et al. 2001; Zhou et al. 2004). SEM fractography of the DLC-coated metallic components is requisite in assessing whether delamination or surface damage is of concern in TJRs. Delamination or spalling of the coating is detrimental as particulate debris can lead to metallosis and metal ion release in the body.

5.8.3 Surface roughness measurements

The final step in completing the tribo-material characterization of TJRs involves measuring the surface roughness of the DLC-coated TJR components via Atomic Force Microscopy (AFM) or Surface Force Microcopy (SFM) (Robertson 2003; Jun Xie and Komvopoulos 2016a; J. Xie and Komvopoulos 2015a; J. Matlak and Komvopoulos 2015; J. Xie and Komvopoulos 2015b).

The effect of surface roughness on the tribological performance of DLC films in TJRs has two possible outcomes which are posited here. First, that the higher surface roughness of the sputtered DLC (sputtered DLC is much more prone to island-like growth in comparison to FCVA or PBIIID (S. Wang, Roy, and Komvopoulos 2021; Robertson 2003; Jun Xie and Komvopoulos 2016a; J. Xie and Komvopoulos 2015a; J. Matlak and Komvopoulos 2015; J. Xie and Komvopoulos 2015b)) act as reservoirs for the lubricant during the articulation. During stages of limited lubricant supply to the joint space, the inherent reservoirs may assist in boundary lubrication, thereby reducing the coefficient of friction and the rate of wear occurring at the site of articulation. The second theory runs contrary to the previous one, claiming that the increase in surface roughness acts as a reservoir for storing wear debris, which would then go on to detrimentally affect the tribological performance by catalyzing three-body wear. A visual of these effects is illustrated in Figure 23.

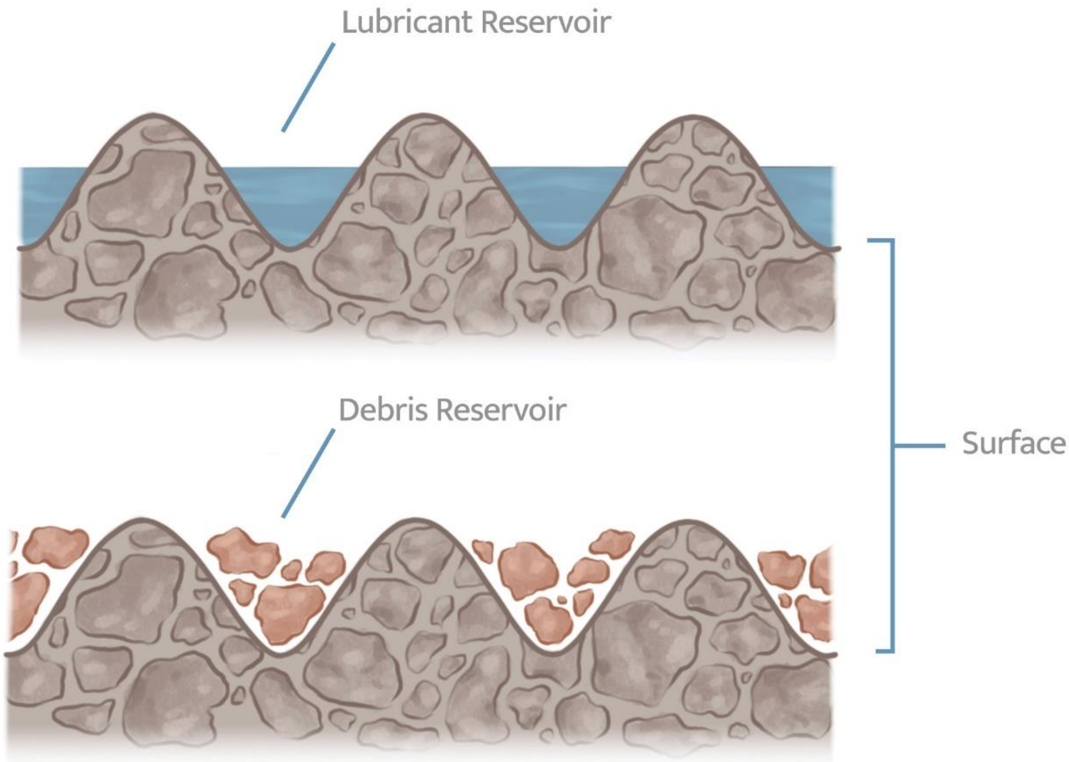

Figure 23 Surface roughness as a lubricant reservoir or debris reservoir hypothesis.

In order to assess requisite tribological performance of DLC coatings in orthopedics, the influence of surface roughness and lubrication regimes in the articulating joint space needs to be examined in future studies. Whether surface roughness acts as a reservoir of lubricant or third body wear debris or both will have serious implications on increasing/decreasing the resilience of DLC-coated metallic components in TJRs. These findings will foretell the likelihood of clinical success for incorporating DLC technology in TJRs.

5.9 Challenges with using DLC in TJRs

In the realm of orthopedics, contemporary formulations of UHMWPE with optimized crosslinking and anti-oxidant technology have majorly rectified the wear-mediated osteolysis problem (Oral and Muratoglu 2011). A further reduction in wear could enhance the lifetime of the TJRs by precluding implant loosening and associated failures. Figure 24 illustrates how wear debris from any source in a joint replacement can culminate in the eventual failure of the implant. Tribological testing which closely simulates the joint space conditions will need to be performed in order to assess DLC-coated metallic components articulating against modern UHMWPE components. This is important as previous wear studies reporting favorable wear outcomes between DLC and UHMWPE were conducted using older formulations of UHMWPE which are no longer clinically relevant (Xu and Pruitt 1999; Tiainen 2001; Oñate et al. 2001; Affatato, Frigo, and Toni 2000; R. Lappalainen, Anttila, and Heinonen 1998; Dong, Shi, and Bell 1999).

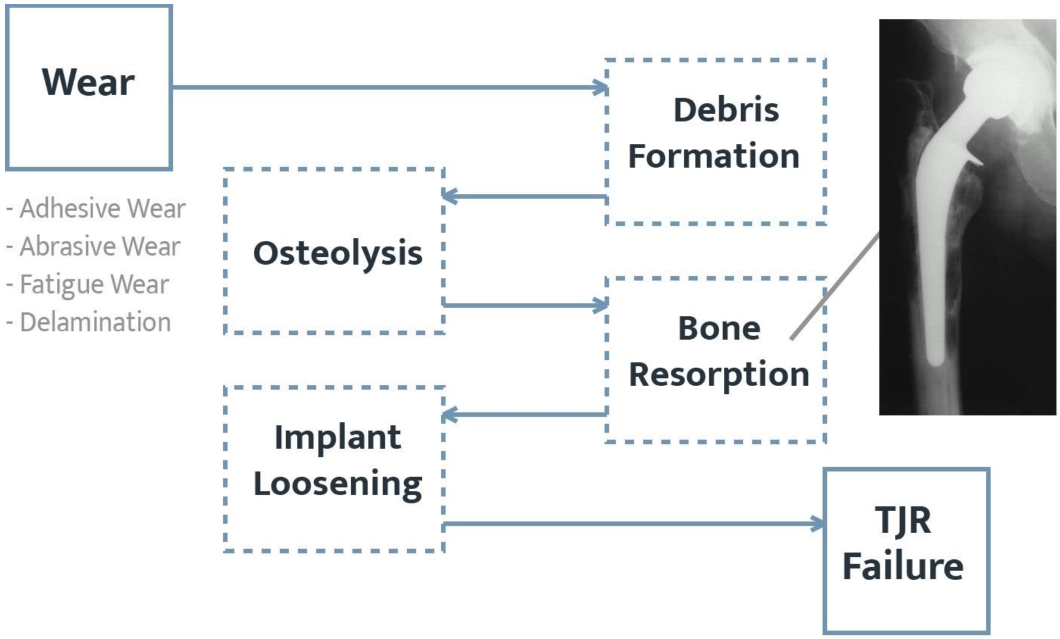

Figure 24 Various modalities of wear leading to the eventual failure of TJRs. Adapted from (Archibeck et al. 2000)

A caution for DLC technology in orthopedics is that some of the tribological literature is not only outdated but also contradictory. Some earlier studies discourage the use of DLC in TJR systems, albeit on older formulations of UHMWPE. In some cases, there were increases in the wear rates for the DLC-coated CoCrMo-UHMWPE coupling (Sheeja et al. 2001; Saikko et al. 2001; H. Liu et al. 2012). Moreover, DLC coatings on Ti substrates showed no tribological improvements when articulating against UHMWPE in comparison to the gold standard of CoCr against UHMWPE under a multidirectional pin-on-disk test setup (Escudeiro et al. 2015).

Some researchers have expressed concerns from their experiments on UHMWPE against DLC-coated ceramic substrates hypothesizing that the UHMWPE-DLC pair might exhibit high adhesion forces which is unfavorable from a tribological standpoint (Choudhury et al. 2015). While the substrates were ceramic in nature, the high adhesion reported between UHMWPE and DLC is irrespective of the underlying substrate material and is cause for concern. Another study found no improvement in the corrosion resistance behavior exhibited by DLC-coated Ti in comparison to bare Ti substrates (Manhabosco and Muller 2009). Finally, there have also been reports of low survivorship (54%) and aseptic loosening of DLC-coated Ti alloy components amongst THR patients barely 90 months after implantation (Taeger et al. 2003).

While DLC shows promise and should be considered for further exploration in TJRs, it does come with some additional caveats. Designers need to be mindful of Hertzian contact stresses during tribological articulation (Arnell et al. 1991); peak stresses that coincide with the DLC coating-metal substrate interface could facilitate delamination, corrosion, and metal-ion release. To surmount this, the coating thickness must be optimized to ensure that the Hertzian stress peak does not coincide with the interface where propensity for delamination is greater.

Another concern is that DLC films are hydrophobic by nature and may interfere with natural lubrication schemes in-vivo (Paul, Das, et al. 2008; Paul, Dalui, et al. 2008). A more hydrophilic material is preferred in TJRs since it draws in the synovial fluid and facilitates lubrication in the joint space. A hydrophobic material's incorporation could potentially exacerbate this tribological challenge and starve the joint space of much-needed natural lubricant. More work is needed in these areas to ascertain whether DLC technology is beneficial in the realm of modern orthopedic devices and material formulations.

5.10 Conclusions and outlook

In summary, it is recommended that the possibility of incorporating DLC films as potential coatings on metallic TJR components be explored further to solve the problems pertaining to wear, metal ion release, and corrosion. With the ever-increasing demand for arthroplasty in both the elderly and younger, more active patient populations, there is a need to find materials that can optimize long-term clinical performance of TJRs. DLC technology with its bio-tribo-thermo-mechanical attributes and tailorability potentially aids in this endeavor.

Chapter 6 – Conclusions and Future Directions

Osteoarthritis has been an affliction affecting humans since time immemorial. In the past six decades, however, the go-to 'cure' for severe cases of osteoarthritis has been to undertake a surgical procedure called total joint replacement (TJR) which encompasses total hip, total knee, and total shoulder replacements. TJRs primarily use a polymer bearing with a ceramic or metallic counter-bearing as articulating components. The polymer of choice for the bearing is Ultra-high molecular weight polyethylene (UHMWPE), which was originally chosen for a multitude of reasons such as its energetic toughness, mechanical strength, biocompatibility, and more. While there have been incremental improvements in the material formulation(s) to improve its bio-tribo-mechanical characteristics, UHMWPE is still plagued by a variety of problems associated with its wear, fatigue, and oxidation when used in TJRs. The metallic components in TJRs are also known to suffer from similar problems pertaining to wear, corrosion, and metal-ion release. This has led to a push for discovering new material systems like Polyether ether ketone (PEEK) and its composites that could potentially substitute the current polymer with augmented performance in-vivo. Moreover, enhancing the surface and sub-surface properties of TJR components via varied surface modification methods ranging from plasma surface processing to coatings (such as Diamond-like carbon) have also been gaining traction lately.

To begin with, this thesis extensively reviews the complex topic of fatigue of polymers. Existing theoretical models that can be employed to predict the fatigue life of polymeric components are included, particularly the total-life and the defect-tolerant philosophies to fatigue are studied in-depth. The fundamental difference between the two being that the former is predicated on the assumption that the material is originally defect-free and that, a significant portion of the fatigue life goes into crack initiation while the latter philosophy starts with the assumption that all materials have initial flaws (or stress concentrations that act as sites of crack nucleation) and that stable crack growth makes up a predominant share of the fatigue life of a component prior to eventual fracture. Both philosophies have underlying assumptions which don't necessarily hold true throughout the entirety of the service life of a structural component. Parameters of interest that dramatically influence the fatigue life and fatigue micro-mechanisms in polymers are identified. These include mechanical variables such as frequency, strain rate, waveform, temperature, and ambient environment. Other microstructural and molecular parameters also have a significant impact on the fatigue life of these components, such as the molecular weight, crystallinity, and crosslinking density. Therefore, it is absolutely incumbent upon researchers and designers to strongly mimic the real-life conditions that a polymeric component will be put through during its time in service, to obtain a realistic estimate of its fatigue life and behavior. The chapter devoted towards fatigue of polymers acts as a centralized repository for researchers, design engineers, and industry professionals by virtue of it encompassing both the classical works as well as latest developments in this field.

Next, PEEK and PEEK composites' bio-tribo-mechanical characteristics are delved into with the aim of comparing it to the current gold standard of UHMWPE for use as a potential substitute material in the polymeric bearings in TJRs. This effort has been hampered by the lack of retrieval studies as well as the deep divide amongst clinical findings and lab testing of PEEK and its composites. Exacerbating the problem further is the lack of a standard for tribo-mechanical testing across different research groups with each one defining their own set of parameters and the technical difficulties witnessed in replicating in-vivo conditions, like the human body's dynamic lubrication regime in the joint space and in capturing the intricacies of the lubricant's behavior with changes in loading, pH, temperature, and other external factors. The conflicting results reported in the wear-related literature don't help either. Despite the aforementioned challenges, some key conclusions can be drawn. First, the wear rate is significantly higher in the case of carbon-fiber reinforced PEEK than that of modern formulations of UHMWPE under high-stress non-conforming contact situations experienced in knee replacements. Therefore, CFR-PEEK is not a potential substitute to UHWMPE in this specific joint space. Rather, their use in low-stress highly conforming geometries as seen in hip joints has found rather encouraging results. Second, the literature overwhelmingly supports the biocompatibility attribute of PEEK and PEEK composites, as ascertained in the bulk (macro-scale) and particulate form (micron-scale) while emphasizing the urgent need to ascertain the same at the nano-level, given the nano-scale wear debris produced in the joint space from the constant articulation between different TJR components in action. Third, numerous factors impacting biocompatibility are identified and analyzed into a parametric model involving factors like particles' size, mass distribution of particles, material type, dosage/concentration of wear particles at the implant site, surface area and volume of wear debris formed, wear debris composition and morphology, and volume fraction of filler material (for PEEK composites). The inherent variations in the methodologies used to assess biocompatibility are also highlighted, such as testing in-vivo or in-vitro, and even amongst in-vivo studies whether it was through animal studies or clinical trials in humans. Biocompatibility evaluation using a bulk implant/fixation device or as a subcutaneous implantation, and the length scale variations in studies, viz. biocompatibility in the bulk form vs at the particulate form are considered. Finally, no conclusive recommendation can be made towards incorporating PEEK and PEEK composites in knee replacements although further exploration is warranted in the context of the hip replacements.

Thereafter, the document pivots towards reporting initial findings in the context of crack initiation behavior in UHMWPE. Fatigue life can be divided into two components- crack initiation and crack propagation. Given the preponderance of crack propagation studies pertaining to UHMWPE that are available in the literature, the focus was directed towards investigating the crack initiation behavior, particularly in the context of clinically relevant geometries and design features that are inherent to TJRs, for instance, notches, undercuts, fillets, etc. This has been accomplished by conducting fatigue tests on medical grade UHMWPE till failure ensues. Two different formulations of UHMWPE, a/W ratios, and notch geometries each are included within the scope of this work. The results confirm the inverse relationship demonstrated between a/W ratio and number of cycles to fatigue failure. The technical explanation for this observation is that as the a/W ratio is increased, it imparts a heightened stress intensity at the crack tip, which in this particular study is the notch root, and a higher stress intensity experienced therein leads to a reduced fatigue life reflected in the smaller number of cycles to crack initiation and eventual fatigue failure. Moreover, the damage accrued via different fatigue loads building up to failure goes on to prove the Palmgren-Miner rule as proven by the markedly higher fatigue lifetimes of specimens tested at the highest loads vis-à-vis incrementally increasing loads that add up. With further experiments, it would be possible to develop a parametric model with input parameters as notch root radii, a/W ratio, and material formulation while crack initiation behavior and fatigue life would be the output parameters of interest.

The final part of the thesis examines the possibility of incorporating Diamond-like Carbon (DLC) as a coating on the metallic components in TJRs with a wider goal of augmenting the quality and increasing the lifetime of these devices inside the body. It would thereby reduce the need for revision surgeries and cater to the needs of the younger, more active demographics that are increasingly being affected by this malaise. The choice of DLC is attributed to its bio-tribo-thermo-mechanical excellence. Its feasibility is assessed as a potential solution for the troika of problems currently plaguing the metallic components of TJRs, i.e. wear, corrosion, and metal-ion release. The advantages as well as anticipated problems with bringing DLC into the orthopedic realm are discussed. Caveats surrounding DLC coatings such as delamination, hydrophobicity of DLC, and conflicting results in the current literature are highlighted. A prudent exploration of DLC coating technology as a potential thin-film coating on the metallic components of TJRs is recommended. The final conclusion remains that DLC should be integrated with TJRs in clinical settings only after all aforementioned challenges and concerns are fully addressed.

In sum, this thesis encapsulates the bio-tribo-mechanical characteristics of orthopedic-grade polymers and diamond-like carbon overcoats for total joint replacement systems. This work has broad implication to the field of orthopedic biomaterials.

REFERENCES

5 Ways to Manage Arthritis | CDC. (2023, June 13). https://www.cdc.gov/arthritis/basics/management.htm

Abdullah, M., Goharian, A., Kadir, M., Wahit, M., 2015. Biomechanical and bioactivity concepts of polyetheretherketone composites for use in orthopedic implants - a review. Journal of Biomedical Materials Research Part A 103, 3689–3702.

Affatato, S., Frigo, M., Toni, A., 2000. An in vitro investigation of diamond-like carbon as a femoral head coating. Journal of Biomedical Materials Research, 53(3), 221–226.

Ahmad, Z.B., Ashby, M.F., Beaumont, P.W.R., 1986. The contribution of particle-stretching to the fracture toughness of rubber modified polymers. Scripta Metallurgica 20(6), 843–848.

Aitasalo, K.M., Piitulainen, J.M., Rekola, J., Vallittu, P.K., 2014. Craniofacial bone reconstruction with bioactive fiber-reinforced composite implant. Head Neck 36(5), 722–728.

Allen, M., Law, F., Rushton, N., 1994. The effects of diamond-like carbon coatings on macrophages, fibroblasts and osteoblast-like cells in vitro. Clinical Materials, 17(1), 1–10.

Allen, M., Myer, B., Rushton, N., 2001. In vitro and in vivo investigations into the biocompatibility of diamond-like carbon (DLC) coatings for orthopedic applications. Journal of Biomedical Materials Research, 58(3), 319–328.

American Society for Testing and Materials, 2012. Standard Practice for Direct Contact Cell Culture Evaluation of Materials for Medical Devices. ASTM International.

Ames, B.N., McCann, J., Yamasaki, E., 1975. Methods for detecting carcinogens and mutagens with the Salmonella/mammalian-microsome mutagenicity test. Mutat. Res.;(Netherlands) 31.

Amjadi, M., Fatemi, A., 2020. Creep and fatigue behaviors of High-Density Polyethylene (HDPE): Effects of temperature, mean stress, frequency, and processing technique. International Journal of Fatigue 141, 105871.

Anders, A., 2008. Physics of plasma-based ion implantation & deposition (PBIID) and high power impulse magnetron sputtering (HIPIMS): A comparison. Physica Status Solidi (a), 205(4), 965–970.

Anderson, T.L., 1995. Fracture Mechanics: Fundamentals and Applications, 2nd Edition. Ann Arbor, MI: CRC Press.

Andrews, E.H., 1969. Fatigue in polymers. In: Brown, W. (Ed.), Testing of Polymers, vol. 4. New York, NY: Wiley, pp. 237–296.

Anne Thomson, L., Law, F. C., Rushton, N., Franks, J., 1991. Biocompatibility of diamond-like carbon coating. Biomaterials, 12(1), 37–40.

Ansari, F., 2015. The Interplay of Design and Materials in Orthopedics: Evaluating the Impact of Notch Geometry on Fatigue Failure of UHMWPE Joint Replacements. In: Ph.D. Thesis, UC Berkeley.

Ansari, F., Gludovatz, B., Kozak, A., Ritchie, R. O., Pruitt, L. A., 2016. Notch fatigue of ultrahigh molecular weight polyethylene (UHMWPE) used in total joint replacements. Journal of the Mechanical Behavior of Biomedical Materials, 60, 267–279.

Ansari, F., Ries, M. D., Pruitt, L., 2016. Effect of processing, sterilization and crosslinking on UHMWPE fatigue fracture and fatigue wear mechanisms in joint arthroplasty. Journal of the Mechanical Behavior of Biomedical Materials, 53, 329–340.

Ansari, F., Ries, M., Pruitt, L., 2016. Effect of processing, sterilization and crosslinking on UHMWPE fatigue fracture and fatigue wear mechanisms in joint arthroplasty. Journal of the Mechanical Behavior of Biomedical Materials 53, 329–340.

Ansari, F., Ries, M.D., Pruitt, L., 2016. "Effect of processing, sterilization and crosslinking on UHMWPE fatigue fracture and fatigue wear mechanisms in joint arthroplasty." Journal of the

Mechanical Behavior of Biomedical Materials 53, 329–340.
Arad, S., Radon, J.C., Culver, L.E., 1971. Fatigue crack propagation in polymethylmethacrylate. Journal of Mechanical Engineering Science 13, 75–81.
Archibeck, M. J., Jacobs, J. J., Black, J., 2000. Alternate Bearing Surfaces in Total Joint Arthroplasty: Biologic Considerations. Clinical Orthopaedics and Related Research (1976-2007), 379, 12–21.
Archibeck, M. J., Jacobs, J. J., Roebuck, K. A., Glant, T. T., 2000. The Basic Science of Periprosthetic Osteolysis. The Journal of Bone and Joint Surgery-American Volume, 82(10), 1478–1489.
Archibeck, M.J., Jacobs, J.J., Black, J., 2000. Alternate bearing surfaces in total joint arthroplasty: biologic considerations. Clinical Orthopedics and Related Research 379, 12–21.
Arevalo, S.E., Arthurs, C., Echeverria Molina, M.I., Pruitt, L., Roy, A., 2023. An overview of the tribological and mechanical properties of PEEK and CFR-PEEK for use in total joint replacements. Journal of the Mechanical Behavior of Biomedical Materials 145, 105974.
Arevalo, S.E., Pruitt, L.A., 2020. Nanomechanical analysis of medical grade PEEK and carbon fiber-reinforced PEEK composites. Journal of the Mechanical Behavior of Biomedical Materials 111, 104008.
Argon, A.S., 1989. The fundamental rate determining process in creep fracture. In: Samala, K., Ravi-Chander, K., Taplin, D.M.R., Rama Rao, P. (Eds.), Proceedings of 7th International Conference on Advances in Fracture Research. New York, NY: Pergamon Press, pp. 3647–3659.
Argon, A.S., Cohen, R.E., 1990. Crazing and toughness of block copolymers and blends. In: Kausch, H.H. (Ed.), Advances in Polymer Science, vol. 91/92. Berlin: Springer, pp. 300–351.
Arnell, R. D., Davies, P. B., Halling, J., Whomes, T. L., 1991. Tribology: Principles and design applications. In New York.
ASTM E647-15e1—Standard Test Method for Measurement of Fatigue Crack Growth Rates. (2015). iTeh Standards.
Atwood, S. A., Van Citters, D. W., Patten, E. W., Furmanski, J., Ries, M. D., Pruitt, L. A., 2011. Tradeoffs amongst fatigue, wear, and oxidation resistance of cross-linked ultra-high molecular weight polyethylene. Journal of the Mechanical Behavior of Biomedical Materials, 4(7), 1033–1045.
Atwood, S.A., Van Citters, D.W., Patten, E.W., et al., 2011. Tradeoffs amongst fatigue, wear, and oxidation resistance of cross-linked ultra-high molecular weight polyethylene. Journal of the Mechanical Behavior of Biomedical Materials 4(7), 1033–1045.
Awaja, F., Zhang, S., Tripathi, M., Nikiforov, A., Pugno, N., 2016. Cracks, microcracks and fracture in polymer structures: Formation, detection, autonomic repair. Progress in Materials Science 83, 536–573.
Azimi, H.R., Pearson, R.A., Hertzberg, R.W., 1996. Fatigue of rubber-modified epoxies: Effect of particle size and volume fraction. Journal of Materials Science 31, 3777–3789.
Baker, D. A., Bellare, A., Pruitt, L., 2003. The effects of degree of crosslinking on the fatigue crack initiation and propagation resistance of orthopedic-grade polyethylene. Journal of Biomedical Materials Research Part A, 66A(1), 146–154.
Baker, D. A., Hastings, R. S., Pruitt, L., 1999. Study of fatigue resistance of chemical and radiation crosslinked medical grade ultrahigh molecular weight polyethylene. Journal of Biomedical Materials Research, 46(4), 573–581.
Baker, D. A., Hastings, R. S., Pruitt, L., 2000. Compression and tension fatigue resistance of medical grade ultra high molecular weight polyethylene: The effect of morphology, sterilization, aging and temperature. Polymer, 41(2), 795–808.
Baker, D.A., Bellare, A., Pruitt, L., 2003. “The effects of degree of crosslinking on the fatigue

crack initiation and propagation resistance of orthopedic-grade polyethylene.". Journal of Biomedical Materials Research Part A An Official Journal of The Society for Biomaterials, The Japanese Society for Biomaterials, and The Australian Society for Biomaterials and the Korean Society for Biomaterials 66(1), 146–154.
Bal, B.S., et al., 2006. Ceramic materials in total joint arthroplasty. Seminars in Arthroplasty 17(3–4), 94–101.
Banasiak, D.H., Grandt, A.F., Montulli, L.T., 1977. Fatigue crack retardation in polycarbonate. Journal of Applied Polymer Science 21, 1297–1309.
Bao, Q.-B., et al., 2007. Nubac disc arthroplasty: preclinical studies and preliminary safety and efficacy evaluations. SAS Journal 1(1), 36–45.
Beardmore, P., Rabinowitz, S., 1975. Treatment Materials Science and Technology 6, 267.
Berrehili, A., Nadot, Y., Castagnet, S., Grandidier, J.C., Dumas, C., 2010. Multiaxial fatigue criterion for polypropylene – Automotive applications. International Journal of Fatigue 32, 1389–1392.
Bhatia, C. S., Anders, S., Brown, I. G., Bobb, K., Hsiao, R., Bogy, D. B., 1998. Ultra-Thin Overcoats for the Head/Disk Interface Tribology. Journal of Tribology, 120(4), 795–799.
Blundell, D., Osborn, B., 1983. The morphology of poly(aryl-ether-ether-ketone). Polymer 24, 953–958.
Bonnheim, N., Ansari, F., Regis, M., Bracco, P., Pruitt, L., 2019. Effect of carbon fiber type on monotonic and fatigue properties of orthopedic grade PEEK. Journal of the Mechanical Behavior of Biomedical Materials 90, 484–492.
Bozic, K. J., Kurtz, S., Lau, E., Ong, K., Chiu, V., Vail, T. P., Rubash, H. E., Berry, D. J., 2009. The Epidemiology of Bearing Surface Usage in Total Hip Arthroplasty in the United States. JBJS, 91(7), 1614.
Bracco, P., Oral, E., 2011. Vitamin E-stabilized UHMWPE for Total Joint Implants: A Review. Clinical Orthopaedics and Related Research®, 469(8), 2286–2293.
Bradford, L., Baker, D., Ries, M. D., Pruitt, L. A., 2004. Fatigue Crack Propagation Resistance of Highly Crosslinked Polyethylene. Clinical Orthopaedics and Related Research®, 429, 68.
Bragdon, R., 1997. Marked improvement in the wear resistance of a new form of UHMWPE in a physiologic hip simulator. J. Bone Joint Surg., B, 79(2), 138.
Brockett, C. L., Abdelgaied, A., Haythornthwaite, T., Hardaker, C., Fisher, J., Jennings, L. M., 2016. The influence of simulator input conditions on the wear of total knee replacements: An experimental and computational study. Proceedings of the Institution of Mechanical Engineers, Part H: Journal of Engineering in Medicine, 230(5), 429–439.
Brockett, C., Carbone, S., Abdelgaied, A., Fisher, J., Jennings, L., 2016. Influence of contact pressure, cross-shear and counterface material on the wear of PEEK and CFR-PEEK for orthopaedic applications. Journal of the Mechanical Behavior of Biomedical Materials 63, 10–16.
Brockett, C.L., Carbone, S., Fisher, J., Jennings, L.M., 2017. PEEK and CFR-PEEK as alternative bearing materials to UHMWPE in a fixed bearing total knee replacement: An experimental wear study. Wear 374–375, 86–91.
Brockett, C.L., et al., 2012. Wear of ceramic-on-carbon fiber-reinforced poly-ether ether ketone hip replacements. Journal of Biomedical Materials Research Part B: Applied Biomaterials 100B(6), 1459–1465.
Bucknall, C.B., Stevens, W.W., 1978. Toughening of Plastics. London: Plastics and Rubber Institute, pp. 24.
Butter, R. S., Lettington, A. H., 1995. DIAMOND-LIKE CARBON FOR BIOMEDICAL APPLICATIONS. In: Applications of Diamond Films and Related Materials, Optica Publishing Group, pp. 683.

Casiraghi, C., Robertson, J., Ferrari, A. C., 2007. Diamond-like carbon for data and beer storage. Materials Today, 10(1), 44–53.
Chamberlain, K.A., Rankin, K.S., Briscoe, A., Deehan, D., Hyde, P.J., 2019. Wear properties of poly-ether-ether-ketone bearing combinations under zero and cross shear kinematics in total knee arthroplasty. Journal of Biomedical Materials Research Part B: Applied Biomaterials 107(2), 445–453.
Charles, D.F., Gnanamoorthy, R., Ravindran, P., 2010. Rolling contact fatigue behavior of polyamide clay reinforced nanocomposite – Effect of load and speed. Wear 269, 565–571.
Charnley, J., 1961. ARTHROPLASTY OF THE HIP: A New Operation. The Lancet, 277(7187), 1129–1132.
Cheah, L. K., Shi, X., Liu, E., Shi, J. R., 1998. Nitrogenated tetrahedral amorphous carbon films prepared by ion-beam-assisted filtered cathodic vacuum arc technique for solar cells application. Applied Physics Letters, 73(17), 2473–2475.
Chekan, N. M., Beliauski, N. M., Akulich, V. V., Pozdniak, L. V., Sergeeva, E. K., Chernov, A. N., Kazbanov, V. V., Kulchitsky, V. A., 2009. Biological activity of silver-doped DLC films. Diamond and Related Materials, 18(5), 1006–1009.
Choudhury, D., Roy, T., Krupka, I., Hartl, M., Mootanah, R., 2015. Tribological investigation of ultra-high molecular weight polyethylene against advanced ceramic surfaces in total hip joint replacement. Proceedings of the Institution of Mechanical Engineers, Part J: Journal of Engineering Tribology, 229(4), 410–419.
Chyr, A., Sanders, A. P., Raeymaekers, B., 2013. A hybrid apparatus for friction and accelerated wear testing of total knee replacement bearing materials. Wear, 308(1), 54–60.
Clark, T.R., Hertzberg, R.W., Nohammadi, N., 1991. In: Bg, A. (Ed.), Proceedings of 8th International Conference on Deformation, Yield and Fracture of Polymers. London: Plastics and Rubber Institute, pp. 31.
Clarke, I.C., 1992. Role of ceramic implants. Design and clinical issues with total hip prosthetic ceramic-to-ceramic bearings. Clinical Orthopedics and Related Research 282, 19–30.
Cogswell, F., Hopprich, M., 1983. Environmental resistance of carbon fibre-reinforced polyether etherketone. Composites 14(3), 251–253.
Connelly, G.M., Rimnac, C.M., Wright, T.M., Hertzberg, R.W., Manson, J.A., 1984. Fatigue crack propagation behavior of ultrahigh molecular weight polyethylene. Journal of Orthopaedic Research 2, 119–125.
Cook, S., Rust-Dawicki, A., 1995. Preliminary evaluation of titanium-coated PEEK dental implants. Journal of Oral Implantology 21(3), 176–181.
Cowie, R.M., Pallem, N.M., Briscoe, A., Jennings, L.M., 2020. Third body wear of UHMWPE-on-PEEK-OPTIMA™. Materials 13(6), 1264.
Cunningham, B.W., et al., 2013. Epidural application of spinal instrumentation particulate wear debris: a comprehensive evaluation of neurotoxicity using an in vivo animal model. Journal of Neurosurgery: Spine 19(3), 336–350.
Dalli, D., Buhagiar, J., Mollicone, P., Schembri Wismayer, P., 2022. A novel hip joint prosthesis with uni-directional articulations for reduced wear. Journal of the Mechanical Behavior of Biomedical Materials, 127, 105072.
Dawes, K., Glover, L.C., 1996. Effects of electron beam and irradiation on polymeric materials. In: Mark, J.E. (Ed.), Physical Properties of Polymers Handbook. New York, NY: AIP Press, pp. 557–576.
de Ruiter, L., et al., 2021. Decreased stress shielding with a PEEK femoral total knee prosthesis measured in validated computational models. Journal of Biomechanics 118, 110270.
de Villiers, D., Shelton, J. C., 2016. Measurement outcomes from hip simulators. Proceedings of

the Institution of Mechanical Engineers, Part H: Journal of Engineering in Medicine, 230(5), 398–405.
Dearnaley, G., Arps, J. H., 2005. Biomedical applications of diamond-like carbon (DLC) coatings: A review. Surface and Coatings Technology, 200(7), 2518–2524.
Di Puccio, F., Mattei, L., 2015. Biotribology of artificial hip joints. World Journal of Orthopedics, 6(1), 77–94.
Dong, H., Shi, W., Bell, T., 1999. Potential of improving tribological performance of UHMWPE by engineering the Ti6Al4V counterfaces. Wear, 225–229, 146–153.
Dowling, D. P., Kola, P. V., Donnelly, K., Kelly, T. C., Brumitt, K., Lloyd, L., Eloy, R., Therin, M., Weill, N., 1997. Evaluation of diamond-like carbon-coated orthopaedic implants. Diamond and Related Materials, 6(2), 390–393.
Dowling, N., 1993. Mechanical Behavior of Materials. Englewood Cliffs, New Jersey: Prentice Hall.
Dwivedi, N., Yeo, R. J., Zhang, Z., Dhand, C., Tripathy, S., & Bhatia, C. S. (2016). Interface Engineering and Controlling the Friction and Wear of Ultrathin Carbon Films: High sp3 Versus High sp2 Carbons. Advanced Functional Materials, 26(10), 1526–1542.
Dwivedi, N., Yeo, R. J., Zhang, Z., Dhand, C., Tripathy, S., Bhatia, C. S., 2017. Direct observation of thickness and foreign interlayer driven abrupt structural transformation in ultrathin carbon and hybrid silicon nitride/carbon films. Carbon, 115, 701–719.
Dworak, M., Rudawski, A., Markowski, J., Blazewicz, S., 2017. Dynamic mechanical properties of carbon fibre-reinforced PEEK composites in simulated body-fluid. Composite Structures 161, 428–434.
East, R.H., Briscoe, A., Unsworth, A., 2015. Wear of PEEK-OPTIMA® and PEEK- OPTIMA®-Wear Performance articulating against highly cross-linked polyethylene. Proceedings of the Institution of Mechanical Engineers, Part H 229(3), 187–193.
Edidin, A. A., Pruitt, L., Jewett, C. W., Crane, D. J., Roberts, D., Kurtz, S. M., 1999. Plasticity-induced damage layer is a precursor to wear in radiation-cross-linked UHMWPE acetabular components for total hip replacement. The Journal of Arthroplasty, 14(5), 616–627.
Eftekhari, M., Fatemi, A., 2016. On the strengthening effect of increasing cycling frequency on fatigue behavior of some polymers and their composites: Experiments and modeling. International Journal of Fatigue 87, 153–166.
Elber, W., 1970. Fatigue crack closure under cyclic tension. Engineering Fracture Mechanics 2, 37–45.
Escudeiro, A., Wimmer, M. A., Polcar, T., Cavaleiro, A., 2015. Tribological behavior of uncoated and DLC-coated CoCr and Ti-alloys in contact with UHMWPE and PEEK counterbodies. Tribology International, 89, 97–104.
Estevez, R., Van der Giessen, E., 2005. Modeling and computational analysis of fracture of glassy polymers. In: Kausch, H.-H. (Ed.), Intrinsic Molecular Mobility and Toughness of Polymers II. Springer, pp.188.
Evans, A., Horton, H., Unsworth, A., Briscoe, A., 2014. The influence of nominal stress on wear factors of carbon fibre–reinforced polyetheretherketone (PEEK- optima® Wear Performance) against zirconia toughened alumina (Biolox®delta ceramic). Proceedings of the Institution of Mechanical Engineers, Part H 228(6), 587–592.
Evans, A.G., Ahmad, Z.B., Gilbert, D.G., Beaumont, P.W.R., 1986. Mechanisms of toughening in rubber toughened polymers. Acta Metallurgica 34, 79–87.
Fan, Z., Yan, L., Liu, H., Li, X., Fan, K., Liu, Q., Li, J. J., Wang, B., 2023. The prevalence of hip osteoarthritis: A systematic review and meta-analysis. Arthritis Research & Therapy, 25(1), 51.
Ferry, J.D., 1961. Viscoelastic Properties of Polymers. New York: Wiley.

Flöck, J., Friedrich, K., Yuan, Q., 1999. On the friction and wear behaviour of PAN- and pitch-carbon fiber reinforced PEEK composites. Wear 225, 304-311.
Furmanski, J., Anderson, M., Bal, S., Greenwald, A. S., Halley, D., Penenberg, B., Ries, M., Pruitt, L., 2009. Clinical fracture of cross-linked UHMWPE acetabular liners. Biomaterials, 30(29), 5572–5582.
Furmanski, J., Kraay, M. J., Rimnac, C. M., 2011. Crack Initiation in Retrieved Cross-Linked Highly Cross-Linked Ultrahigh-Molecular-Weight Polyethylene Acetabular Liners: An Investigation of 9 Cases. The Journal of Arthroplasty, 26(5), 796–801.
Furmanski, J., Pruitt, L. A., 2007. Peak stress intensity dictates fatigue crack propagation in UHMWPE. Polymer, 48(12), 3512–3519.
Furmanski, J., Pruitt, L. A., 2018. Static mode fatigue crack propagation and generalized stress intensity correlation for fatigue–brittle polymers. International Journal of Fracture, 210(1), 213–221.
Gang, Tao, Zihui, Xia, 2009. Biaxial fatigue behavior of an epoxy polymer with mean stress effect. International Journal of Fatigue 31, 678–685.
Garcea, S.C., Mavrogordato, M.N., Scott, A.E., Sinclair, I., Spearing, S.M., 2014. Fatigue micromechanism characterisation in carbon fibre reinforced polymers using synchrotron radiation computed tomography. Composites Science and Technology 99, 22–30.
Garcea, S.C., Sinclair, I., Spearing, S.M., 2015. In situ synchrotron tomographic evaluation of the effect of toughening strategies on fatigue micromechanisms in carbon fibre reinforced polymers. Composites Science and Technology 109, 32–39.
Gelb, H., Ralph Schumacher, H., Cuckler, J., Baker, D.G., 1994. In vivo inflammatory response to polymethylmethacrylate particulate debris: effect of size, morphology, and surface area. Journal of Orthopedic Research 12(1), 83–92.
Gencur, S. J., Rimnac, C. M., Kurtz, S. M., 2003. Failure micromechanisms during uniaxial tensile fracture of conventional and highly crosslinked ultra-high molecular weight polyethylenes used in total joint replacements. Biomaterials, 24(22), 3947–3954.
Gencur, S.J., Rimnac, C.M., Kurtz, S.M., 2006. Fatigue crack propagation resis- tance of virgin and highly crosslinked, thermally treated ultra-high molecular weight polyethylene. Biomaterials 27(8), 1550–1557.
Ghadirinejad, K., Day, C. W., Milimonfared, R., Taylor, M., Solomon, L. B., Hashemi, R., 2023. Fretting Wear and Corrosion-Related Risk Factors in Total Hip Replacement: A Literature Review on Implant Retrieval Studies and National Joint Replacement Registry Reports. Prosthesis, 5(3), 3.
Glant, T.T., Jacobs, J.J., 1994. Response of three murine macrophage populations to particulate debris: bone resorption in organ cultures. Journal of Orthopedic Research 12(5), 720–731.
Goldman, M., Gronsky, R., Pruitt, L., 1998. The influence of sterilization technique and aging on the structure and morphology of medical-grade ultrahigh molecular weight polyethylene. Journal of Materials Science Materials in Medicine 9, 207–212.
Goldman, M., Pruitt, L., 1998. Comparison of the effects of gamma radiation and low temperature hydrogen peroxide gas plasma sterilization on the molecular structure, fatigue resistance, and wear behavior of UHMWPE. Journal of Biomedical Materials Research 40, 378–384.
Green, T., Fisher, J., Stone, M., Wroblewski, B., Ingham, E., 1998. Polyethylene particles of a 'critical size'are necessary for the induction of cytokines by macrophages in vitro. Biomaterials 19(24), 2297–2302.
Green, T.R., Fisher, J., Matthews, J.B., Stone, M.H., Ingham, E., 2000. Effect of size and dose on bone resorption activity of macrophages by in vitro clinically relevant ultra high molecular weight polyethylene particles. Journal of Biomedical Materials Research 53(5), 490–497.

Grill, A., 1997. Tribology of diamondlike carbon and related materials: An updated review. Surface and Coatings Technology, 94–95, 507–513.
Grill, A., 2003. Diamond-like carbon coatings as biocompatible materials—An overview. Diamond and Related Materials, 12(2), 166–170.
Grupp, T., Kabir, K., Fritz, B., Schwiesau, J., Bloemer, W., Jansson, V., 2014. Evaluation of carbon-fibre-reinforced PEEK as material for intervertebral disc replacement. In: Orthopaedic Proceedings 96-B(11), 223.
Grupp, T.M., et al., 2010. Biotribology of alternative bearing materials for unicompartmental knee arthroplasty. Acta Biomaterilia 6(9), 3601–3610.
Gutensohn, K., Beythien, C., Bau, J., Fenner, T., Grewe, P., Koester, R., Padmanaban, K., Kuehnl, P., 2000. In Vitro Analyses of Diamond-like Carbon Coated Stents: Reduction of Metal Ion Release, Platelet Activation, and Thrombogenicity. Thrombosis Research, 99(6), 577–585.
Hallab, N.J., McAllister, K., Brady, M., Jarman-Smith, M., 2012. Macrophage reactivity to different polymers demonstrates particle size-and material-specific reactivity: PEEK-optima® particles versus UHMWPE particles in the submicron, micron, and 10 micron size ranges. Journal of Biomedical Materials Research Part B: Applied Biomaterials 100(2), 480–492.
Harris, J.S., Ward, I.M., 1973. Fatigue-crack propagation in vinyle urethane polymers. Journal of Materials Science 8, 1655–1665.
Hauert, R., 2003. A review of modified DLC coatings for biological applications. Diamond and Related Materials, 12(3), 583–589.
Hertzberg, R.W., 1996. Deformation and Fracture Mechanics of Engineering Materials, fourth ed. New York, NY: Wiley.
Hertzberg, R.W., Manson, J.A., 1980. Fatigue of Engineering Plastics. New York, NY: Academic Press.
Hertzberg, R.W., Manson, J.A., 1983. Environment, frequency and temperature effects on fatigue in engineering plastics. In: Burke, J.J., Weiss, V. (Eds.), Sagamore Army Materials Research Conference Proceedings, vol. 27. Boston, MA: Springer.
Hertzberg, R.W., Manson, J.A., 1986. Encyclopedia of Polymer Science and Engineering. New York: Wiley, pp. 378.
Hertzberg, R.W., Manson, J.A., Skibo, M., 1975. Frequency sensitivity of fatigue processes in polymeric solids. Polymer Engineering & Science 15, 252–260.
Hertzberg, R.W., Skibo, M.D., Manson, J.A., 1979. Fatigue Fracture Micromechanisms in Engineering Plastics Fatigue Mechanisms, ASTM STP 675. Philadelphia, PA: American Society for Testing and Materials, pp. 471–491.
Hip & Knee Revision Surgery Recovery Timeline. (2021, April 6). University of Utah Health | University of Utah Health. https://healthcare.utah.edu/orthopaedics/specialties/joint-replacement/hip-knee-revision/recovery
Howling, G., et al., 2003. Biological response to wear debris generated in carbon based composites as potential bearing surfaces for artificial hip joints. Journal of Biomedical Materials Research Part B: Applied Biomaterials 67(2), 758–764.
Ingram, J., et al., 2002. Comparison of the biological activity of grade GUR 1120 and GUR 415HP UHMWPE wear debris. Biomedical Materials and Engineering 12(2), 177–188.
J. Yeo, R., Dwivedi, N., Zhang, L., Zhang, Z., H. Lim, C. Y., Tripathy, S., Bhatia, C.S., 2017. Superior wear resistance and low friction in hybrid ultrathin silicon nitride/carbon films: Synergy of the interfacial chemistry and carbon microstructure. Nanoscale, 9(39), 14937–14951.
Jockisch, K., Brown, S., Bauer, T., Merritt, K., 1992. Biological response to chopped-carbon-fiber-reinforced peek. Journal of Biomedical Materials Research 26(2), 133–146.
Joyce, T., 2005. The wear of two orthopaedic biopolymers against each other. Journal of Applied

Biomaterials and Biomechanics 3(3), 141–146.
Kandemir, G., Smith, S., Joyce, T.J., 2019. Wear behaviour of CFR PEEK articulated against CoCr under varying contact stresses: Low wear of CFR PEEK negated by wear of the CoCr counterface. Journal of the Mechanical Behavior of Biomedical Materials 97, 117–125.
Kanters, M.J.W., Stolkb, J., Govaerta, L.E., 2015. Direct comparison of the compliance method with optical tracking of fatigue crack propagation in polymers. Polymer Testing 46, 98–107.
Katzer, A., Marquardt, H., Westendorf, J., Wening, J., Von Foerster, G., 2002. Polyetheretherketone—cytotoxicity and mutagenicity in vitro. Biomaterials 23(8), 1749–1759.
Kausch, H.H., Williams, J.G., 1986. Encyclopedia of Polymer Science and Engineering. New York, NY: Wiley, p. 341.
Kerner, J., et al., 1999. Correlation between pre-operative periprosthetic bone density and post-operative bone loss in THA can be explained by strain-adaptive remodeling. Journal of Biomechanics 32, 695–703.
Khonsari, R.H., Berthier, P., Rouillon, T., Perrin, J.-P., Corre, P., 2014. Severe infectious complications after PEEK-derived implant placement: report of three cases. Journal of Oral and Maxillofacial Surgery, Medicine, and Pathology 26(4), 477–482.
Kim, Y.H., et al., 2013. Mechanical properties of carbon/PEEK composites according to the fiber ply orientation and sizing removal of carbon fiber for artificial hip joint. In: Advanced Engineering Materials III. In: Advanced Materials Research, 750, Trans Tech Publications Ltd, pp. 164–175.
Kinloch, A.J., Guild, F.J., 1996. Predictive modelling of the properties and toughness of rubber-toughened epoxies. In: Keith, C. (Ed.), Advances in Chemistry, Series 252: Toughened Plastics II: Novel Approaches in Science and Engineering. Washington, DC: American Chemical Society, pp. 1–25.
Kishi, H., Matsuda, S., Imade, J., et al., 2021. The effects of the toughening mechanism and the molecular weights between cross-links on the fatigue resistance of epoxy polymer blends. Polymer 223. 123712.
Klapperich, C., Komvopoulos, K., Pruitt, L., 1999. Tribological Properties and Microstructure Evolution of Ultra-High Molecular Weight Polyethylene. Journal of Tribology, 121(2), 394–402.
Klimkeit, B., Nadot, Y., Castagnet, S., et al., 2011. Multiaxial fatigue life assessment for reinforced polymers. International Journal of Fatigue 33, 766–780.
Koh, Y.G., et al., 2019. Total knee arthroplasty application of polyetheretherketone and carbon-fiber-reinforced polyetheretherketone: A review. Materials Science and Engineering: C 100, 70–81.
Komvopoulos, K., 1996. Surface engineering and microtribology for microelectromechanical systems. Wear, 200(1), 305–327.
Kramer, E.J., Berger, L.L., 1990. Fundamental processes of craze growth and fracture. In: Kausch, H.H. (Ed.), Advances in Polymer Science, vol. 91/92. Berlin: Springer, pp. 1–68.
Krause, D., 2016. A physically based micromechanical approach to model damage initiation and evolution of fiber reinforced polymers under fatigue loading conditions. Composites Part B Engineering 87, 176–195.
Kremers, H.M., et al., 2015. Prevalence of total hip and knee replacement in the United States. The Journal of Bone and Joint Surgery 97(17), 1386.
Krzypow, David J., Rimnac, Clare M., 2000. Cyclic steady state stress–strain behavior of UHMW polyethylene. Biomaterials vol 21, 2081–2087.
Kumar, A., Yap, W.T., Foo, S.L., Lee, T.K., 2018. Effects of sterilization cycles on PEEK for medical device application. Bioengineering 5(1), 18.
Kumar, S., Anderson, D., Adams, W., 1986. Crystallization and morphology of poly(aryl-ether-ether-ketone). Polymer 27, 329–336.

Kurtz, S. M., 2009. UHMWPE Biomaterials Handbook: Ultra High Molecular Weight Polyethylene in Total Joint Replacement and Medical Devices. Academic Press.
Kurtz, S. M., Lau, E., Ong, K., Zhao, K., Kelly, M., Bozic, K. J., 2009. Future Young Patient Demand for Primary and Revision Joint Replacement: National Projections from 2010 to 2030. Clinical Orthopaedics and Related Research®, 467(10), 2606.
Kurtz, S. M., Oral, E., 2016. In Vivo Oxidation of UHMWPE. In S. M. Kurtz (Ed.), UHMWPE Biomaterials Handbook (Third Edition) (pp. 488–505). William Andrew Publishing.
Kurtz, S., 2012a. An Overview of PEEK Biomaterials. In: PEEK Biomaterials Handbook, pp. 1–7.
Kurtz, S., et al., 2005. Prevalence of primary and revision total hip and knee arthroplasty in the United States from 1990 through 2002. The Journal of Bone and Joint Surgery 87(7), 1487–1497.
Kurtz, S., et al., 2009. Future Young patient demand for primary and revision joint replacement: National projections from 2010 to 2030. Clinical Orthopaedics and Related Research®, 467, 2606–2612.
Kurtz, S., Ong, K., Lau, E., Mowat, F., Halpern, M., 2007. Projections of Primary and Revision Hip and Knee Arthroplasty in the United States from 2005 to 2030: The Journal of Bone & Joint Surgery, 89(4), 780–785.
Kurtz, S.M. (Ed.), 2009. UHMWPE Biomaterials Handbook Ultra High Molecular Weight Polyethylene in Total Joint Replacement and Medical Devices. Academic Press.
Kurtz, S.M., 2009. UHMWPE Biomaterials Handbook: Ultra High Molecular Weight Polyethylene in Total Joint Replacement and Medical Devices. Academic Press.
Kurtz, S.M., 2012b. Applications of polyaryletheretherketone in spinal implants: Fusion and motion preservation. In: Modjarrad, K., Ebnesajjad, S. (Eds.), Handbook of Polymer Applications in Medicine and Medical Devices. In: Plastics Design Library, William Andrew Publishing, Oxford, pp. 231–251.
Kurtz, S.M., Bartel, D.L., Rimnac, C.M., 1994. Transactions of the 40th Annual Meeting Of The Orthopedic Research Society. San Francisco: Orthopaedic Research Society.
Kurtz, S.M., Devine, J.N., 2007. PEEK biomaterials in trauma, orthopedic, and spinal implants. Biomaterials 28(32), 4845–4869.
Lampman, S., 2003. Characterization and Failure Analysis of Plastics. ASM International.
Landel, R.F., Nielsen, L.E., 1993. Mechanical Properties of Polymers and Composites. CRC press.
Lang, R.W., Manson, J.A., Hertzberg, R.W., Schirrer, R., 1984. Craze development in poly(methl methacrylate) during stable fatigue crack propagation. Polymer Engineering & Science 24, 833–842.
Lappalainen, R., Anttila, A., Heinonen, H., 1998. Diamond coated total hip replacements. Clinical Orthopaedics and Related Research, 352, 118–127.
Lappalainen, R., Heinonen, H., Anttila, A., Santavirta, S., 1998. Some relevant issues related to the use of amorphous diamond coatings for medical applications. Diamond and Related Materials, 7(2), 482–485.
Latif, A.M., et al., 2008. Pre-clinical studies to validate the MITCH PCR™ Cup: a flexible and anatomically shaped acetabular component with novel bearing characteristics. Journal of Materials Science: Materials in Medicine 19(4), 1729–1736.
Lettington, A. H., 1998. Applications of diamond-like carbon thin films. Carbon, 36(5), 555–560.
Li, C.S., Vannabouathong, C., Sprague, S., Bhandari, M., 2015. The use of carbon-fiber-reinforced (CFR) PEEK material in orthopedic implants: a systematic review. Clinical Medicine Insights: Arthritis and Musculoskeletal Disorders 8, 33-45.
Liao, C., Li, Y., Tjong, S.C., 2020. Polyetheretherketone and its composites for bone replacement and regeneration. Polymers 12(12), 2858.

Liu, H., Leng, Y., Tang, J., Wang, S., Xie, D., Sun, H., Huang, N., 2012. Tribological performance of ultra-high-molecular-weight polyethylene sliding against DLC-coated and nitrogen ion implanted CoCrMo alloy measured in a hip joint simulator. Surface and Coatings Technology, 206(23), 4907–4914.
Liu, J., Wang, X., Wu, B. J., Zhang, T. F., Leng, Y. X., Huang, N., 2013. Tribocorrosion behavior of DLC-coated CoCrMo alloy in simulated biological environment. Vacuum, 92, 39–43.
Loos, M.R., Yang, J., Feke, D.L., et al., 2013. Enhancement of fatigue life of polyurethane composites containing carbon nanotubes. Composite Part B 44, 740–744.
Lorber, V., et al., 2014. Elevated cytokine expression of different PEEK wear particles compared to UHMWPE in vivo. Journal of Materials Science: Materials in Medicine 25(1), 141–149.
Luo, J. K., Fu, Y. Q., Le, H. R., Williams, J. A., Spearing, S. M., Milne, W. I., 2007. Diamond and diamond-like carbon MEMS. Journal of Micromechanics and Microengineering, 17(7), S147.
Lvhua, L., Yanyan, Z., Lifang, Z., Chengdong, X., 2017. Bioactive polyetheretherketone implant composites for hard tissue. Progress in Chemistry 29(4), 450.
Ma, H., et al., 2021. PEEK (polyether-ether-ketone) and its composite materials in orthopedic implantation. Arabian Journal of Chemistry 14(3), 102977.
Ma, W. J., Ruys, A. J., Mason, R. S., Martin, P. J., Bendavid, A., Liu, Z., Ionescu, M., Zreiqat, H., 2007. DLC coatings: Effects of physical and chemical properties on biological response. Biomaterials, 28(9), 1620–1628.
MacDonald, S.J., 2004. Metal-on-metal total hip arthroplasty: The concerns. Clinical Orthopedics and Related Research 429, 86–93.
Malito, L. G., Arevalo, S., Kozak, A., Spiegelberg, S., Bellare, A., Pruitt, L., 2018. Material properties of ultra-high molecular weight polyethylene: Comparison of tension, compression, nanomechanics and microstructure across clinical formulations. Journal of the Mechanical Behavior of Biomedical Materials, 83, 9–19.
Manhabosco, T. M., Muller, I. L., 2009. Electrodeposition of diamond-like carbon (DLC) films on Ti. Applied Surface Science, 255(7), 4082–4086.
Manson, J.A., Hertzberg, R.W., Bretz, P.E., 1981. Normalization of fatigue crack propagation behavior in polymers. In: Francois, D. (Ed.), Advances in Fracture Research. Oxford: Pergamon Press, pp. 443–448.
Marciano, F. R., Bonetti, L. F., Santos, L. V., Da-Silva, N. S., Corat, E. J., Trava-Airoldi, V. J., 2009. Antibacterial activity of DLC and Ag–DLC films produced by PECVD technique. Diamond and Related Materials, 18(5), 1010–1014.
Mars, W.V., Fatemi, A., 2004. Factors that affect the fatigue life of rubber: A literature survey. Rubber Chemistry and Technology 77, 391–412.
Matlak, J., 2017. Synthesis and Characterization of Amorphous Carbon Films for Heat-Assisted Magnetic Storage. In: Ph.D. Thesis, UC Berkeley.
Matlak, J., Komvopoulos, K., 2015. Friction properties of amorphous carbon ultrathin films deposited by filtered cathodic vacuum arc and radio-frequency sputtering. Thin Solid Films, 579, 167–173.
Matlak, J., Komvopoulos, K., 2018. Ultrathin amorphous carbon films synthesized by filtered cathodic vacuum arc used as protective overcoats of heat-assisted magnetic recording heads. Scientific Reports, 8(1), 9647.
Matlak, J., Rismaniyazdi, E., Komvopoulos, K., 2018. Nanostructure, structural stability, and diffusion characteristics of layered coatings for heat-assisted magnetic recording head media. Scientific Reports, 8(1), 9807.
Matthews, J.B., et al., 2000a. Evaluation of the response of primary human peripheral blood mononuclear phagocytes to challenge with in vitro generated clinically relevant UHMWPE

particles of known size and dose. Journal of Biomedical Materials Research 52(2), 296–307.
Matthews, J.B., et al., 2000b. Comparison of the response of primary murine peritoneal macrophages and the U937 human histiocytic cell line to challenge with in vitro generated clinically relevant UHMWPE particles. Biomedical Materials and Engineering 10(3, 4), 229–240.
Medel, F. J., Peña, P., Cegoñino, J., Gómez-Barrena, E., Puértolas, J. A., 2007. Comparative fatigue behavior and toughness of remelted and annealed highly crosslinked polyethylenes. Journal of Biomedical Materials Research Part B: Applied Biomaterials, 83B(2), 380–390.
Medel, F., Kurtz, S.M., Klein, G., et al., 2009. Revisiting the clinical wear performance of poly II tibial inserts after long-term implantation. In: Proceedings of the Transaction of the 2009 AAOS Meeting, Las Vegas.
Mehta, V., Cooper, J. S., 2003. Review and analysis of PEM fuel cell design and manufacturing. Journal of Power Sources, 114(1), 32–53.
Mills, N.J., Walker, N., 1976. Craze growth and crack growth in poly(viny chloride) under monotonic and fatigue loading. Polymer 17, 335–344.
Miner, M. A., 1945. Cumulative Damage in Fatigue. Journal of Applied Mechanics, 12(3), A159–A164.
Miner, M.A., 1945. Cumulative damage in fatigue. Journal of Applied Mechanics 3, 159–164.
Mitura, E., Mitura, S., Niedzielski, P., Has, Z., Wolowiec, R., Jakubowski, A., Szmidt, J., Sokołowska, A., Louda, P., Marciniak, J., Koczy, B., 1994. Diamond-like carbon coatings for biomedical applications. Diamond and Related Materials, 3(4), 896–898.
Monich, P.R., Henriques, B., Novaes de Oliveira, A.P., Souza, J.C., Fredel, M.C., 2016. Mechanical and biological behavior of biomedical PEEK matrix composites: A focused review. Materials Letters 185, 593–597.
Morrison, C., et al., 1995. In vitro biocompatibility testing of polymers for orthopaedic implants using cultured fibroblasts and osteoblasts. Biomaterials 16 (13), 987–992. Nieminen, T., et al., 2008. Amorphous and crystalline polyetheretherketone: Mechanical properties and tissue reactions during a 3-year follow-up. Journal of Biomedical Materials Research Part A 84(2), 377–383.
Mortazavian, S., Fatemi, A., 2015. Fatigue behavior and modeling of short fiber reinforced polymer composites: A literature review. International Journal of Fatigue 70, 297–321.
Moser, E. M., Urech, R., Hack, E., Künzli, H., Müller, E., 1998. Hydrocarbon films inhibit oxygen permeation through plastic packaging material. Thin Solid Films, 317(1), 388–392.
Moskala, E.J., 1991. In: Proceedings of 8th International Conference on Deformation, Yield and Fracture of Polymers, Plastics and Rubber Institute, London 51/1.
Movahedi-Rad, A.V., Keller, T., Vassilopoulos, A.P., 2019. Modeling of fatigue behavior based on interaction between time-and cyclic-dependent mechanical properties. Composites Part A Applied Science and Manufacturing 124, 105469.
Mukherjee, B., Burns, D. J., 1971. Fatigue-crack growth in polymethylmethacrylate: Effect of frequency, mean and range of stress-intensity factor are covered by the authors in this paper. Experimental Mechanics, 11, 433-439.
Murakami, R., Noguchi, S., Akizono, K., Ferguson, W.G., 1987. Fatigue crack propagation and crack closure behavior in polycarbonate and fibre reinforced polycarbonate. Fatigue 10, 461–470.
Naebe, M., Abolhasani, M.M., Khayyam, H., Amini, A., Fox, B., 2016. Crack Damage in Polymers and Composites: A Review. Polymer Reviews 56(1), 31–69.
Nugent, M., Young, S. W., Frampton, C. M., Hooper, G. J., 2021. The lifetime risk of revision following total hip arthroplasty. The Bone & Joint Journal, 103-B(3), 479–485.
O'Connell, P.A., McKenna, G.B., 2002. Yield and crazing in polymers. In: Matyjaszewski, K. (Ed.), Encyclopedia of Polymer Science and Technology. Wiley.
Olborska, A., Swider, M., Wolowiec, R., Niedzielski, P., Rylski, A., Mitura, S., 1994. Amorphous

carbon—Biomaterial for implant coatings. Diamond and Related Materials, 3(4), 899–901.
Oñate, J. I., Comin, M., Braceras, I., Garcia, A., Viviente, J. L., Brizuela, M., Garagorri, N., Peris, J. L., Alava, J. I., 2001. Wear reduction effect on ultra-high-molecular-weight polyethylene by application of hard coatings and ion implantation on cobalt chromium alloy, as measured in a knee wear simulation machine. Surface and Coatings Technology, 142–144, 1056–1062.
Oral, E., Muratoglu, O. K., 2011. Vitamin E diffused, highly crosslinked UHMWPE: A review. International Orthopaedics, 35(2), 215–223.
Osteoarthritis (OA) | Arthritis | CDC. (2020, August 4). https://www.cdc.gov/arthritis/basics/osteoarthritis.htm
Pace, N., Marinelli, M., Di Matteo, R., 2005a. Elemental and histological analysis of a retrieved peek composite-ceramic bearing couple, 28 months after implantation. Transactions of the International Society for Technology in Arthroplasty (ISTA) 18, 13.
Pace, N., Marinelli, M., Spurio, S., 2008. Technical and histologic analysis of a retrieved carbon fiber–reinforced poly-ether-ether-ketone composite alumina-bearing liner 28 months after implantation. The Journal of Arthroplasty 23(1), 151–155.
Pace, N., Marinelli, M., Spurio, S., Di Matteo, R., 2005b. Primary total hip arthroplasty with carbon fibre reinforced poly-ether-ether-ketone composite acetabular cup component 36 months results. Transactions of the International Society for Technology in Arthroplasty (ISTA) 18, 2–6.
Pace, N., Spurio, S., Rizzato, G., 2004. Clinical trial of a new CF-PEEK acetabular insert in hip arthroplasty: P080. Hip International 14(2), 132–133.
Palmgren, A., 1924. Die lebensdauer von kugellagern (The service life of ball bearings). Zeitschrift des Vereines Deutscher Ingenieure 68(14), 339–341.
Palmgren, A., 1924. Die Lev/bensdauer von kugellagern (The service life of ball bearings). 68(14), 339–341.
Paris, P.C., Gomez, M.P., Anderson, W.P., 1961. A rational analytic theory of fatigue. Trends in Engineering 13, 9–14.
Pastukhov, L.V., Kanters, M.J.W., Engels, T.A.P., Govaert, L.E., 2020. Physical background of the endurance limit in poly(ether ketone). Journal of Polymer Science 58(5), 716–736.
Patten, E. W., Carney, M. E., Johnson, P. M., Hong, T., Almaguer, A. J., Pruitt, L. A., 2013. A Multi-Directional Tribo-System: Testing the Wear of UHMWPE Under Sliding, Rolling, and Rotation. 1177–1178.
Patten, E. W., Cruz, C., Mehdizadeh, A., Assadian, S., Pruitt, L. A., 2011. Fatigue Crack Propagation of Ultra-High Molecular Weight Polyethylene – Conformity of Compact Tension Specimen Geometry to ASTM E647. Society For Biomaterials, Abstract #041.
Paul, R., Dalui, S., Das, S. N., Bhar, R., Pal, A. K., 2008. Hydrophobicity in DLC films prepared by electrodeposition technique. Applied Surface Science, 255(5, Part 1), 1705–1711.
Paul, R., Das, S. N., Dalui, S., Gayen, R. N., Roy, R. K., Bhar, R., Pal, A. K., 2008. Synthesis of DLC films with different sp 2 /sp 3 ratios and their hydrophobic behaviour. Journal of Physics D: Applied Physics, 41(5), 055309.
Pearson, R., Pruitt, L., 1999. Fatigue crack propagation in polymer blends. In: Paul, D.R., Bucknall, C.B. (Eds.), Polymer Blends Formulation and Performance 27. New York: John Wiley and Sons, Inc, pp. 269–299.
Petillo, O., et al., 1994. In vivo induction of macrophage Ia antigen (MHC class II) expression by biomedical polymers in the cage implant system. Journal of Biomedical Materials Research 28(5), 635–646.
Piitulainen, J.M., et al., 2015. Paediatric cranial defect reconstruction using bioactive fibre-reinforced composite implant: early outcomes. Acta Neurochirurgica 157, 681–687.
Pippan, R., Hohenwarter, A., 2017. Fatigue crack closure: A review of the physical phenomena.

Fatigue & Fracture of Engineering Materials & Structures 40(4), 471–495.
Pitoniak, F.J., Grandt, A.F., Montulli, L.T., Packman, P.F., 1974. Fatigue crack retardation and closure in polymethylmethacrylate. Journal of Engineering Fracture Mechanics 6, 663–670.
Plummer, C.J.G., Kausch, H.H., 1996. Deformation and entanglement in semicrystalline polymers. Journal of Macromolecular Science, Part B Physics 35(3–4), 637–657.
Polineni, V.K., et al., 1998. Characterization of carbon fiber-reinforced PEEK composite for use as a bearing material in total hip replacements. In: Alternative Bearing Surfaces in Total Joint Replacement. ASTM International.
Posti, J.P., et al., 2016. A glass fiber-reinforced composite–bioactive glass cranioplasty implant: a case study of an early development stage implant removed due to a late infection. Journal of the Mechanical Behavior of Biomedical Materials 55, 191–200.
Pruitt, L. A., Simis, K. S., Bistolfi, A., Bellare, A., 2005. The Role of Microstructure on the Fatigue and Fracture Properties of Medical Grade Ultra High Molecular Weight Polyethylene. International Congress on Fracture ICF, 11.
Pruitt, L., 1993. Cyclic Damage Ahead of Fatigue Cracks in Amorphous Solids: Theory, Experiments and Implications. In: Phd Thesis, Brown University.
Pruitt, L., Herman, R., Suresh, S., 1992. Fatigue crack growth in polymers subjected to fully compressive cyclic loads. Journal of Materials Science 27, 1608–1616.
Pruitt, L., Rondinone, D., 1996. The effect of specimen thickness and stress ratio on the fatigue behavior of polycarbonate. Polymer Engineering & Science 36, 1300–1305.
Pruitt, L., Suresh, S., 1993. Cyclic stress-fields for fatigue cracks in amorphous solids experimental measurement and their implications. Philosophical Magazine A 67, 1219–1245.
Pruitt, L., Suresh, S., 1994. Cyclic stress-fields ahead of tension fatigue cracks in amorphous polymers. Polymer 35, 3221–3229.
Pruitt, L., Roy, A., Smith, B., 2023. Fatigue of Polymers. In: Comprehensive Structural Integrity 2nd Edition 4, 146-161.
Pruitt, L., Wat, A., Malito, L., 2022. Fatigue and Fracture Mechanisms in Polymers. In: Characterization and Failure Analysis of Plastics, ASM Handbook, 11B.
Pruitt, L.A., Ansari, F., Kury, M., et al., 2013. Clinical trade-offs in cross-linked ultrahigh-molecular-weight polyethylene used in total joint arthroplasty. Journal of Biomedical Materials Research Part B Applied Biomaterials 101(3), 476–484.
Pruitt, L.A., Chakravartula, A.M., 2011. Mechanics of Biomaterials: Fundamental Principles for Implant Design. Cambridge University Press.
Qin, W., Li, Y., Ma, J., Liang, Q., Tang, B., 2019. Mechanical properties and cytotoxicity of hierarchical carbon fiber-reinforced poly (ether-ether-ketone) composites used as implant materials. Journal of the Mechanical Behavior of Biomedical Materials 89, 227–233.
Quaresimin, M., Salviato, M., Zappalorto, M., 2015. Toughening mechanisms in nanoparticle polymer composites: experimental evidences and modeling. In Toughening Mechanisms in Composite Materials. Woodhead Publishing. pp. 113–133.
Rader, C.P., Sterner, T., Jakob, F., Schütze, N., Eulert, J., 1999. Cytokine response of human macrophage-like cells after contact with polyethylene and pure titanium particles. The Journal of Arthroplasty 14(7), 840–848.
Rahmitasari, F., et al., 2017. PEEK with reinforced materials and modifications for dental implant applications. Dentistry Journal 5(4), 35.
Randive, M. R., Kumar, R., Goyal, A., 2015. Analysis of Artificial Support Structure for Knee Joint. International Journal of Applied Engineering Research, 10(54), 71-77.
Regis, M., Bellare, A., Pascolini, T., Bracco, P., 2017. Characterization of thermally annealed PEEK and CFR-PEEK composites: Structure-properties relationships. Polymer Degradation and

Stability 136, 121–130.
Regis, M., Lanzutti, A., Bracco, P., Fedrizzi, L., 2018. Wear behavior of medical grade PEEK and CFR PEEK under dry and bovine serum conditions. Wear 408–409, 86–95.
Reitman, M., Jaekel, D., Siskey, R., 2012. Morphology and Crystalline Architecture of Polyaryletherketones. In PEEK biomaterials handbook, William Andrew Publishing, pp. 49–60.
Rice, J.R., 1967. Mechanics of Crack Tip Deformation and Extension by Fatigue. Fatigue Crack Propagation, ASTM STP 415. Philadelphia, PA: ASTM, p. 247.
Ries, M. D., Pruitt, L., 2005. Effect of Cross-linking on the Microstructure and Mechanical Properties of Ultra-High Molecular Weight Polyethylene. Clinical Orthopaedics and Related Research (1976-2007), 440, 149–156.
Rimnac, C.M., Wright, T.M., Klein, R.W., 1988. J integral measurements of ultra high molecular weight polyethylene. Polymer Engineering & Science 28, 1586–1589.
Ritchie, R., 2002. Fatigue of brittle materials. In: Milne, I., Ritchie, R., Karihaloo, B.L. (Eds.), Comprehensive Structural Integrity Cyclic Loading and Fatigue. Elsevier.
Ritchie, R.O., 1988. Mechanisms of fatigue crack propagation in metals, ceramics and composites: Role of crack tip shielding. Materials Science and Engineering 103, 15–28.
Ritchie, R.O., 2000. Mechanisms of fatigue crack propagation in ductile and brittle solids. International Journal of Fracture 100, 55–83.
Ritchie, R.O., Liu, D., 2021. Introduction to Fracture Mechanics. Elsevier. ISBN 978-0323898225.
Rivard, C.-H., Rhalmi, S., Coillard, C., 2002. In vivo biocompatibility testing of peek polymer for a spinal implant system: a study in rabbits. Journal of Biomedical Materials Research 62(4), 488–498.
Robertson, J., 2001. Ultrathin carbon coatings for magnetic storage technology. Thin Solid Films, 383(1), 81–88.
Robertson, J., 2002. Diamond-like amorphous carbon. Materials Science and Engineering: R: Reports, 37(4), 129–281.
Robertson, J., 2003. Requirements of ultrathin carbon coatings for magnetic storage technology. Tribology International, 36(4), 405–415.
Rotini, R., et al., 2015. Proximal humeral fracture fixation: multicenter study with carbon fiber peek plate. Musculoskeletal Surgery 99(1), 1–8.
Roy, A., Wang, S., Komvopoulos, K., 2023. A review of plasma-assisted deposition methods for amorphous carbon thin and ultrathin films with a focus on the cathodic vacuum arc technique. Journal of Materials Research, 38(3), 586–616.
Roy, R. K., Lee, K.R., 2007. Biomedical applications of diamond-like carbon coatings: A review. Journal of Biomedical Materials Research Part B: Applied Biomaterials, 83B(1), 72–84.
Saikko, V., Ahlroos, T., Calonius, O., Keränen, J., 2001. Wear simulation of total hip prostheses with polyethylene against CoCr, alumina and diamond-like carbon. Biomaterials, 22(12), 1507–1514.
Saikko, V., Calonius, O., 2002. Simulation of wear rates and mechanisms in total knee prostheses by ball-on-flat contact in a five-station, three-axis test rig. Wear, 253(3), 424–429.
Sancheź-Valencia, A., Smerdova, O., Hutchings, L.R., De Focatiis, D.S., 2017. The roles of blending and of molecular weight distribution on craze initiation. Macromolecules 50(23), 9507–9514.
Santavirta, S., Konttinen, Y. T., Lappalainen, R., Anttila, A., Goodman, S. B., Lind, M., Smith, L., Takagi, M., Gómez-Barrena, E., Nordsletten, L., Xu, J.W., 1998. Materials in total joint replacement. Current Orthopaedics, 12(1), 51–57.
Sauer, J.A., Hara, M., 1990. Effect of molecular variable on crazing and fatigue. In: Kausch, H.H. (Ed.), Advances in Polymer Science, vol. 91/92. Berlin: Springer, pp. 69–118.

Sauer, J.A., Richardson, G.C., 1980. Fatigue of polymers. International Journal of Fracture 16, 499–532.
Schliemann, B., et al., 2015. Treatment of proximal humerus fractures with a CFR- PEEK plate: 2-year results of a prospective study and comparison to fixation with a conventional locking plate. Journal of Shoulder and Elbow Surgery 24(8), 1282–1288.
Scholes, S., Unsworth, A., 2009. Wear studies on the likely performance of CFR- PEEK/CoCrMo for use as artificial joint bearing materials. Journal of Materials Science: Materials in Medicine 20(1), 163.
Scholes, S., Unsworth, A., 2010. The wear performance of PEEK-OPTIMA based self- mating couples. Wear 268(3), 380–387.
Scholes, S.C., Unsworth, A., 2007. The wear properties of CFR-PEEK-OPTIMA articulating against ceramic assessed on a multidirectional pin-on-plate machine. Proceedings of the Institution of Mechanical Engineers, Part H 221(3), 281–289.
Scholz, R., Knyazeva, M., Porchetta, D., et al., 2018. Development of biomimetic in vitro fatigue assessment for UHMWPE implant materials. Journal of the Mechanical Behavior of Biomedical Materials 85, 94–101.
Schwitalla, A., Müller, W.-D., 2013. PEEK dental implants: a review of the literature. Journal of Oral Implantology 39(6), 743–749.
Schwitalla, A.D., Spintig, T., Kallage, I., Müller, W.-D., 2015. Flexural behavior of PEEK materials for dental application. Dental Materials 31(11), 1377–1384.
Scotchford, C.A., Garle, M.J., Batchelor, J., Bradley, J., Grant, D.M., 2003. Use of a novel carbon fibre composite material for the femoral stem component of a THR system: in vitro biological assessment. Biomaterials 24(26), 4871–4879.
Sgouras, D., Duncan, R., 1990. Methods for the evaluation of biocompatibility of soluble synthetic polymers which have potential for biomedical use: 1—Use of the tetrazolium-based colorimetric assay (MTT) as a preliminary screen for evaluation of in vitro cytotoxicity. Journal of Materials Science: Materials in Medicine 1(2), 61–68.
Shah, R., Gashi, B., Hoque, S., Marian, M., Rosenkranz, A., 2021. Enhancing mechanical and biomedical properties of protheses—Surface and material design. Surfaces and Interfaces, 27, 101498.
Shanbhag, A.S., Jacobs, J.J., Black, J., Galante, J.O., Glant, T.T., 1994. Macrophage/particle interactions: effect of size, composition and surface area. Journal of Biomedical Materials Research 28(1), 81–90.
Shanbhag, A.S., Jacobs, J.J., Black, J., Galante, J.O., Glant, T.T., 1995. Human monocyte response to particulate biomaterials generated in vivo and in vitro. Journal of Orthopedic Research 13(5), 792–801.
Sheeja, D., Tay, B. K., Lau, S. P., Nung, L. N., 2001. Tribological characterisation of diamond-like carbon coatings on Co–Cr–Mo alloy for orthopaedic applications. Surface and Coatings Technology, 146–147, 410–416.
Sih, G.C., 1973. Handbook of Stress Intensity Factors. Bethlehem, PA: Lehigh University Press.
Simis, K. S., Bistolfi, A., Bellare, A., Pruitt, L. A., 2006. The combined effects of crosslinking and high crystallinity on the microstructural and mechanical properties of ultra high molecular weight polyethylene. Biomaterials, 27(9), 1688–1694.
Singh, A., Ehteshami, G., Massia, S., He, J., Storer, R. G., Raupp, G., 2003. Glial cell and fibroblast cytotoxicity study on plasma-deposited diamond-like carbon coatings. Biomaterials, 24(28), 5083–5089.
Sirimamilla, A., Rimnac, C. M., 2019. Crack initiation from a clinically relevant notch in a highly-crosslinked UHMWPE subjected to static and cyclic loading. Journal of the Mechanical Behavior

of Biomedical Materials, 91, 366–372.
Sirimamilla, P. A., Furmanski, J., Rimnac, C. M., 2011. Effect of Non-Uniform Material De-Cohesion on Crack Initiation From Notches in Crosslinked UHMWPE. ASME 2011 Summer Bioengineering Conference, Parts A and B, 1321–1322.
Sirimamilla, P. A., Furmanski, J., Rimnac, C. M., 2013. Application of viscoelastic fracture model and non-uniform crack initiation at clinically relevant notches in crosslinked UHMWPE. Journal of the Mechanical Behavior of Biomedical Materials, 17, 11–21.
Sirimamilla, P. A., Rimnac, C. M., Furmanski, J., 2018. Viscoplastic crack initiation and propagation in crosslinked UHMWPE from clinically relevant notches up to 0.5 mm radius. Journal of the Mechanical Behavior of Biomedical Materials, 77, 73–77.
Sobieraj, M. C., Kurtz, S. M., Rimnac, C. M., 2005. Notch strengthening and hardening behavior of conventional and highly crosslinked UHMWPE under applied tensile loading. Biomaterials, 26(17), 3411–3426.
Sobieraj, M. C., Kurtz, S. M., Wang, A., Manley, M. M., Rimnac, C. M., 2008. Notched stress–strain behavior of a conventional and a sequentially annealed highly crosslinked UHMWPE. Biomaterials, 29(35), 4575–4583.
Sobieraj, M. C., Murphy, J. E., Brinkman, J. G., Kurtz, S. M., Rimnac, C. M., 2013. Monotonic and fatigue behavior of five clinically relevant conventional and highly crosslinked UHMWPEs in the presence of stress concentrations. Journal of the Mechanical Behavior of Biomedical Materials, 28, 244–253.
Sobieraj, M. C., Rimnac, C. M., 2009. Ultra high molecular weight polyethylene: Mechanics, morphology, and clinical behavior. Journal of the Mechanical Behavior of Biomedical Materials, 2(5), 433–443.
Solavy, 2017. Sterilization Compatibility Overview – High-Performance Medical-Grade Plastics. Technical Report.
Steffen, H. J., Schmidt, J., Gonzalez-Elipe, A., 2000. Biocompatible surfaces by immobilization of heparin on diamond-like carbon films deposited on various substrates†. Surface and Interface Analysis, 29(6), 386–391.
Stratton-Powell, A.A., Pasko, K.M., Brockett, C.L., Tipper, J.L., 2016. The biologic response to polyetheretherketone (PEEK) wear particles in total joint replacement: a systematic review. Clinical Orthopedics and Related Research 474, 2394–2404.
Suresh, S., 1983. Micromechanisms of fatigue crack growth retardation following overloads. Engineering Fracture Mechanics 18, 577–593.
Suresh, S., 1998. Fatigue of Materials, second ed. Cambridge: Cambridge University Press.
Sze, J. Y., Tay, B. K., 2006. Carbon ion implantation of ultra-high molecular weight polyethylene using filtered cathodic vacuum arc with substrate pulse biasing. Surface and Coatings Technology, 200(12), 4104–4110.
Taeger, G., Podleska, L. E., Schmidt, B., Ziegler, M., Nast-Kolb, D., 2003. Comparison of Diamond-Like-Carbon and Alumina-Oxide articulating with Polyethylene in Total Hip Arthroplasty. Materialwissenschaft Und Werkstofftechnik, 34(12), 1094–1100.
Takemori, M.T., 1982. Fatigue fracture of polycarbonate. Polymer Engineering & Science 22, 937–945.
Teoh, S.H., 2000. Fatigue of biomaterials: A review. International Journal of Fatigue 22(10), 825–837.
Thyssen, J., Jakobsen, S., Engkilde, K., 2009. The association between metal allergy, total hip arthroplasty and revision. Acta Orthopaedica 80, 646–652.
Tiainen, V.M., 2001. Amorphous carbon as a bio-mechanical coating—Mechanical properties and biological applications. Diamond and Related Materials, 10(2), 153–160.

Total Hip Replacement—OrthoInfo—AAOS. (2024). https://www.orthoinfo.org/en/treatment/total-hip-replacement/
Total Knee Replacement—OrthoInfo—AAOS. (2024). https://www.orthoinfo.org/en/treatment/total-knee-replacement/
Toth, J.M., et al., 2006. Polyetheretherketone as a biomaterial for spinal applications. Biomaterials 27(3), 324–334.
Urish, K. L., Giori, N. J., Lemons, J. E., Mihalko, W. M., Hallab, N., 2019. Trunnion Corrosion in Total Hip Arthroplasty – Basic Concepts. The Orthopedic Clinics of North America, 50(3), 281–288.
Utzschneider, S., et al., 2010. Inflammatory response against different carbon fiber- reinforced PEEK wear particles compared with UHMWPE in vivo. Acta Biomaterialia 6(11), 4296–4304.
Uwais, Z. A., Hussein, M. A., Samad, M. A., Al-Aqeeli, N., 2017. Surface Modification of Metallic Biomaterials for Better Tribological Properties: A Review. Arabian Journal for Science and Engineering, 42(11), 4493–4512.
Verma, S., Sharma, N., Kango, S., Sharma, S., 2021. Developments of PEEK (polyetheretherketone) as a biomedical material: A focused review. European Polymer Journal 147, 110295.
von Knoch, M., et al., 2004. The effectiveness of polyethylene versus titanium particles in inducing osteolysis in vivo. Journal of Orthopedic Research 22(2), 237–243.
Wang, A., 1997. Effect of Radiation Dosage on the Wear of Stabilized UHMWPE Evaluated by Hip and Knee Joint Simulators. Transactions of the 23rd Society Congress on Biomaterials, 1997.
Wang, A., Essner, A., Polineni, V. K., Stark, C., Dumbleton, J. H., 1998. Lubrication and wear of ultra-high molecular weight polyethylene in total joint replacements. Tribology International, 31(1), 17–33.
Wang, A., Essner, A., Polineni, V., Stark, C., Dumbleton, J., 1998a. Lubrication and wear of ultra-high molecular weight polyethylene in total joint replacements. Tribolology International 31(1–3), 17–33.
Wang, A., Essner, A., Stark, C., Dumbleton, J. H., 1996. Comparison of the size and morphology of UHMWPE wear debris produced by a hip joint simulator under serum and water lubricated conditions. Biomaterials, 17(9), 865–871.
Wang, A., et al., 1997. The significance of nonlinear motion in the wear screening of orthopaedic implant materials. Journal of Testing and Evaluation 25(2), 239–245.
Wang, A., et al., 1998b. Carbon fiber reinforced polyether ether ketone composite as a bearing surface for total hip replacement. Tribology International 31(11), 661–667.
Wang, A., Lee, R., Herrera, L., Korduba, L., 2013. Wear of ultra-high molecular weight polyethylene moving along a circular path in a hip simulator. Wear, 301(1), 157–161.
Wang, A., Lin, R., Stark, C., Dumbleton, J., 1999. Suitability and limitations of carbon fiber reinforced PEEK composites as bearing surfaces for total joint replacements. Wear 225–229, 724–727.
Wang, N., Komvopoulos, K., 2013. The multilayered structure of ultrathin amorphous carbon films synthesized by filtered cathodic vacuum arc deposition. Journal of Materials Research, 28(16), 2124–2131.
Wang, N., Komvopoulos, K., 2014. The effect of deposition energy of energetic atoms on the growth and structure of ultrathin amorphous carbon films studied by molecular dynamics simulations. Journal of Physics D: Applied Physics, 47(24), 245303.
Wang, S., Komvopoulos, K., 2020. Structure evolution during deposition and thermal annealing of amorphous carbon ultrathin films investigated by molecular dynamics simulations. Scientific Reports, 10(1), 8089.
Wang, S., Roy, A., Komvopoulos, K., 2021. Thermal stability and diffusion characteristics of

ultrathin amorphous carbon films grown on crystalline and nitrogenated silicon substrates by filtered cathodic vacuum arc deposition. Scientific Reports, 11(1), 13106.
Wenz, L., Merritt, K., Brown, S., Moet, A., Steffee, A., 1990. In vitro biocompatibility of polyetheretherketone and polysulfone composites. Journal of Biomedical Materials Research 24(2), 207–215.
Williams, D., McNamara, A., Turner, R., 1987. Potential of polyetheretherketone (PEEK) and carbon-fibre-reinforced PEEK in medical applications. Journal of Materials Science Letters 6(2), 188–190.
Williams, J. G., 1977. Fracture mechanics of polymers. Polymer Engineering & Science, 17(3), 144–149.
Willis-Owen, C. A., Keene, G. C., Oakeshott, R. D., 2011. Early metallosis-related failure after total knee replacement: A REPORT OF 15 CASES. The Journal of Bone & Joint Surgery British Volume, 93-B(2), 205–209.
Willis-Owen, C., Keene, G., Oakeshott, R., 2011. Early metallosis-related failure after total knee replacement: a report of 15 cases. The Journal of Bone and Joint Surgery (British volume) 93(2), 205–209.
Wnuk, M.P., 1974. Quasi-static extension of a tensile crack contained in a viscoelastic-plastic solid. Journal of Applied Mechanics 41(1), 234–242.
Wright, T.M., Astion, D.J., Bansal, M., et al., 1988. Failure of carbon fiber-reinforced polyethylene total knee-replacement components. Journal of Bone and Joint Surgery 70(6), 926–932.
Wright, T.M., Rimnac, C.M., Stulberg, S.D., et al., 1992. Wear of polyethylene in total joint replacements – Observations from retrieved PCA knee implants. Clinical Orthopaedics 276, 126–134.
Wu, Y., Li, H., Ji, L., Ye, Y., Chen, J., Zhou, H., 2013. Preparation and properties of MoS2/a-C films for space tribology. Journal of Physics D: Applied Physics, 46(42), 425301.
Xie, J., Komvopoulos, K., 2015a. Hybridization and tribomechanical properties of ultrathin amorphous carbon films synthesized by radio-frequency low-pressure plasma discharges. Surface and Coatings Technology, 262, 15–20.
Xie, J., Komvopoulos, K., 2015b. The Role of Duty Cycle of Substrate Pulse Biasing in Filtered Cathodic Vacuum Arc Deposition of Amorphous Carbon Films. IEEE Transactions on Magnetics, 51(12), 1–9.
Xie, J., Komvopoulos, K., 2016a. Bilayer amorphous carbon films synthesized by filtered cathodic vacuum arc deposition. Journal of Materials Research, 31(20), 3161–3167.
Xie, J., Komvopoulos, K., 2016b. Friction, nanostructure, and residual stress of single-layer and multi-layer amorphous carbon films deposited by radio-frequency sputtering. Journal of Materials Research, 31(13), 1857–1864.
Xie, J., Komvopoulos, K., 2016c. The effect of Argon ion irradiation on the thickness and structure of ultrathin amorphous carbon films. Journal of Applied Physics, 119(9), 095304.
Xu, T., Pruitt, L., 1999. Diamond-like carbon coatings for orthopaedic applications: An evaluation of tribological performance. Journal of Materials Science: Materials in Medicine, 10(2), 83-90.
Yang, J., Liu, J., 2001. Cavitation of rubber particles in high-impact polystyrene. Polymer Journal 33(12), 952–954.
Yeo, R. J., Dwivedi, N., Tripathy, S., Bhatia, C. S., 2015. Excellent wear life of silicon nitride/tetrahedral amorphous carbon bilayer overcoat on functional tape heads. Applied Physics Letters, 106(9), 091604.
Zenkert, D., Burman, M., 2009. Tension, compression and shear fatigue of a closed cell polymer foam. Composites Science and Technology 69, 785–792.
Zhang, Y., Jordan, J. M., 2010. Epidemiology of Osteoarthritis. Clinics in Geriatric Medicine,

26(3), 355–369.
Zheng, X., et al., 2019. "Mechanical characteristics of medical grade UHMWPE under dynamic compression.". Journal of Materials Science Materials in Medicine 30.5, 1–12.
Zhou, J., Chakravartula, A., Pruitt, L., Komvopoulos, K., 2004. Tribological and Nanomechanical Properties of Unmodified and Crosslinked Ultra-High Molecular Weight Polyethylene for Total Joint Replacements. Journal of Tribology, 126(2), 386–394.
Zhou, J., Komvopoulos, K., 2005. Wear Mechanisms of Untreated and Gamma Irradiated Ultra-High Molecular Weight Polyethylene for Total Joint Replacements. Journal of Tribology, 127(2), 273–279.
Zhou, Y.Q., Brown, N., 1992. The mechanism of fatigue failure in a polyethylene copolymer. Journal of Polymer Science: Polymer Physics 30, 477–487.
Zysk, S., et al., 2005. Particles of all sizes provoke inflammatory responses in vivo. Clinical Orthopaedics and Related Research 433, 258–264.